Circumarctic landcover diversity considering wetness gradients

Annett Bartsch[1], Aleksandra Efimova[1], Barbara Widhalm[1], Xaver Muri[1], Clemens von Baeckmann[1], Helena Bergstedt[1], Ksenia Ermokhina[2], Gustaf Hugelius[3,4], Birgit Heim[5], and Marina Leibmann[6]

[1]b.geos, Industriestrasse 1, 2100 Korneuburg, Austria
[2]A.N. Severtsov Institute of Ecology and Evolution, Russian Academy of Sciences, Moscow, Russia
[3]Department of Physical Geography, Stockholm University, Stockholm, Sweden
[4]Bolin Centre for Climate Research, Stockholm University, Stockholm, Sweden
[5]Alfred Wegener Institute for Polar and Marine Research, Potsdam
[6]Earth Cryosphere Institute, Tyumen Scientific Centre SB RAS

Correspondence: Annett Bartsch (annett.bartsch@bgeos.com)

Abstract. Landcover heterogeneity information considering soil wetness across the entire Arctic tundra is of interest for a wide range of applications targeting climate change impacts and ecological research questions. Patterns potentially link to permafrost degradation and affect carbon fluxes. First a landcover unit retrieval scheme which provides unprecedented detail by fusion of satellite data using Sentinel-1 (synthetic aperture radar) and Sentinel-2 (multispectral) has been was adapted. Patterns of lakes, wetlands, general soil moisture conditions and vegetation physiognomy are represented interpreted at 10 m nominal resolution. Units with similar patterns are were identified with a k-means approach and documented through statistics derived from comprehensive in situ records for soils and vegetation (more than 3500 samples). The result goes beyond the capability of existing landcover maps which have deficiencies in spatial resolution, thematic content and accuracy although landscape heterogeneity related to moisture gradients cannot be fully resolved at 10 m. Wetness gradients have been eventually were assessed and measures for landscape heterogeneity were derived north of the treeline. About 40 % of the area north of the treeline falls into three units of dry types with limited shrub growth. Wetter regions have higher landcover diversity than drier regions. 4566 % of the analysed Arctic landscape is highly heterogeneous with respect to wetness considering 1kmx1km units at a 1-km scale (representative scale of frequently used regional landcover and permafrost modelling products). Wetland areas cover on average 9 % and moist tundra types 32 %, what is potentially which is of relevance for methane flux upscaling.

1 Introduction

Landsurface hydrology, moisture gradients, wetting and drying processes play a major role in the context of Arctic biodiversity studies, carbon flux upscaling, carbon pools quantification, permafrost mapping and human impact assessment. In order to address such processes both open water fraction and soil moisture related information is essential. In the Arctic, the landscape heterogeneity and especially the occurrence of lakes, has so far been a major limiting factor for retrieval of near surface soil moisture time series using microwave satellite data as commonly applied on regional to global scale due to spatial resolution (Hogstrom and Bartsch, 2017; Högström et al., 2018; Wrona et al., 2017). Landcover properties are therefore often used as proxy for subground conditions. Multi-spectral satellite data, especially from Landsat (30m) have been 30 m) were regionally employed for characterizing typical tundra landscape types reflecting moisture regimes and vegetation physiognomy previously (Bartsch et al., 2016b). Soil characteristics are for example required for parameterization of heat transfer modelling for permafrost studies (Westermann et al., 2017). Global landcover maps are currently used although deficiencies for the Arctic are known. This relates to thematic content as well as high landcover heterogeneity not reflected by the comparably coarse spatial resolution. For example, the accuracy of the Landcover CCI dataset (300 m) for high latitude wetlands ~~has been~~ was determined to be only 19 % (Palmtag et al., 2022). Nevertheless it ~~has been used for~~ was used for example for permafrost modelling (Westermann et al., 2017) and wetland delineation (Olefeldt et al., 2021; Albuhaisi et al., 2023) accepting the uncertainties in the absence of a better alternative.

The issue of spatial resolution ~~has been~~ was extensively discussed for water bodies (Liljedahl et al., 2016; Muster et al., 2019) and also for further landcover features on regional scale (e.g. fluxes (Virtanen and Ek, 2014), soils (Siewert et al., 2015), carbon balance and landscape heterogeneity (Treat et al., 2018)). All studies call for very high resolution data, in the order of few meters or sub-meter scale, for which availability and access is limited (Bartsch et al., 2023). A scheme with high thematic content (with respect to tundra) ~~has been~~ was previously implemented based on ~~1kmx1km~~ 1 km x 1 km data using multispectral data (AVHRR - Advanced Very High Resolution Radiometer; Walker et al. (2005); Raynolds et al. (2019)). This widely used Circumpolar Vegetation Map (CAVM) provides vegetation community information but does not provide a measure of the high spatial heterogeneity of Arctic landscapes.

Recently, data from the multispectral Sentinel-2 mission which provides ~~10-20m~~ 10-20 m detail came into focus. This provides an advance compared to for example Landsat (~~30m~~30 m) although still lacking some detail. Such data ~~have been~~ were also shown of added value in combination with C-band radar information from Sentinel-1 with similar resolution to obtain landcover related information (Bartsch et al., 2019a, 2020; Scheer et al., 2023). For example the approach by Bartsch et al. (2019a, b) is based on a combination of Sentinel-1 and Sentinel-2 using a k-means unsupervised classification. The application potential of the obtained landcover units (21 classes) ~~has been~~ was shown in regional studies (Bartsch et al., 2019a; Bergstedt et al., 2020; Kraev et al., 2022; Spiegel et al., 2023). The approach targets use of landcover information as proxy for soil conditions, specifically wetness gradients. This is achieved through focus on the use of selected bands of Sentinel-2 and the choice of frozen state acquisitions of Sentinel-1.

Wetness patterns are known to drive the occurrence of certain vegetation communities in tundra environment (e.g. Silvertown et al. (2014); Dvornikov et al. (2016); Ackerman et al. (2017)). A commonly used multispectral index is the Tasseled Cap Wetness Index. This index ~~has been~~ was demonstrated of value for longterm change studies targeting permafrost degradation in tundra (Nitze and Grosse, 2016). Whereas the commonly used Normalized Vegetation Index NDVI utilizes the red and near infrared information only, the Tasseled Cap Wetness index also considers green and short-wavelength infrared information (Crist, 1985). Considering Sentinel-2, bands available at ~~10m~~ 10 m as well as ~~20m~~ 20 m nominal resolution are of interest.

The use of Sentinel-1 is usually confined to unfrozen conditions in order to use the moisture information reflected in the backscatter measurements (e.g. for the Arctic, Reschke et al. (2012); Ou et al. (2016)). High backscatter is associated with high soil moisture. Other scattering mechanisms, such as surface roughness, however, also contribute to backscatter increase. It ~~has been~~ was shown that relevant information can be also derived from C-band SAR data acquired under frozen conditions (Bartsch et al., 2016b; Widhalm et al., 2015). It ~~has been~~ was for example demonstrated in Bartsch et al. (2016b) that C-band frozen backscatter at HH polarization (horizontally sent and horizontally received) can be used as proxy for estimation of near surface soil organic carbon in tundra regions. For tundra environments, this also coincides with specific landsurface wetness gradients what ~~has been~~ was initially shown for ENVISAT ASAR (Advanced Synthtic Aperure Radar) Global monitoring mode (~~1km~~1 km) by Widhalm et al. (2015). The derived CAWASAR (CircumArctic Wetlands based on Advanced Aperture Radar) map ~~has been~~ was previously applied for a permafrost equilibrium model soil parameterization (Obu et al., 2019) as well as for a recent estimation of the global methane budget (wetlands as input for landsurface modelling (Saunois et al., 2016), global wetland map compilation (Zhang et al., 2021)) and climate change vulnerability assessment (Kåresdotter et al., 2021).

Bartsch et al. (2019a) demonstrated that the different landscape units derived based on selected Sentinel-1/2 data reflect differences in soil wetness as can be determined by seasonal subsidence patterns derived through SAR Interferometry. Ice in the soil pores melts and commonly leads to subsidence throughout the summer. This effect is less pronounced for dryer soils. The initial land-cover map covered Western Siberia with 20 m nominal resolution (Bartsch et al., 2019b). On regional scale, classes ~~have been~~ were also matched to vegetation community descriptions. The classification accuracy ranged between 70 and 83.3 % for central Yamal (Bartsch et al., 2019b). The approach does however consider bands of Sentinel-2 which have 10 m as well as ~~20m~~ 20 m resolution. Adapted super-resolution processing can be ~~, however,~~ used for transformation to ~~10m~~ 10 m nominal resolution. This ~~has been~~ was shown applicable in case for Sentinel-2 for Arctic environments ~~before~~ (Bartsch et al., 2021b). Bartsch et al. (2021b) also demonstrate the feasibility of Sentinel-1/2 for circumpolar processing, but with focus on artificial objects. Circumpolar implementation of a landcover unit retrieval with high detail is, however, still lacking. A map for tundra regions based on Sentinel-1/2 and digital elevation information ~~has been~~ was previously published, but with lower thematic content (ten classes, CALC-2020, (Liu et al., 2023)). Topographic information was used in addition and shown to be the dominating factor in the random forest method based retrieval. In addition, shrub growth patterns which are a key characteristic of tundra landscapes (Raynolds et al., 2019) are not distinguished (Liu et al., 2023).

The purpose of this study was to provide an account of tundra land cover heterogeneity, considering wetness gradients and diversity. (1) Landcover units at comparably high resolution (~~10m~~10 m) and thematic content needed to be derived for the entire Arctic north of the treeline (Circumarctic Landcover Units - CALU). (2) Heterogeneity ~~has been~~ was assessed with respect to the scale of current global permafrost modelling (~~1km~~1 km). (3) The landcover units also ~~have been~~ were documented with in situ data regarding their vegetation and soil properties to facilitate further use.

This requires an approach feasible to be implemented for the entire Arctic. A strategy is needed to extent the prototype landcover units as suggested in Bartsch et al. (2019a) which ~~can be~~ were distinguished by combining the multispectral and C-band synthetic aperture radar data for representative regions (climatic gradients). The original approach considered only top of atmosphere radiance, ~~20m~~ 20 m resampled data and flat to moderate terrain. The latter allowed the use of σ^0 for Sentinel-1 backscatter with a simplified normalization approach (Widhalm et al., 2018). Mountain regions are ~~included~~ present on circumpolar scale, what requires the use of γ^0 instead (Small, 2011). Overall, a retraining of the classifier is needed considering the enhanced pre-processing techniques.

2 Data

2.1 Satellite data

Data acquired from ~~both the Copernicus~~ the Sentinel-1 ~~and~~ (synthetic aperture radar - SAR) as well as Sentinel-2 ~~mission have been~~ (mutli-spectral) mission were used for the retrieval. ~~Both~~ These missions are part of ESA's Copernicus program. ~~Whereas~~ Data from both Sentinel-1 ~~carries synthetic aperture radar systems, Sentinel-2 provides multi-spectral data.~~

~~Two satellites were so far usedfor the Sentinel-1 mission, both with~~ satellites were used. Both have a near-polar, sun-synchronous orbit ~~,~~ and they are 180 degrees apart from each other. ~~The two earth observation satellites~~ Sentinel-1A (launched in April 2014) and Sentinel-1B (launched in April 2016, operation stopped in December 2020) have an identical C-band SAR sensor on board (Schubert et al., 2017). Several modes are available. The Interferometric Wide Swath (IW) mode is of main interest for this study. It combines a swath width of 250 km with a relatively good ground resolution of 5×20 m. ~~A pixel spacing of 10×10 m is commonly used for nominal resolution of derived products. This is also the case for~~ The Ground Range Detected (GRD) products as distributed by Copernicus ~~. Information can be captured~~ are supplied with 10 m nominal resolution. GRD products are detected, multi-looked, and projected to ground range using an Earth ellipsoid model (ESA, 2012). The SAR sensors can capture information in dual polarization (HH+HV or VV+VH; H - horizontal, V - vertical). Mostly VV+VH is available for the Arctic land area for this mode and resolution. Greenland and several high Arctic islands are an exception. They are covered in HH+HV mode due to requirements of glacial monitoring.

~~GRD products are detected, multi-looked, and projected to ground range using an Earth ellipsoid model (ESA, 2012). As temporal variations of backscatter can occur with changes in liquid water content (Bergstedt et al., 2018; Bartsch et al., 2023), only winter data~~ Only data acquired during mid-winter (December and/or January; frozen soil conditions) ~~are~~ is used for cross-Arctic consistency and comparability as temporal variations of backscatter can occur with changes in liquid water content (Bergstedt et al., 2018; Bartsch et al., 2023).

The Sentinel-2 constellation has also two ~~twin satellites,~~ satellites. Sentinel-2A (launched June 2015) and -2B ~~,~~ (launched March 2017) are in a sun-synchronous orbit, 180° apart from each other. ~~Sentinel-2A was launched in June 2015 and Sentinel-2B in March 2017. The optical sensor samples~~ Data from 13 spectral bands is available. The spatial resolution depends on the ~~used~~ band: four bands have a spatial resolution of 10 m, six bands of 20 m, and three bands of 60 m (ESA, 2015). Bands 3 (green, 10 m), 4 (red, 10 m), 8 (near infrared, 10 m), 11 (SWIR, 20 m), 12 (SWIR, 20 m) ~~have been~~ were used for the classification following the prototype scheme (Bartsch et al., 2019a, b).

2.2 Landcover prototype

The original prototype covered a transect reaching from the Yamal peninsula into the northern part of the West Siberian Lowlands (Figure 1). Four bioclimatic zones are covered. The processing is based on Sentinel-1 and Sentinel-2 images with bands sampled to ~~20m~~20 m. Top of atmosphere radiance was originally used for Sentinel-2 and normalized σ^0 for Sentinel-1. 25 classes were considered, including three water classes, but excluding permanent snow/ice and shadows as the ~~analyses~~ analysis region did not include steep mountain or high Arctic areas. The classes were determined with a k-means approach and labeled based on field data and expert knowledge (Bartsch et al., 2019a).

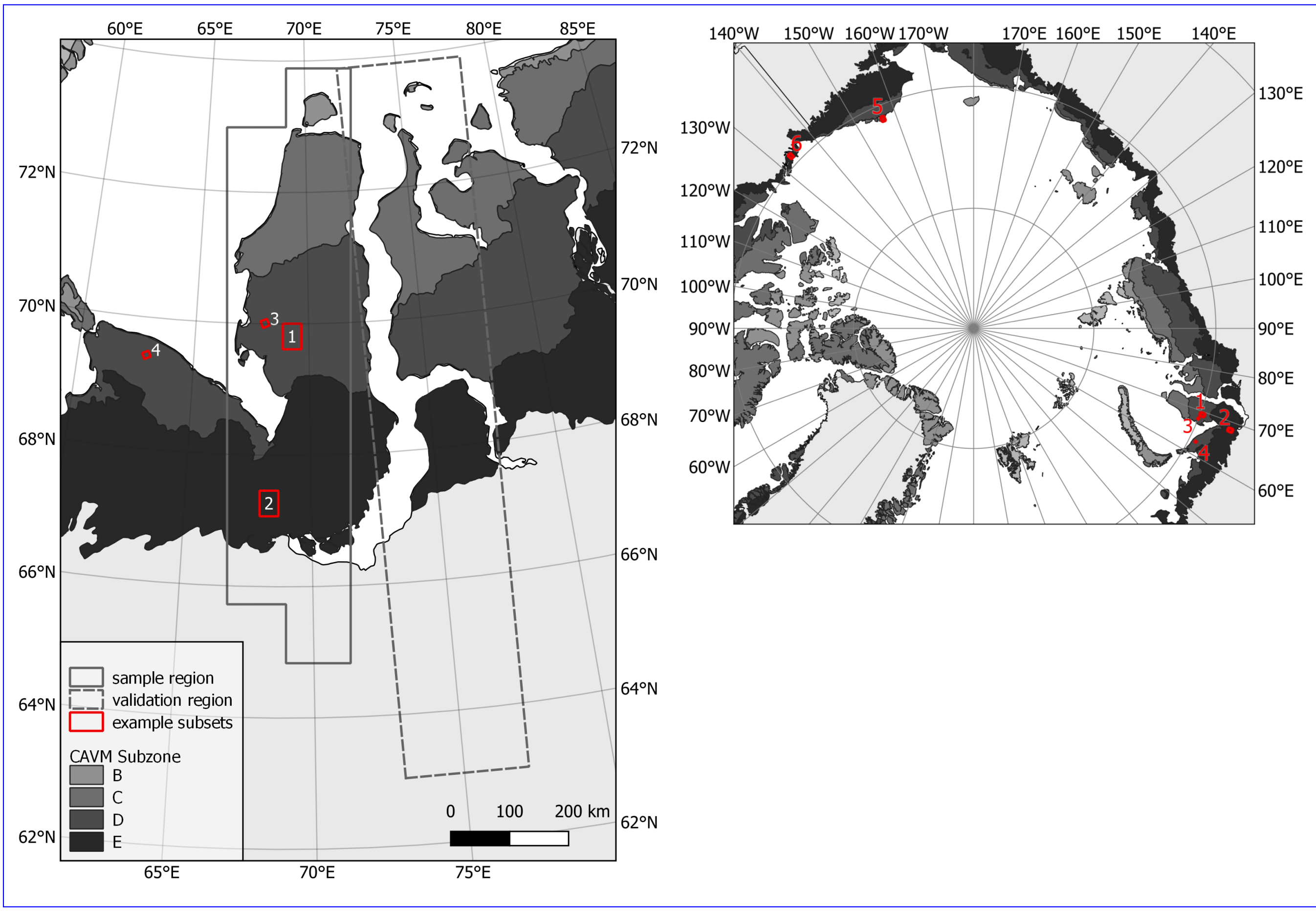

Figure 1. Location of subsets discussed in the study. Left: the training region for the Maximum Likelihood approach used for transfer to the circumpolar domain based on the prototype (K-Means analyses; 'sample ~~transect~~region') ~~,~~ and the evaluation region ('validation ~~transect~~region')~~and~~ . Right: sites of examples of the results presented in Figure 14 (subset 1), Figure 15 (subset 2), Figure 16 (subset 5), Figure 17 (subset 6) and Figure 19 (subsets 3 and 4). Example locations are shown in both maps. CAVM - ~~Circumarctic~~ Circumpolar Vegetation Map (Raynolds et al., 2019) with subzones ~~A) High Arctic tundra,~~ B) Arctic tundra: northern variant, C) Arctic tundra southern variant, D) Northern hypo-Arctic tundra, E) Southern hypo-Arctic tundra.

2.3 In situ data

Three types of in situ records are available: (1) full pedon descriptions for key regions, (2) field data of soil surface organic horizon depth available from multiple sites across the northern hemisphere, (3) vegetation coverage records from the Russian Arctic Vegetation Archive for Western Siberia (over view map in Figure A1). More than 3500 in situ data records ~~have been~~ were used.

~~355 pedons were available for #1.~~ The field soil sampling took place between 2006 and ~~2019.~~ 2019, and produces 355 pedons available for this analysis. Protocols for field sampling, laboratory analyses and data is detailed in Palmtag et al. (2022). Surface organic horizon depth was available for 788 non forest samples~~were available for #2. The data was~~ , extracted from several different sources, including (Hugelius et al., 2013, 2014, 2020) and (Palmtag et al., 2022). Soil horizons ~~are defined as surface soil horizons~~ were defined as organic when their organic carbon content ~~is ≥~~was ≥17 % (equivalent to ca. 30 % organic matter content) (Hugelius et al., 2020). ~~Many of the sites for (1) and (2) overlap.~~

We used the information from the Russian Arctic Vegetation Archive (AVA standardized protocol, Zemlianskii et al. (2023)), which contains relevés (geobotanical plots) made in accordance with the Braun-Blanquet tradition (available for download at the AVA website, https://avarus.space). The relevés include species lists and species' cover estimations, as well as vegetation and habitat characteristics. They cover square plots with an area of 1-400 m^2 (74 % cover 100 m^2, 12 % cover 4 m^2, other variants comprise less than 10 %). These plots are typically distributed across a 10x10 km site to ensure the representation of various plant communities with a statistically significant number of plots. The AVA data used in this study ~~was obtained during fieldworks~~ were obtained during fieldwork conducted from 2007 to 2020. 2705 relevé locations overlapped the analysis extent (area within CAVM boundary).

The following in situ measurements are used for the assessment and assignment of unit descriptions:

1. sites with full pedon descriptions (Palmtag et al., 2022)
   - Volumetric Water content (%)
   - Organic volumetric content (%)
   - Mineral volumetric content (%)
   - Wet and dry bulk density
   - Soil organic carbon and total nitrogen density
2. sites with soil surface organic horizon depth (cm) (partial overlap with #(1))
3. vegetation coverage (%) (from AVA https://avarus.space/profile/about/ , Zemlianskii et al. (2023))
   - Trees
   - Tall shrubs
   - Low shrubs

- Erect dwarf shrubs
- Prostrate dwarf shrub
- Graminoids
- Tussok graminoids
- Forbs
- Seedless vascular plants
- Mosses and liverworts
- Lichen
- Crust
- Algae
- Bare soil
- Bare rock
- Litter

The AVA dataset (#3) also includes a general wetness description (dry, moist, wet and aquatic) and open water fraction.

2.4 Auxiliary data

The ~~analyses~~ analysis extent also includes disturbances, specifically ~~wild fire affected~~ wildfire-affected areas within the tundra-taiga transition zone, which need to be considered in the assessment. The Alaska Large Fire Database (https://www.frames.gov/catalog/1046 contains current and historical reported fire locations and fire perimeters. It builds on Kasischke et al. (2002). The database covers all of Alaska and contains about 4600 polygons for fire extent dating back to breakouts in 1942. Polygons which overlap with the analyses extent date back to 2002. The latest fires represented are from October 2021.

Digital elevation data are required for pre- and post-processing of the satellite data. The Copernicus DEM GLO 90 was used. It represents the surface of the Earth including buildings, infrastructure and vegetation at ~~90m~~ 90 m spatial resolution. It covers the full global landmass of the time frame of data acquisition (2011-2015). The Copernicus DEM is based on the SAR-derived WorldDEM dataset provided by Airbus and acquired by the TanDEM-X mission. According to official statistics published by the Copernicus in the DEM Product Handbook, overall absolute vertical accuracy of the dataset is 90 %, confidence level is > 4 m. For Svalbard the ~~20m~~ 20 m spatial resolution DEM of the Norwegian Polar Institute was used Melvaer (2014). This DEM is based on stereo models of aerial photos. ~~In areas where these were not available the DEM is built on elevation contours.~~

Air temperature ~~has been~~ was derived from ERA5 reanalysis data which combines model data with observations to provide a globally consistent dataset (Hersbach et al., 2023). The data ~~was~~ were available from the European Centre for Medium-Range Weather Forecasts (ECMWF) and accessed via the Climate Data Store (CDS). We used air temperature at ~~2m~~ 2 m above the surface in a temporal resolution of 2 hours at 0.25° spatial resolution for selection of Sentinel-1 observations. Precipitation was

Table 1. Landcover datasets considered for cross-comparison. CCI - ESA land cover Climate Change Initiative (CCI) (2017) project (http://maps.elie.ucl.ac.be/CCI/viewer/index.php, last access: 1 September 2023)., CAVM - ~~Circumarctic~~ Circumpolar Arctic Vegetation Map, ~~CALC~~ CALC-2020 - Circumarctic Landcover, LCP - Land Cover Prototype, CALU - Circumarctic Landcover Units.

Dataset	**C3S/Landcover CCI**	**CAVM**	**~~CALC2020~~CALC-2020**	**LCP**	**CALU**
Reference	~~Defourny et al. (in preparation)~~ ESA CCI (2017)	Raynolds et al. (2019)	Liu et al. (2023)	Bartsch et al. (2019a)	this study
Spatial resolution	~~300m~~ 300 m	~~1000m~~ 1000 m	~~10m~~ 10 m	~~20m~~ 20 m	~~10m~~ 10 m
Primary source	Sentinel-3 OLCI 2019	AVHRR 2000	Sentinel-1/2, DEM	Sentinel-1/2	Sentinel-1/2
Extent	Global	North of treeline	As defined in CAVM	Western Siberia	As defined in
Classes/Units	38	16	10	21	23

used in addition in order to clarify anomalous weather conditions (drought and flooding conditions) impacting the results in the final maps.

2.5 Existing land cover information for comparison

Two circumpolar and one global landcover dataset ~~have been~~ were compared to the landcover units (Table 1). The spatial resolution ranges from ~~10m to 1000m~~10 m to 1000 m. The raster version of the CAVM (Circumpolar Arctic Vegetation Map, Raynolds et al. (2019)) is considered a key benchmark dataset as it ~~has been~~ was developed specifically for the Arctic by vegetation experts. It provides a similar level of detail regarding shrub types and soil wetness.

The CAVM also includes information on bioclimatic subzones. In total ~~six~~ five subzones are distinguished for the Arctic~~of which five~~ , of which four can be found along the validation and calibration ~~transect~~ region (Figure 1).

3 Methods

In a first step, a landcover unit retrieval scheme ~~has been~~ was adapted in order to achieve 10 m nominal resolution, consider atmospheric correction, address issues in mountainous regions and ~~in order to~~ allow additional classes such as recent fire scars, snow and shadow. Results ~~have been~~ were cross-compared to results of the original processing scheme and to external datasets including classical landcover maps and soil and vegetation in situ records. The latter was used to provide an example for description of the units.

Statistics ~~have been derived for 1km x 1km~~ were derived for 1 km x 1 km areas in a second step in order to quantify landcover diversity in general and specifically for wetland areas.

3.1 Landcover units retrieval scheme adaption

The retrieval ~~schemes~~ scheme expands the prototype (Bartsch et al., 2019b) from Western Siberia to the entire Arctic, incorporating advanced pre-processing and a postprocessing step ~~is~~ was introduced. The final classes are referred to as landcover units, the entire map as CALU - Circumarctic Landcover Units. The prototype is based on an unsupervised k-means classification.

The resulting classes are units of similar reflectance of the shortwave incoming radiation (Sentinel-2) and radar backscatter at C-VV (Sentinel-1). Names for the prototype units were assigned by regional experts to the 23 resulting classes.

The processing ~~has been~~ was based on Sentinel-2 granules as defined by the data provider. Granules have an extent of 100 km by 100 km. They partially overlap as they are aligned with respect to UTM projection zones. Only granules including ice free land areas were considered. All Sentinel-1 images ~~have been~~ were subset to the granules.

Sentinel-2 data are available in UTM projection and largely at Level 2A (orthorectified, top of atmosphere). Atmospheric correction ~~is~~ was required in order to account for related differences between the dates. We therefore applied atmospheric correction using sen2cor on the Sentinel-2 data, which also ~~generates~~ generated a cloud mask during the process. Sentinel-2 provides spatial resolution of 10 m for some bands but not for all. Enhancement of spatial resolution of the coarser band therefore ~~needs~~ needed to be considered to exploit the multi-spectral capabilities offered by Sentinel-2. We therefore performed super-resolution based on the tool Dsen2 (Lanaras et al., 2018), which ~~uses~~ used a convolutional neural network. Lanaras et al. (2018) showed that their approach clearly ~~outperforms~~ outperformed simpler upsampling methods and better ~~preserves~~ preserved spectral characteristics. The original model was trained on Level-1 data, which ~~have not been~~ were not atmospherically corrected, and global sampling. Bartsch et al. (2021a) retrained and tested the model on Level-2 data (output of sen2cor) using the same published training and testing routines for selected granules from our study sites. After the super-resolution step, clouds were masked using the cloud mask output from sen2cor. In case of frequent fractional cloud cover also subsets of scenes ~~have been~~ were used. Mostly mid-growing season acquisitions ~~have been~~ were considered for Sentinel-2, this means mid July to mid August. This time frame ~~has been~~ was slightly extended in some cases ~~of lack of cloud free~~ with limited cloud-free acquisitions. Up to eight ~~granules have been considered~~Sentinel-2 acquisition dates were selected for individual granule locations. A minimum of three has been collected if available. In a next step the median of ~~three, if available, acquisition dates are~~ theacquisition dates was calculated which further ~~mitigates~~ mitigated errors due to undetected clouds.

Acquisitions ~~need~~ needed to represent frozen conditions in case of Sentinel-1, but at maximum -10 °C to minimize the effect of temperature on backscatter at C-band (Bergstedt et al., 2018; Bartsch et al., 2023). This ~~requires~~ required the use of spatially consistent temperature data across all analysed areas. Reanalyses data (ERA5) was therefore used for scene selection. Processing steps of Sentinel-1 ~~include~~ included border noise removal, based on the bidirectional all-samples method of Ali et al. (2018), calibration, thermal noise removal and orthorectification using the Copernicus ~~90m~~ 90 m resolution DEM. These steps ~~are~~ were carried out with the SNAP toolbox provided by ESA and γ^0 ~~is~~ was derived. After normalization, data ~~has been~~ was reprojected and subset to match the Sentinel-2 granules and temporal averaging ~~has been~~ was performed.

A ~~transect~~ training area spanning nine degrees in latitude and representing different landscape gradients and thus all units (Figure 1) ~~has been~~ was selected from the prototype landcover unit map in order to transfer the retrieval (re-training of the maximum likelihood classifier) to the entire Arctic as well as to the output of the enhanced preprocessing (super-resolution processing, atmosphere correction and use of γ^0 instead of σ^0). The units remained largely the same. ~~Additional training data have been included in case of the disturbance unit. This~~ 18 of the 21 original classes were assigned to the new units. The remaining three classes were modified and split up. First, the original mixed and coniferous forest units were both split regionally (bioclimatic zone E versus B to D) to address misclassification of tundra as forest. Pixels in zones B and D were joined and assigned to a new unit. The disturbance unit originally combined different disturbance types which lead to vegetation removal, geomorphological processes as well as fires. ~~Training~~ A k-means classification was applied targeting two units. Results were preliminary assessed with data from recently burned areas ~~were included into the training dataset for a separate class. The~~ within the prototype extent in Western Siberia. The new 'recently burned' unit was then validated over Alaska. The originally three water units ~~have been~~ were merged into one water unit. The modified prototype classification was then used to train the maximum likelihood classifier. Further on, a snow ~~unit has been~~ and a shadow unit were introduced based on training data from Svalbard resulting in 23 units.

Illumination conditions impact the reflectance in the Sentinel-2 bands in mountainous areas. ~~This has been addressed in two steps. First a other/shadow unit was introduced based on training data obtained over Svalbard.~~ Not all shadow areas ~~can be however identified~~could be identified, due to similarities in reflectance ~~over~~ with water bodies and wetlands. Therefore a second post-processing step based on the slope derived from the Copernicus DEM data was introduced. 'Water', 'Permanent wetlands' or 'shallow water' on slopes larger than 7° ~~have been~~ were set to 'other'. Shadow in regions with low slope (less than 3°) ~~has been~~ was set to 'water'.

3.2 Evaluation and documentation of landcover units

Unit specific validation was carried out for the new disturbance unit which targets burned ~~areasusing~~ areas using the Alaska Fire Database.

The description of the units ~~is~~ was based on the comprehensive soil and a vegetation in situ dataset. The first ~~has been~~ was previously used similarly in conjunction with a global landcover map (Palmtag et al., 2022). The second data set is part of a tundra specific international standardization and archive effort (Zemlianskii et al., 2023). Common statistics (mean, standard deviation) ~~have been~~ were derived and are supplied with the dataset documentation.

Unit descriptions consider abundance of vegetation types including shrub growth form/height as well as moisture conditions. The following shrub types ~~are~~ were considered (following the differentiation of the CAVM, Raynolds et al. (2019) and Walker et al. (2018)):

- Prostrate dwarf shrub – approximately 5 cm, also referred to as prostrate shrub
- Erect dwarf shrub – up to 40 cm, also referred to as dwarf shrub
- Low shrub – up to ~~2m~~ 2 m
- Tall shrubs – tundra biome species taller than ~~2m~~ 2 m

The comparison to Landcover CCI and the CAVM (see table 4) ~~requires~~ required resampling. The coarser resolution maps ~~have been resampled to 10m (~~were resampled to 10 m (the same resolution as CALU). Classes ~~have been~~ were grouped for comparison due to the large differences in thematic content. ~~The translation tables are provided in the supplement.~~ A simplified set of nine units was developed that allowed cross-comparison between the CALU and the three external maps. Table 2 shows the grouping for the CALU, and Appendix C shows the groupings for the external maps. In addition, the new classification ~~has~~

been was compared with the original prototype (20m20 m, 21 classes). A different transect has been training area was used for the evaluation than for the re-training of the transfer samples (Figure 1).

A direct comparison can could only be made for common or merged classes which include included water, snow/ice, other, wetland, grasslandgraminoids, lichen/moss, dwarf to low shrub tundra, forest and barren (without graminoids). The grouping of CALU for the comparison has been was primarily guided by the presence of shrubs. If more than 20 % of erect dwarf to low shrubs are were found on average the class is unit was assigned to shrub tundra. The assignment is referred to as grouping A (Table 2).

3.3 Heterogeneity assessment

Landscape heterogeneity is eventually was addressed through assessment of (1) richness with respect to the CAVM classification specifications and (2) wetness diversity, both for 1km grid cells. The chosen cell size matches the grid of the permafrost model CryoGRID (Obu et al., 2021) as well as the rater raster version of the CAVM (Raynolds et al., 2019). The number of identified units (minimum 1 % fraction) within 1km x 1km cells has been 1 km x 1 km cells was counted for the CAVM classes. Permanent snow and shadow have been were excluded from the richness assessment. In addition, units have have been were grouped with respect to wetness (wet, moist, dry) for wetland and tundra classes, also excluding permanent snow and shadow as well as water, forest and recently burned areas. Groups (referred to as B, Table 2) have been were summed up resulting in values of one (homogeneous) to three (heterogeneous).

4 Results

4.1 Coverage

1266 Sentinel-2 granules which overlap with the Arctic as identified in the CAVM (Raynolds et al., 2019) have been were identified (Figure 2). The use of three Sentinel-2 acquisitions was targeted to account for anomalies due to undetected clouds and hydrological extremes (droughts, flooding) what could be which was achieved in 75 % of the cases (Figure 3). Only two images were available for 4 % of all granules. More than 3600 Sentinel-2 images at granule extent have been were included in the processing.

No suitable Sentinel-2 acquisitions have been were available in 52 (4 %) cases and in addition 66 (5 %) cases with no Sentinel-1 data (Figure 2). The latter is related to the general Sentinel-1 acquisition strategy for IW mode. Data are were missing specifically for Greenland and the Canadian High Arctic islands. Nevertheless, 97 % of the target area (CAVM extent) could be processed. In 13 % of the area the availability of data was very limited and led to lower quality results or gaps (Figure 2 and 3). This results from acquisition date issues or inconsistencies in the used Copernicus DEM (no data: 23 times in case of some inland water bodies and 2 times general gaps). 19 % have been were flagged as medium and 3 % as low quality. Medium quality usually results resulted from anomalous meteorological/hydrological conditions in certain years (evaluated with re-analyses), including flooding or droughts which impact landcover and vegetation optical properties. Low quality is was

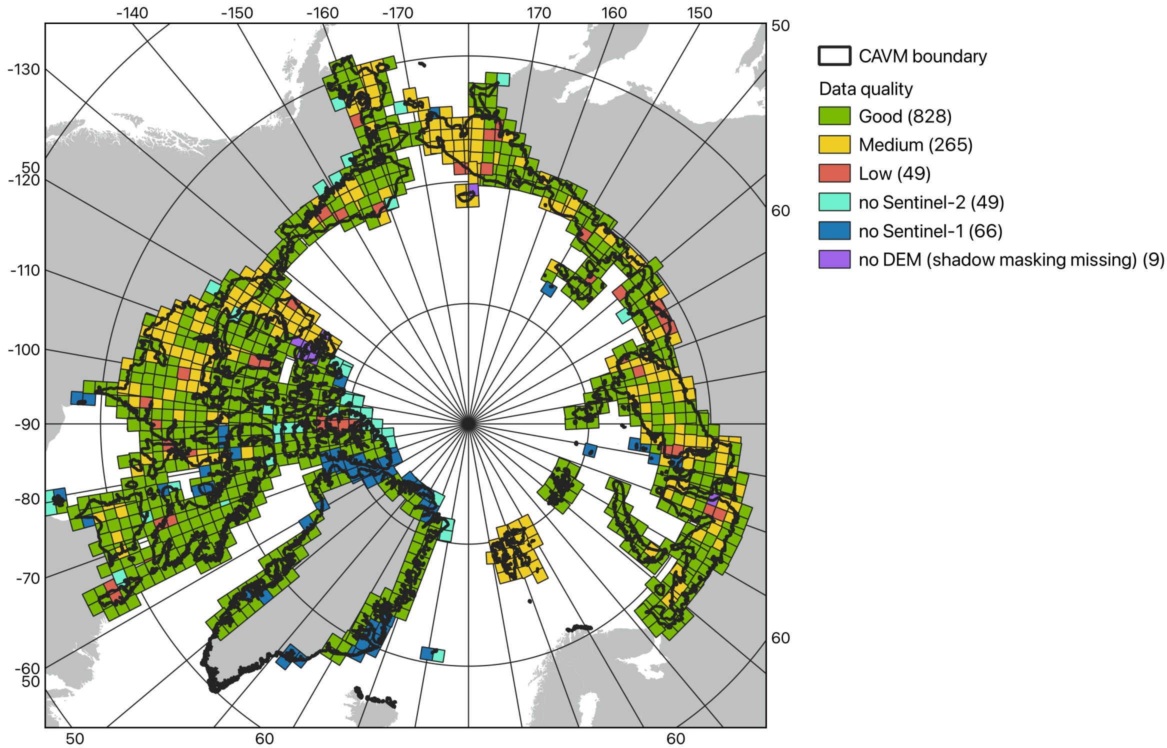

Figure 2. Data quality by granules within ~~CAVM~~ within the Circumpolar Arctic Vegetation map (Raynolds et al., 2019) boundary and number of granules in parenthesis.

usually caused by acquisitions ~~too late or too early in the season~~close to mid-July and mid-August in years with deviations in phenology (early or late spring).

4.2 Identified landcover units

23 unit types ~~are eventually~~ were derived for the CALU (Circumarctic Landcover Units) map (Table 2). Descriptions ~~are~~ were assigned summarizing the statistics of the in situ data, referring to wetness, vegetation physiognomy and abundance. The most common unit within the extent of the CAVM ~~is~~ was unit #6 'dry to moist tundra, partially barren, prostrate shrubs' with overall 22.5 % (original 10x10m) and 28.5 % in the majority (1x1km) respectively. This unit ~~can~~ could be specifically found in the Canadian High Arctic and on the Taimyr peninsula (Russia). Units with shrubs of dwarf and higher growth form ~~sum~~ summed up to about 32 % and wetlands to about 9 %. A higher occurrence in the majority retrieval ~~indicates~~ indicated relatively homogeneous patterns. This ~~applies specifically to class~~ applied specifically to unit #6 as well as #21 (partially barren). The contrary ~~is~~ was the case for wetland ~~classes~~ units #2 and #3 reflecting ~~occurrence patches~~patchy occurrence at a scale of < 1 km^2. Regarding wetness, 40 % ~~are~~ of the circumarctic area were assigned to the dry and 32 % to the moist group.

Table 2. ~~Classes~~ Example of representation of the Circumarctic Landcover Units (CALU) based on in situ records (see Figure A1) and grouping (A) ~~grouping~~ for comparison ~~,~~ with other landcover maps and (B) ~~grouping~~ for wetness heterogeneity assessment. In addition, ~~P)~~ the proportion within the CAVM (Circumpolar Arctic Vegetation map; Raynolds et al. (2019)) extent is provided in % ~~M~~(P) and the majority proportion (1km grid cells) in % (M). * sparse tree cover along treeline. Full documentation of classes 1 to 21 is available in ~~Appendix A~~the Appendices.

ID	Description example	Gr. A	Gr. B	P	M
1	water	Water	-	5.9	7.1
2	shallow water / abundant macrophytes	Wetland	wet	2.9	0.8
3	wetland, permanent	Wetland	wet	2.6	1.5
4	wet to aquatic tundra (seasonal), abundant moss	Wetland	wet	3.5	3.4
5	moist to wet tundra, abundant moss, prostrate shrubs	~~Grassland~~ Graminoids	moist	1.3	0.9
6	dry to moist tundra, partially barren, prostrate shrubs	Lichen/Moss	dry	22.5	28.5
7	dry tundra, abundant lichen, prostrate shrubs	Lichen/Moss	dry	3.5	2.4
8	dry to aquatic tundra, dwarf shrubs*	~~Shrub tundra~~ Dwarf to low shrub tundraa	moist	0.9	0.2
9	dry to moist tundra, prostrate to low shrubs	~~Shrub~~ Dwarf to low shrub tundra	moist	7.5	9.2
10	moist tundra, abundant moss, prostrate to low shrubs	~~Shrub~~ Dwarf to low shrub tundra	moist	6.0	7.0
11	moist tundra, abundant moss, dwarf and low shrubs	~~Shrub~~ Dwarf to low shrub tundra	moist	8.5	11.6
12	moist tundra, dense dwarf and low shrubs*	~~Shrub~~ Dwarf to low shrub tundra	moist	1.3	0.7
13	moist to wet tundra, dense dwarf and low shrubs*	~~Shrub~~ Dwarf to low shrub tundra	moist	0.2	0.02
14	moist tundra, low shrubs	~~Shrub~~ Dwarf to low shrub tundra	moist	2.9	2.0
15	dry to moist tundra, partially barren	~~Shrub~~ Dwarf to low shrub tundra	moist	2.6	1.3
16	moist tundra, abundant forbs, dwarf to tall shrubs	~~Shrub~~ Dwarf to low shrub tundra	moist	1.6	1.5
17	recently burned or flooded, partially barren	~~Shrub~~ Dwarf to low shrub tundra	-	0.6	0.1
18	forest (deciduous) with dwarf to tall shrubs	Forest	-	0.3	0.2
19	forest (mixed) with dwarf to tall shrubs	Forest	-	0.5	0.3
20	forest (needle leave) with dwarf and low shrubs	Forest	-	0.1	0.1
21	partially barren	Barren	dry	14.5	16.3
22	snow/ice	Snow/ice	-	2.1	3.4
23	other (incl. shadow)	Other	-	2.3	1.6
nd	-	-	-	6.1	-

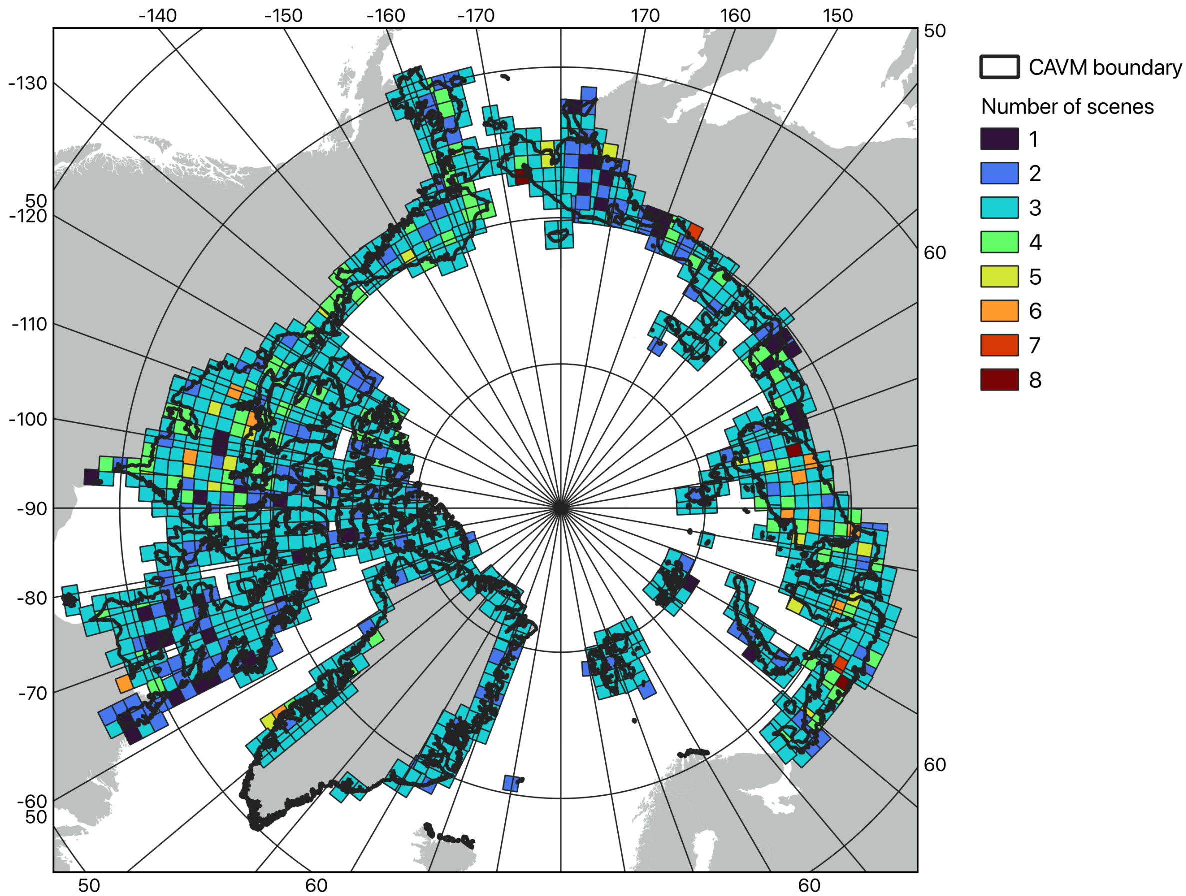

Figure 3. Number of ~~used~~ Sentinel-2 scenes used, by ~~granules~~ Sentinel granule, within ~~CAVM~~ the Circumpolar Arctic Vegetation map (Raynolds et al., 2019) boundary.

4.3 Characterization through in situ records

All ~~classes can~~ units could be assigned distinct vegetation compositions and water/mineral volumetric content (Table 3, Figures 4~~and 5~~, 5 and 6). There ~~are~~ were differences in in situ data availability between the landcover units which ~~need~~ needed to be considered. Soil data ~~are~~ were largely unavailable for forest and disturbed sites (Tables A2, A1). The dry tundra unit #7 which ~~has~~ had the most abundant lichen coverage ~~has only~~ had little pedon data but good vegetation description. Unit #13 ~~lacks~~ lacked both pedon and vegetation description as it represents vegetation along incised creek channels (moist tundra, dense dwarf and low shrubs, Figure B41) which ~~are~~ were rarely sampled. Soil samples for inundated areas (unit #2) ~~are~~ were unavailable. Vegetation samples for this ~~class~~ unit are expected to be located at the boundary of shallow water bodies with macrophytes, but in the same pixel. They ~~have been~~ were nevertheless included in the tables and figures. The lack ~~of soil wetness description~~

or very low samples of soil volumetric water content data for some units can (#2 and #7) could be partially compensated by general wetness information contained in the vegetation records (Figure 6).

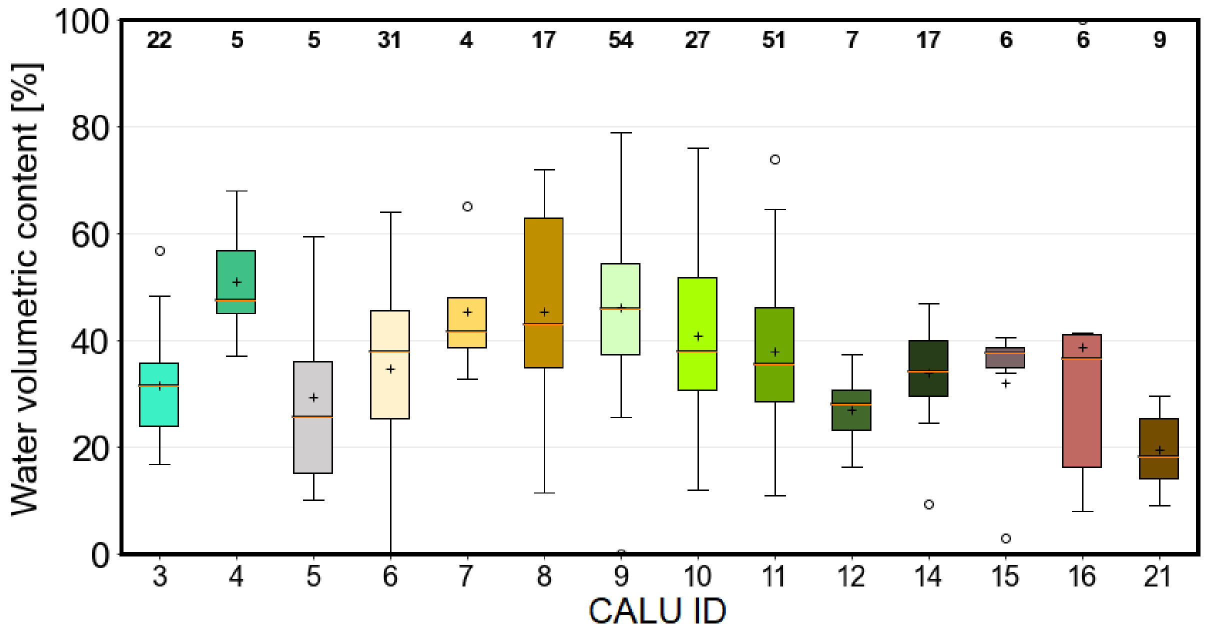

Figure 4. Volumetric water content statistics (box plot representing quartiles, median, mean as '+' and outliers as '°') for Circumarctic Landcover Units (CALU) based on (Palmtag et al., 2022)in situ data from Palmtag et al. (2022). Number of samples per unit are shown on top. For unit details and colors see Table 2.

4.3.1 Vegetation

Mosses and graminoids are were common across all units with moss being most dominant (48 % overall average coverage) and graminoids second (20 % overall average coverage) (Table 3). Lichens occur on average had on average only 12 % and are reaching more than cover, and had over 20 % cover only for units with comparably dry parts. Forbs are were less abundant except for one case, unit #16 for which the average is cover was 41 %. Mosses also show showed the highest standard deviation within the landcover units (Figure ??Table 3).

The 'Barren' unit #21 has had the highest bare ground fraction with on average 32 % for soil and 2 % for bare rock. Bare rock is was most common in unit #6 with 11 % cover.

Unit #2 represents shallow water along lakes and seashores which is are not are not well represented in the AVA or soil records . (see example in Appendix Figure B2). Vegetation and soil records (in case of organic layer thickness) are taken on land along the lake margins. Presence of open water in the proximity is reported in the AVA records in some cases (Figure B1). Macrophytes are abundant, emerging through the course of the summer season as observed during alternative field surveys

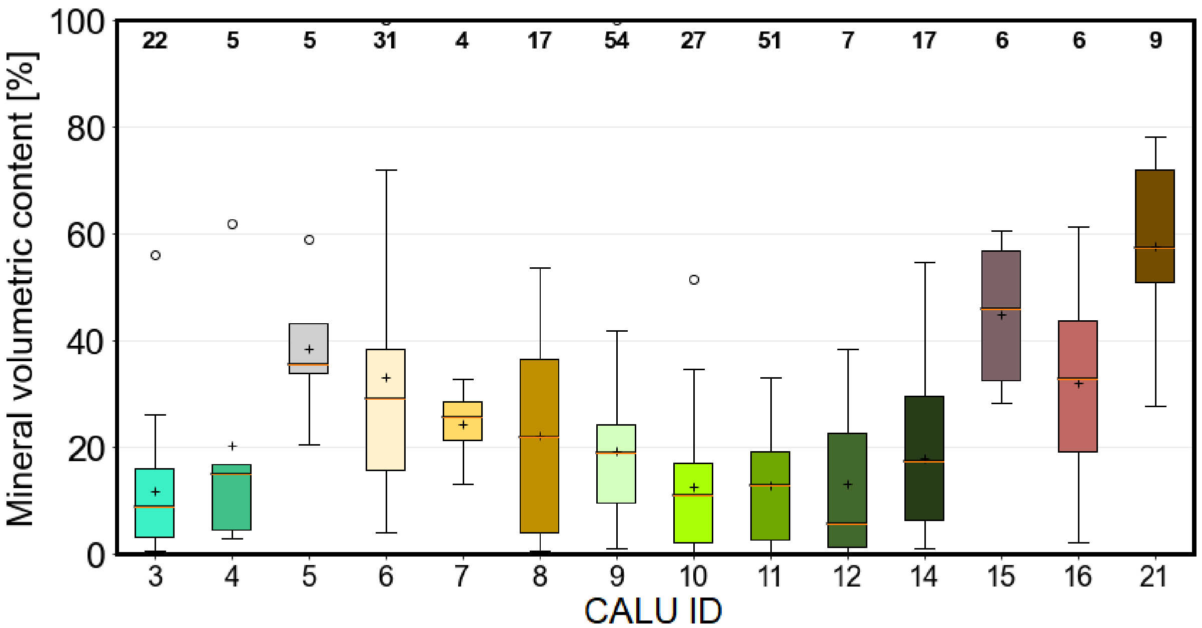

Figure 5. Mineral volumetric content statistics (box plot representing quartiles, median, mean as '+' and outliers as '°') for Circumarctic Landcover Units (CALU) based on (Palmtag et al., 2022)in situ data from Palmtag et al. (2022). Number of samples per unit are shown on top. For unit details and colors see Table 2.

(see photograph B3). The average open water fraction in the AVA records is mostly close to zero (Appendix B) except for #2 (7.5%), #3 (permanent wetland; 12%), #8 (dry to aquatic tundra; 7%) and #17 (recently burned area; 21%). Western Siberia Arctic Vegetation Archive average standard deviation of coverage within CAL units.

Several classes units with tall shrubs in proximity to the treeline also can include needle leave trees (needle-leave trees (#8, #12 and #13, see Table 3). The latter are of limited height and also diameter due to the harsh environment and is common for commonly occur in the North American treeline zone (Pictures B24 and B42). Areas These areas correspond to the 'woodlands' and 'open stands' definition level III according to Viereck et al. (1992) (10 to 24 % crown canopy cover, and 24 to 60 % respectively).

4.3.2 Soils

The units with a certain barren fraction (#6, #15 and #21, see Table 3) show showed all comparably high mineral volumetric content (Table 3 and Figure 5). Higher wetness (>40 % volumetric content on average) can could be found in permanent wetlands (#4) and several moist tundra units with differing types of shrub physiognomy. The permanent wetland class has one of the lowest standard deviations, the seasonal wetland class one of the highest representing homogeneous and heterogeneous conditions respectively. The number of available samples is, however, too low for generalization. The 'barren' unit is was most

Table 3. Average coverage of different lifeforms for each ~~unit for~~ Circumarctic Landcover Unit(CALU) based on Russian Arctic Vegetation Archive ~~types~~plots, Western Siberia (Zemlianskii et al., 2023).

Unit	**2**	**3**	**4**	**5**	**6**	**7**	**8**	**9**	**10**	**11**	**12**	**13**	**14**	**15**	**16**	**17**	**18**	**19**	**20**	**21 ~~Mean~~**
Number of Samples	51	56	47	68	412	142	85	354	348	293	78	20	193	95	181	7	29	18	45	95 ~~131~~
Tree layer	0	1	0	0	0	0	8	0	0	0	2	4	1	2	1	4	28	7	43	0 ~~5~~
Tall shrubs	3	3	0	0	0	0	2	1	0	1	2	5	1	0	10	0	11	26	2	0 ~~3~~
Low shrubs	4	2	1	1	5	3	8	11	7	19	36	23	21	4	17	6	13	26	10	3 ~~11~~
Erect dwarf shrubs	5	2	7	1	5	5	19	6	6	12	20	11	7	11	9	15	18	18	49	1 ~~11~~
Prostr. dwarf shrubs	11	6	9	14	11	13	6	13	15	10	5	8	6	8	4	0	1	1	1	10 ~~8~~
Graminoids	18	30	30	27	20	14	22	20	24	18	9	24	18	19	17	30	19	19	5	9 ~~20~~
Tussok graminioids	3	1	2	1	3	2	1	4	6	6	2	2	2	4	2	0	2	2	0	1 ~~2~~
Forbs	12	7	9	4	11	2	10	6	9	9	9	19	12	12	41	12	29	12	9	9 ~~12~~
Seedless vasc. pl.	3	3	0	1	1	1	3	1	2	1	1	3	2	1	4	0	11	5	1	5 ~~2~~
Mosses and liverw.	33	37	74	65	41	33	40	54	71	63	54	43	58	38	43	43	37	54	62	17 ~~48~~
Lichen	8	15	5	11	16	27	23	14	9	10	13	11	12	26	3	0	3	5	17	7 ~~12~~
Crust	3	9	2	0	2	6	1	2	1	1	1	1	1	1	0	0	1	1	0	2 ~~2~~
Algae	0	2	0	0	1	1	0	0	0	0	0	0	1	0	0	0	0	0	0	0 ~~0~~
Bare soil	9	4	2	1	3	11	3	3	1	1	4	1	2	4	2	21	0	3	0	32 ~~5~~
Bare rock	3	1	0	0	11	1	2	2	1	1	2	3	3	6	2	0	0	0	0	2 ~~2~~
Litter	9	22	14	24	8	10	22	13	18	11	14	15	11	9	17	25	43	15	22	3 ~~16~~

dry. Unit #16 ~~shows~~ showed the highest total nitrogen density values (Table A2) with at the same time comparably high mean organic layer thickness (Figure 7, Table A1) but only 6 pedon samples ~~are~~ were available.

~~SOC and TN are~~ Soil organic carbon (SOC) and total nitrogen (TN) were lowest for the 'Barren' unit (CALU #21, Table A2). Unit #10 and 11 (moist tundra, abundant moss and shrubs) ~~show~~ showed the highest SOC values with more than 35 $kgCm^2$.

AVA records which include wetness descriptions ~~show~~ showed in sum more than 50 % in the categories wet and aquatic in units #3, 4 and 8 (Figure 6). Unit 15 (dry to moist tundra, partially barren) also ~~has~~ had a comparably high fraction of moist and aquatic samples. The AVA records ~~complement~~ complemented the soil description for specifically unit #6 (only four pedon records). The AVA records ~~confirm~~ confirmed that it is a relatively dry landcover type.

4.4 Fire disturbance assessment

The majority of input data for the landcover classification ~~has been~~ was acquired between 2017 and 2020. The assignment to the disturbance unit #17 ~~does occur~~ occured up to four years after a burn event (Figure 8). A specific year ~~cannot~~ could not be determined in most cases due to averaging over up to three years. Burned areas from events before 2014 ~~are~~ were represented through other ~~classes~~ units (vegetation recovery).

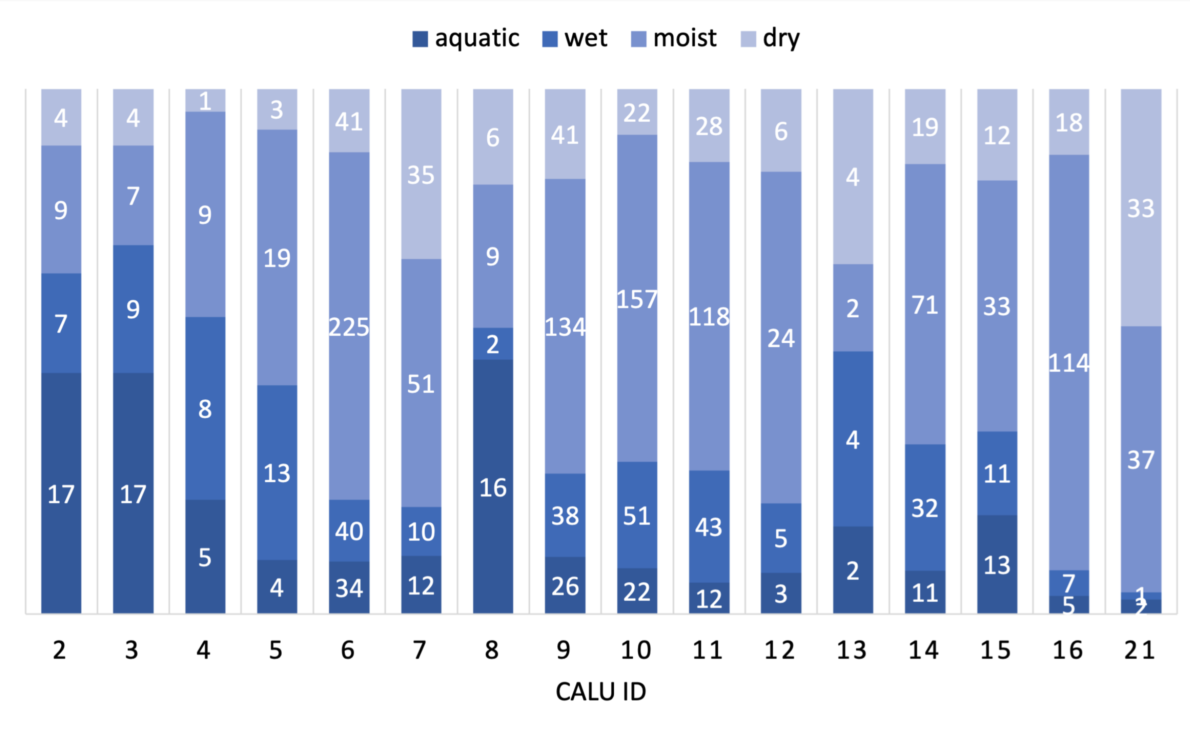

Figure 6. ~~Western Siberia~~ Wetness categories for Circumarctic Landcover Units (CALU) based on Arctic Vegetation Archive ~~wetness categories~~ plots, Western Siberia (~~only~~ Zemlianskii et al. (2023); units with at least 10 data points).

The disturbance unit #17 ~~occurs~~ occured within recently burned areas in approximately 72 % of all cases documented for Alaska. The majority of remaining unit #17 areas ~~occurs~~ occured along shorelines of lakes with varying extent. This ~~is~~ was specifically the case on the Alaskan North Slope (Figure 9).

4.5 Heterogeneity

Landcover diversity (richness based on fractions - at least 1 percent - within ~~1x1km areas) is~~ 1x1 km areas) was lowest in the higher Arctic and higher towards south (Figure 10). The average number of landcover units ~~ranges~~ ranged from 4 to 9, depending on the majority unit type. The barren unit dominated regions ~~have~~ had the lowest richness (Figure 11). 81 % of the CAVM extent had at least 1 % wetland within the 1x1 km cells (considering the sum of all types - units # 2, 3, and 4), but only 0.7 % were cells with pure wetlands. The average wetland fraction across the entire CAVM region was 8.8 %.

The CAVM class W3 (Sedge, moss, low-shrub wetland complex) ~~shows~~ showed the highest diversity with almost 9 units on average (Figure 12). In general, wetter regions ~~have~~ had a higher diversity than drier ones. This ~~can be also~~ could also be confirmed through the wetness group assessment. In 59 % of cases when wet types ~~are~~ were present, dry and moist ~~can~~ could be found at the same time~~(Figure 13 right). 45~~. 66 % of the CAVM extent ~~is~~ was heterogeneous regarding wetness (group sum

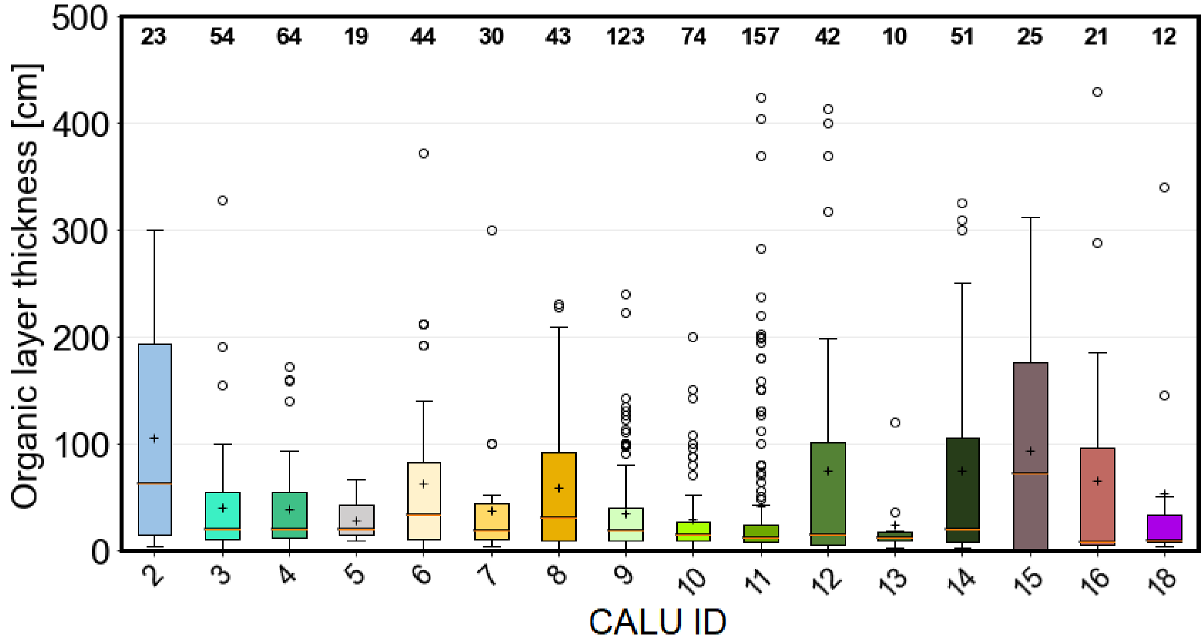

Figure 7. Soil surface organic horizon depth statistics for ~~classes~~ units with at least 10 data points. Box plot representing quartiles, median, mean as '+' and outliers as '°' for Circumarctic Landcover Units (CALU) based on in situ data. Number of samples per unit are shown on top. For unit details and colors see Table 2.

three, areas with no data excluded) and only ~~10~~12 % homogeneous (group sum one) (Figure 13 left). ~~81% of the CAVM extent has at least 1% wetland within the 1x1km cells (considering the sum of all types), but only 0.7% are cells with pure wetlands. The average wetland fraction across the entire CAVM region is 8.8%.~~ The fraction of areas with a sum of three reduced when the heterogeneous unit #6 was assigned to 'moist' instead of 'dry' but remained comparably high with 48 %.

4.6 Comparison with existing datasets

~~Distinct difference can~~ Subsets of selected regions in Western Siberia, Alaska and Canada were investigated. This included regions with dwarf to low shrubs with patches of wetlands (Figures 14 and 15) within the original prototype extent (see Figure 1). The prototype (20 m), CCI landcover (300 m), the CAVM (1km) and CALC-2020 (10 m) were compared with CALU (10 m). Distinct differences could be found between CALU and other landcover maps which ~~do not only relate~~ are not only related to the spatial resolution difference~~(Figures 14 and 15)~~. Wetland areas are considerably more extensive in the CALC-2020 (which is the only classification largely driven by terrain information) than in all other maps, including CALU. Wetlands are more extensive in CALU than in CCI landcover and CALC-2020 in the example from the Alaskan Coastal plain (Figure 16). Patterns are mostly similar for the example from the Tuktoyaktuk region (Figure 17). Only CALC-2020 differs, where graminoids dominate instead of dwarf to low shrubs.

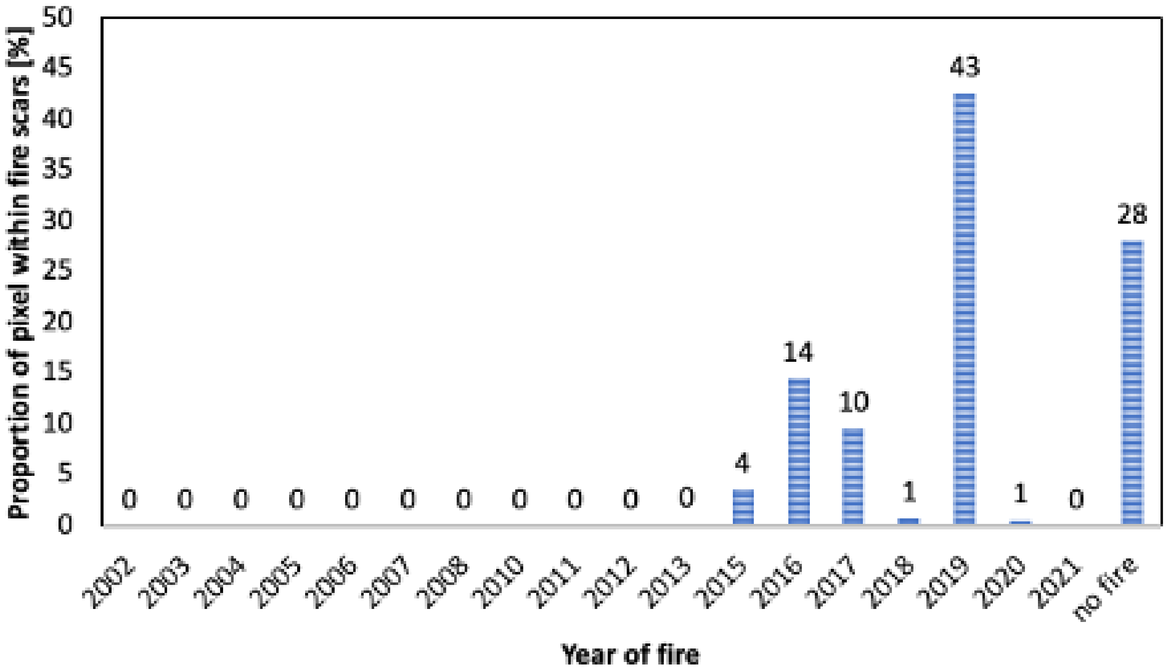

Figure 8. Year of fire for pixels in unit 17 (recently burned or flooded, partially barren) for Alaska (source: Alaska Fire database)

4.6.1 Prototype

Results well ~~demonstrate~~ demonstrated the resolution difference between the prototype with ~~20m~~ 20 m and the CALU with ~~10m~~ 10 m (Figure 18). The patchiness of shrub tundra ~~leads~~ lead to a reassignment to other vegetation ~~classes~~units. About 15 % of the dwarf to low shrub tundra group ~~have been~~ were reassigned to other groups, mostly to wetlands (5 %) and ~~grassland~~graminoids/lichen/moss (5 %). The new disturbance ~~classes result~~ units resulted in a shift of area from lichen/moss to the group barren (which ~~is~~ was largely only partially barren according to description of ~~CAL units~~ units (CALU)). Pixels originally classified as disturbed ~~have been~~ were assigned to vegetation ~~classes.~~ units units, specifically #8 (dry to aquatic tundra, with 42 %; Figure D1). The maximum fraction of a prototype class within a new unit ranged from 17 % (disturbed) to 96 % (water) and was on average 50 %.

4.6.2 Landcover CCI

The barren group of CCI Landcover ~~is~~ was predominant in all tundra vegetation groups of CALU (Figure 18). In case of the lichen/moss group of CALU, less than 30 % ~~are~~ were in the same group in CCI Landcover. Also the shrub and forest groups ~~are~~ were most abundant in shrub tundra and forest respectively. More than 88 % percent of the CCI Landcover group barren

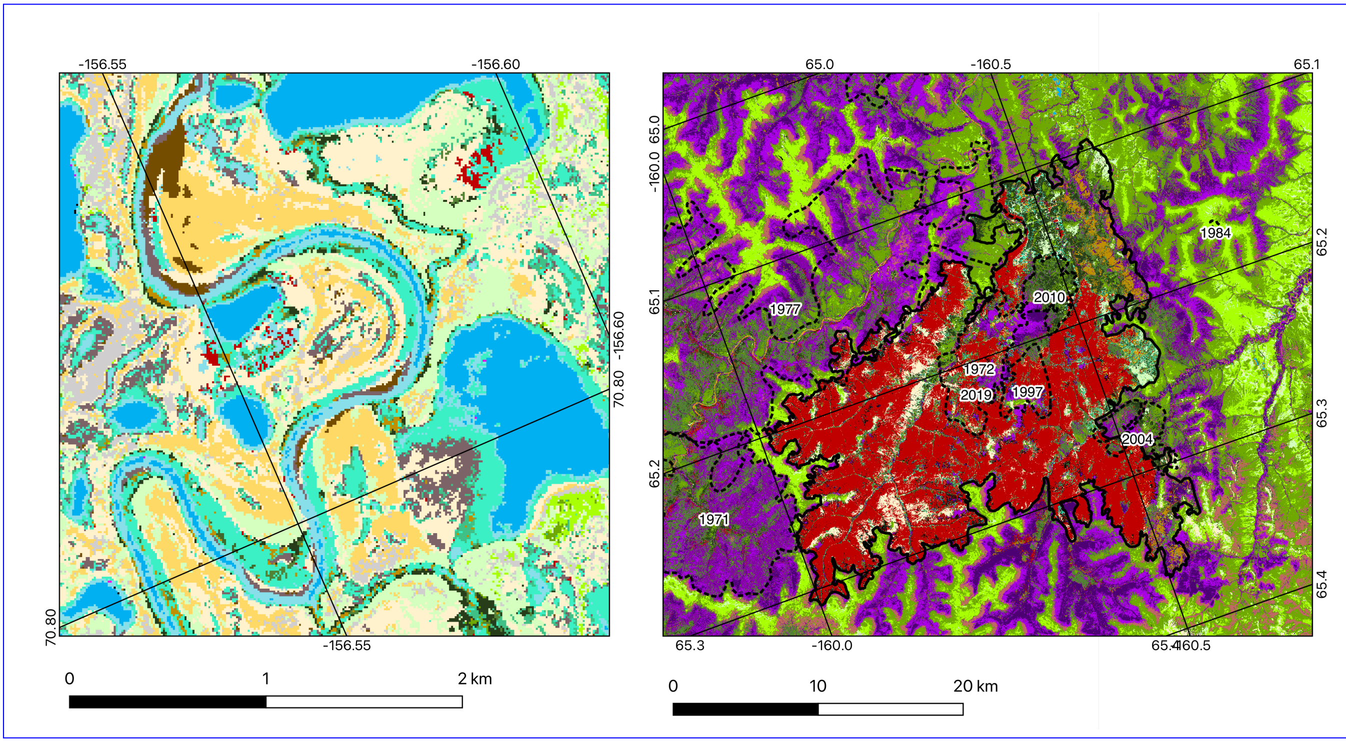

Figure 9. Examples for ~~class~~ CALU #17 'recently burned or flooded' (shown in red). Left: ~~Thaw lake~~ Lakes within a river floodplain on the Alaskan North Slope; right: Burned areas in southwestern Alaska (outlines and years from Alaska Fire Database). Dashed lines – boundaries of fires before 2019, bold line - fire extent 2019. For detailed legend see Table 2.

~~are~~ were actually characterized by vegetation (example maps in Figures 14 and 15). ~~63% are~~ 60 % were dwarf to low shrub tundra and about 9 % ~~grassland~~ graminoids and 16 % lichen/moss (Table ~~11~~4).

About 80 % of the CCI Landcover class forest ~~are~~ were in the shrub tundra group of CALU. The overlap ~~applies~~ applied specifically to unit 12 'dry to moist tundra, dense dwarf and low shrubs'. Low shrubs ~~are~~ were abundant and very dense in the proximity to the treeline (see picture in B39).

4.6.3 CAVM

The shrub tundra group of the CAVM ~~is~~ was present with more than 40 % in all CALU groups (Figure 18). This can be attributed largely to the spatial resolution difference. The spatial patterns ~~are~~were, however, similar (Figures 14 and 15)). Overlapping areas with the group forest ~~correspond~~ corresponded mostly to shrub tundra as the CAVM does not have a forest class. Less than 1 % of ~~CAL~~ CALU within the CAVM boundary ~~has been~~ was identified as mixed or needle leaf forest.

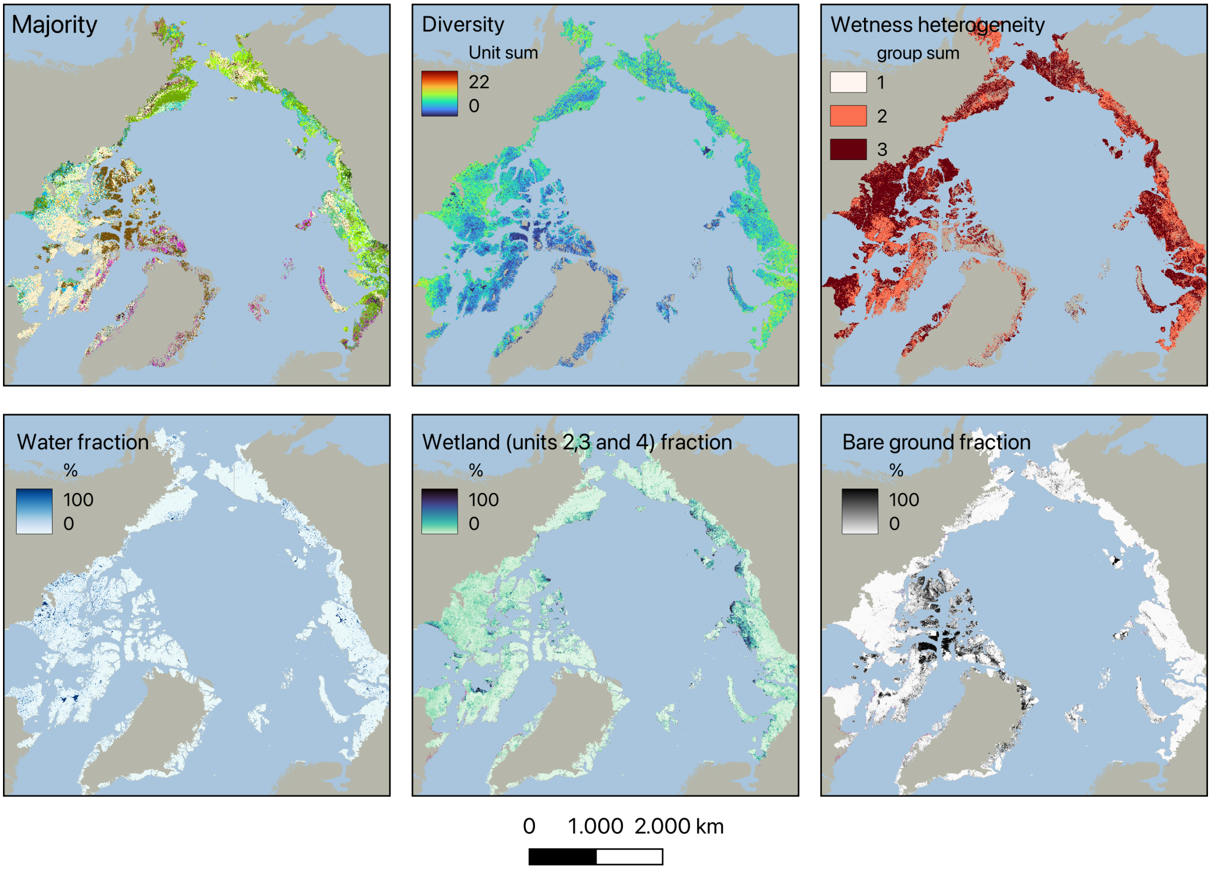

Figure 10. Statistics for ~~1x1km~~ CALU (10 m original resolution) for 1x1 km areas. For legend of majority, wetness groups and unit IDs see Table 2.

4.6.4 CALC-2020

There ~~is~~ was a substantial mismatch between the two datasets for the group 'dwarf to low shrub tundra' and 'wetland' (Figure 18). About 80 % of this group ~~has been labeled as grassland~~ was labeled as graminoids and most of the remaining part to wetland in the CALC-2020. Large proportions of wetlands ~~are~~ were also found in the CALU groups lichen/moss as well as forest as a larger proportion of the landscape.

~~A comparison of CALC-2020 with the CAVMhas been made for further investigation of the differences (Figure ??) . Similar to CALU, CALC-2020 grassland is found most abundant in the CAVM group shrub tundra. Also the proportion of the wetland class in the groups grassland and shrub tundra are high . The analyses by CALC-2020 group (Figure ??b) shows a high proportion of CAVM shrub tundra in all groups and especially grassland. The spread of tundra shrubs across all classes is similar to the comparison with CALU (see Figure 18) as this can be attributed partially to the resolution difference. But in case of grassland it is much higher (about 90% for CALC-2020 (Figure ??) compared to about 50% for CALU.~~

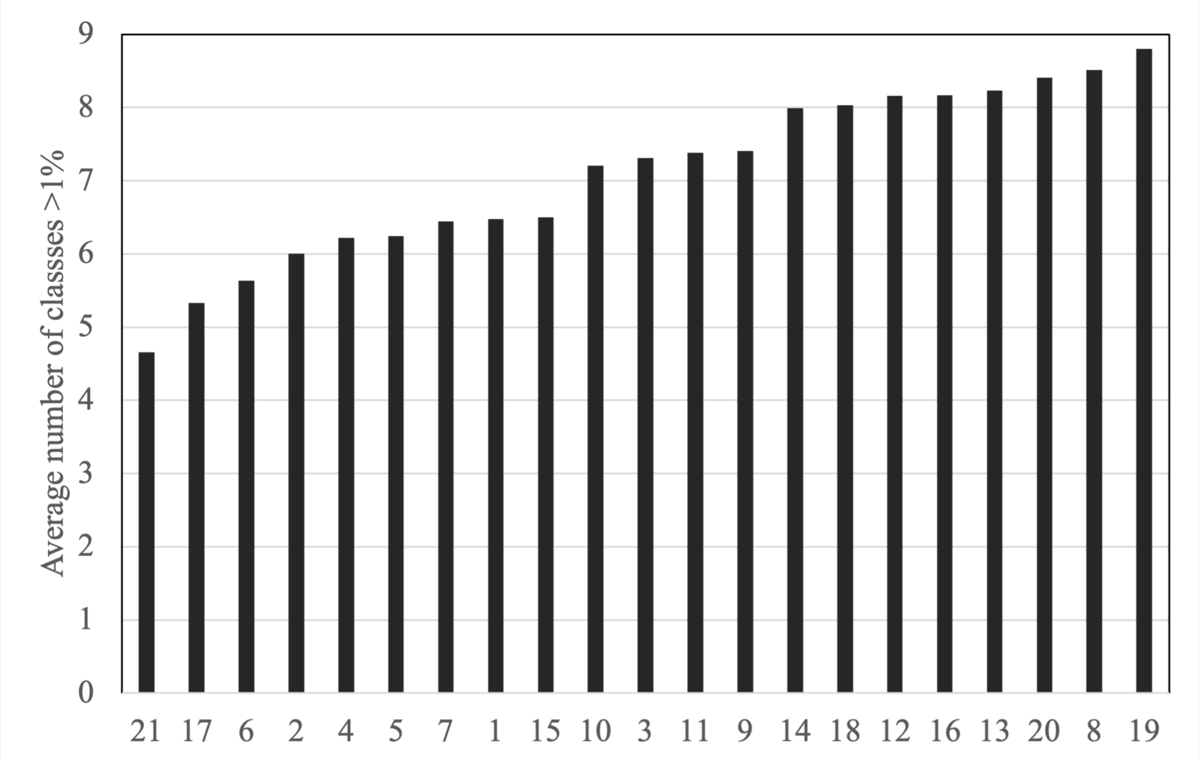

Figure 11. Diversity (average number of ~~CAL Units~~ units (CALU) within ~~1km~~ 1 km x ~~1km~~ 1 km cells) versus majority, for unit IDs see Table 2. Sorted by diversity.

~~Since dwarf and low shrubs are very common over the evaluation region, there is a widespread mismatch (Figure 15) . Comparison for landcover groups – CAVM versus CALC 2020. For grouping schemes see Tables C2 and C3.~~

5 Discussion

~~The high richness for shrub tundra and wetland complexes (as defined in the CAVM) underlines the importance of spatial resolution and need for thematic content. The largest differences in class assignment between the prototype with 20m and the new version with 10m occurred also for the shrub tundra groups what reflects the high heterogeneity. Especially wetlands~~

5.1 Adjustment of the prototype retrieval scheme

The high richness for shrub tundra and wetland complexes (as defined in the CAVM; figure 12) underlines the importance of spatial resolution and need for thematic content. The prototype was developed at 20m nominal spatial resolution as also the 20m-bands of Sentinel-2 have been used to better exploit the spectral capabilities. In this study a super-resolution approach

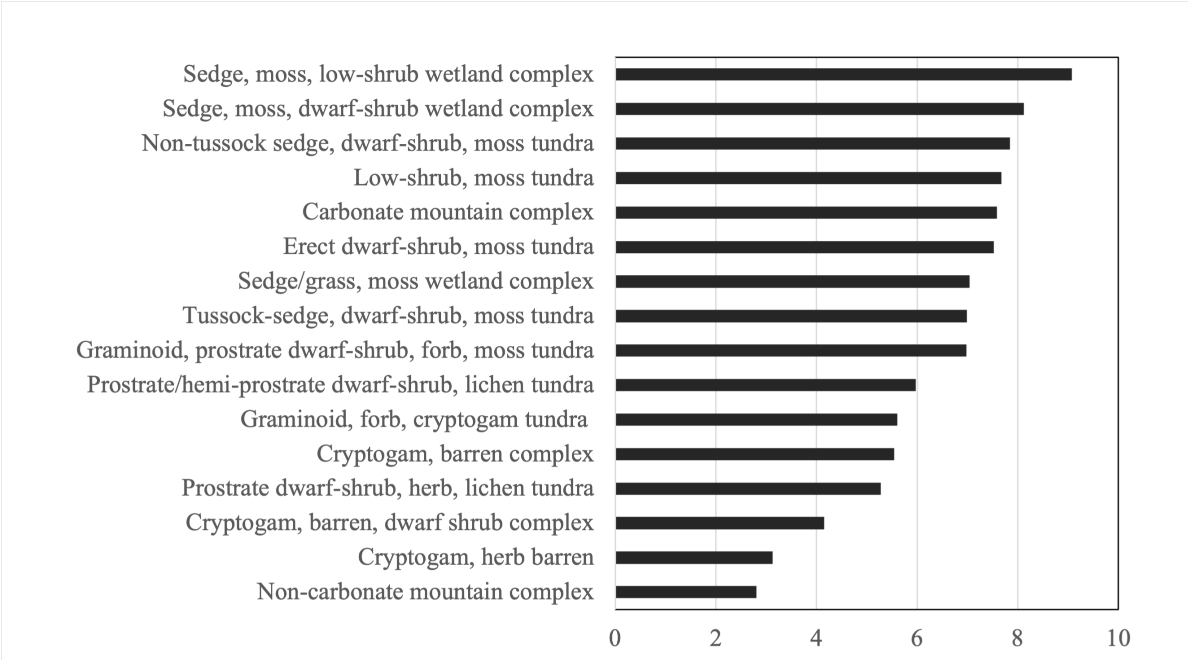

Figure 12. Landcover diversity for CAVM (Circum Arctic vegetation map (Raynolds et al., 2019)) classes: average number of CAL Units units (CALU) within 1km 1 km x 1km 1 km cells.

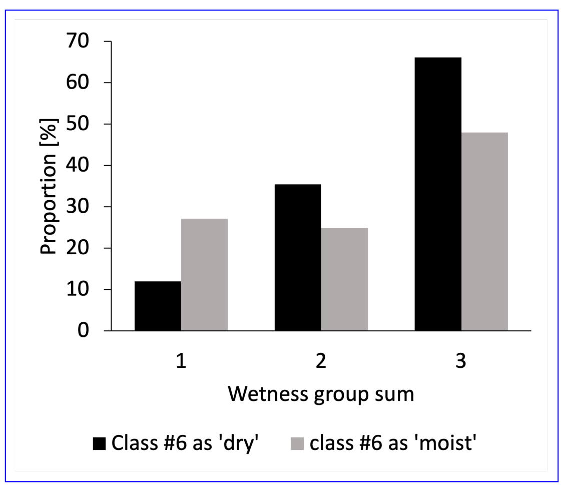

Figure 13. Wetness diversity within 1km 1 km x 1km 1 km areas (sum of groups B: dry, moist, wet; see Table 2; minimum 1% fraction for each type), (left) all CAVM (Circum Circumpolar Arctic vegetation map Vegetation Map (Raynolds et al., 2019)) region , (right) spatial subset for group B excluding areas with 'wetno data'(see Table 2).

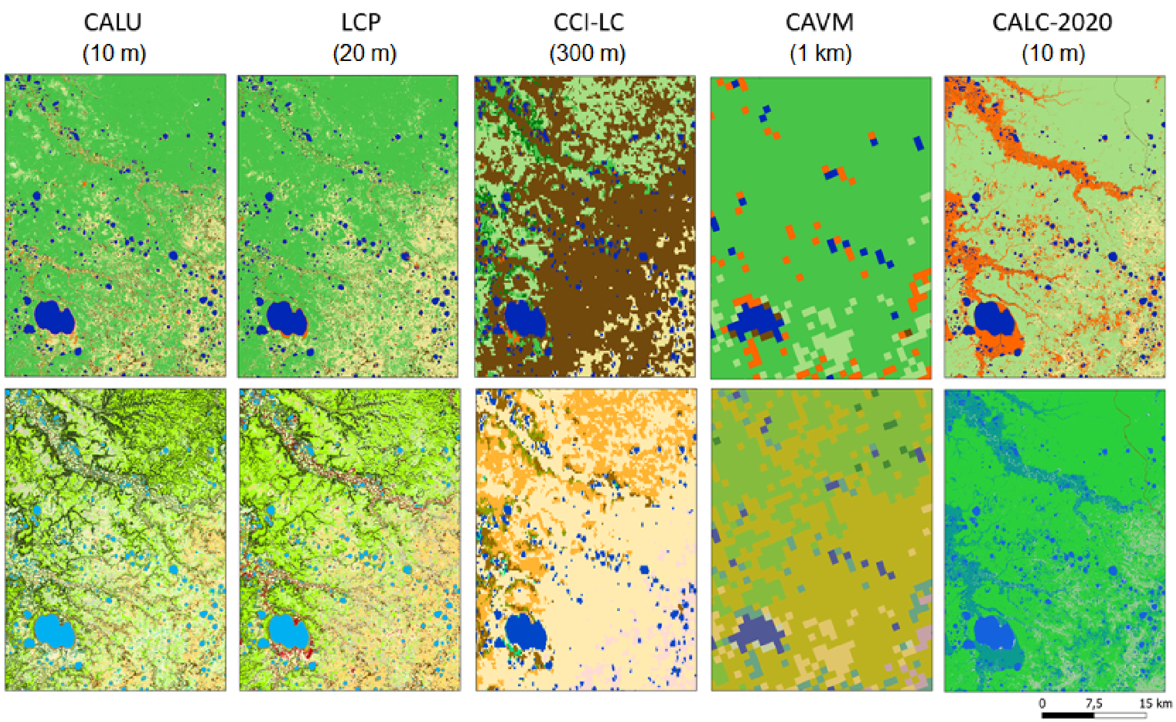

Figure 14. Comparison across all evaluated products for a region dominated by shrub tundra with patches of wetland .(CALU - Circumarctic Landcover Units, LCP refers to the - landcover prototype, CCI-LC - Climate Change Initiative - Landcover, CAVM - Circumpolar vegetation map, CALC - Circumarctic landcover 2020). Upper row- grouped classes (with name of source and spatial resolution), lower row – original classes (for detailed legend see Tables 1, 2, C1, C2 and C3). For location see Figure 1 (number 1).

(convolutional neural networks) adjusted to Arctic environments was now applied to bring these bands to 10 m. Nevertheless, the higher original resolution might contribute to issues in unit representation at 10 m due to the high heterogeneity.

The re-assignment of the units between the prototype and CALU reflects the high heterogeneity. The largest differences in unit assignment between the prototype with 20 m and the new version with 10 m occurred for the shrub tundra groups (Figure D1). The splitting of the 'disturbed' unit into two resulted in re-assignments across more types than initially foreseen (Figure D1). Pixels were also re-assigned to wetlands, the heterogeneous unit #8 (dry to aquatic tundra) and unit #6 (dry to moist prostrate shrub tundra, partially barren) in addition to the new units #15 (dry to moist tundra, partially barren) and #17 (disturbed, including burned areas). #15 consists now also of areas previously assigned to #6. All partially barren units might potentially include disturbed areas, e.g. wind blown sands and landslide scars as common across the Yamal peninsula.

5.2 Expansion of the approach across the Arctic

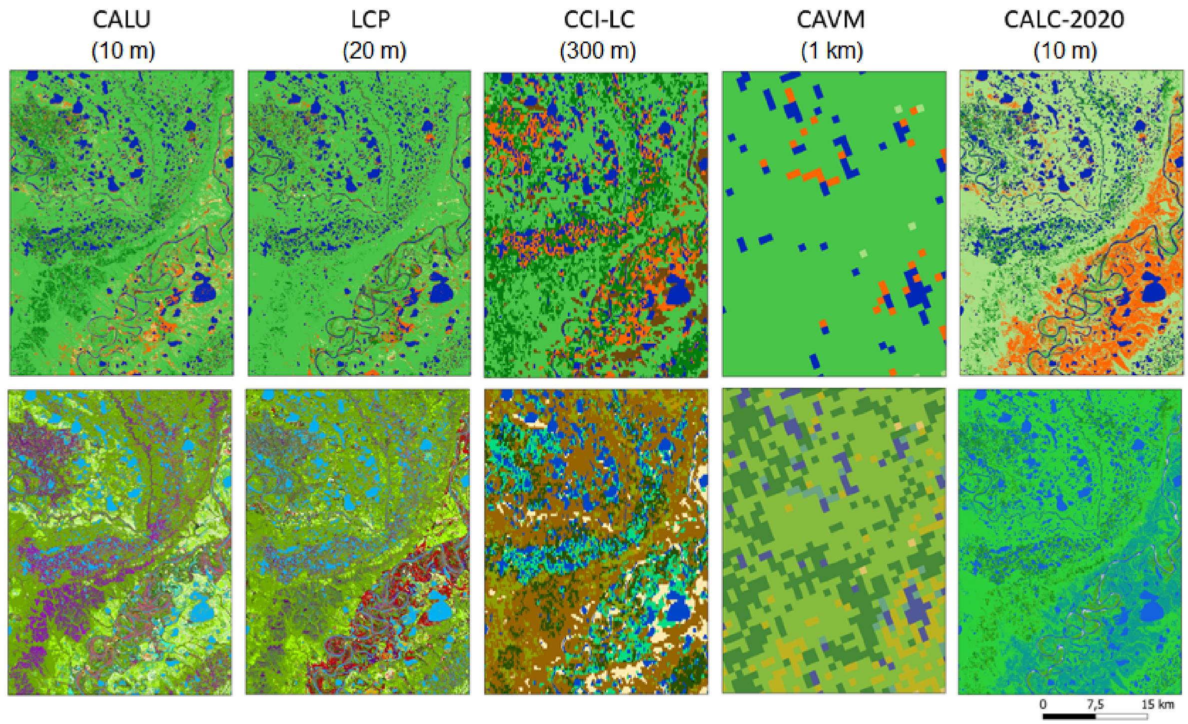

Figure 15. Comparison across all evaluated products for a region dominated by shrub tundra with patches of forest and wetland -(CALU - Circumarctic Landcover Units, LCP refers to the - landcover prototype, CCI-LC - Climate Change Initiative - Landcover, CAVM - Circumpolar vegetation map, CALC - Circumarctic landcover 2020). Upper row- grouped classes (with name of source and spatial resolution), lower row – original classes (for detailed legend see Tables 21, 2, C1,C2 and C3). For location see Figure 1 (number 2).

Environmental conditions distinct from Western Siberia occur specifically where coastal plains and river deltas can be found. Example comparisons with other circumpolar/global maps for the Alaskan North Slope (coastal plain) and the Canadian Tuktoyaktuk peninsula document nevertheless similar results as for Western Siberia.

Regional maps which offer comparably high thematic content are available specifically for North America. These are, however, based on Landsat. The lower spatial resolution (30 m) does therefor limit the applicability for cross-validation on their basis. Several units are expected to be assigned to the classes due to landcover heterogeneity. Examples are provided in supplement Figures 2 and 3.

The high number of units requires cloud free Sentinel-2 at the peak vegetation season. Several years are therefore needed to assemble the circumpolar mosaic. Ingested images span a wide range of acquisition years which may limit application of landcover change studies. Such analyses should be carried out only locally and the documentation of acquisition dates consulted. In addition, years can differ regarding landsurface hydrology and vegetation state. Wet years with flooding and dry years leading to drought are expected to impact the detectability of specifically the wetland units. Haze caused by forest fires

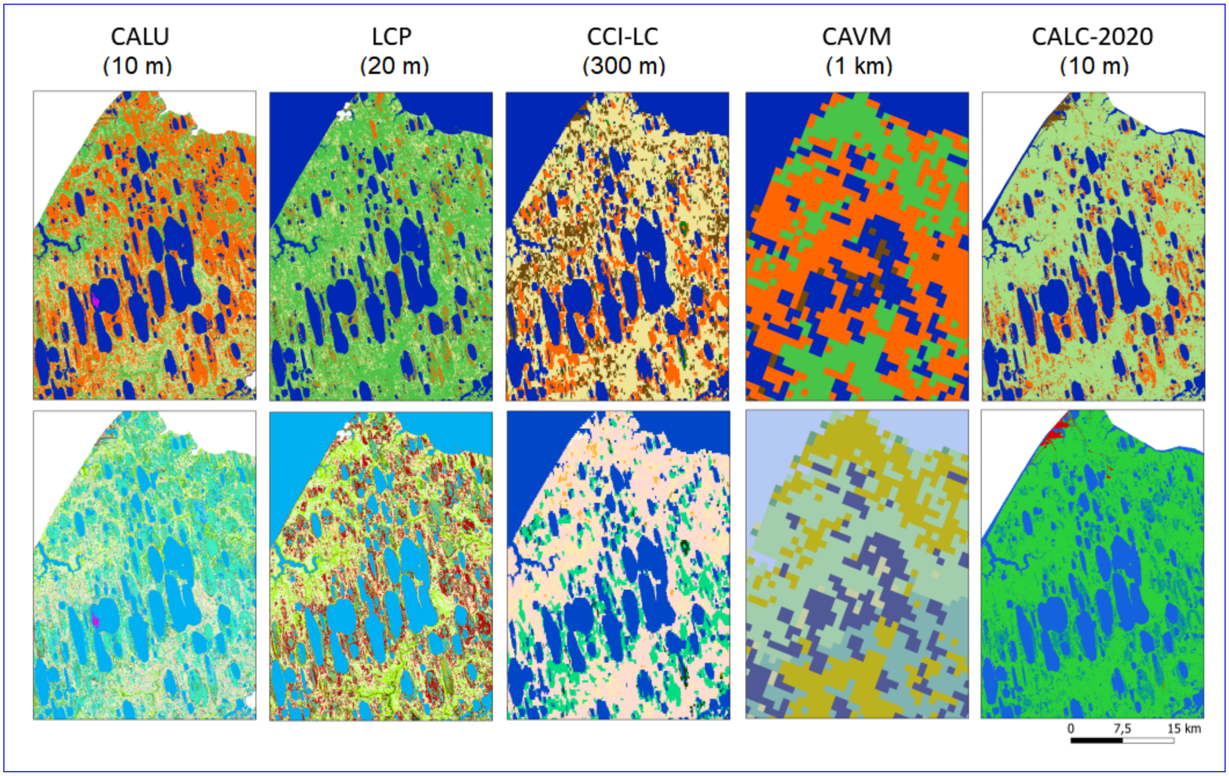

Figure 16. Comparison across all evaluated products for a region dominated by wetlands and lakes (CALU - Circumarctic Landcover Units, LCP - landcover prototype, CCI-LC - Climate Change Initiative - Landcover, CAVM - Circumpolar vegetation map, CALC - Circumarctic landcover 2020). Upper row- grouped classes (with name of source and spatial resolution), lower row – original classes (for detailed legend see Tables 1, 2, C1,C2 and C3). For location see Figure 1 (number 5)

465 in general cannot be corrected with the tools used. Affected scenes can not be used. This reduces the number of usable scenes considerably, as fires are abundant and smoke is transported to the tundra area.

Issues with wrong assignment are common for lakes in the northern parts. Late floating ice fragments are identified as ice/snow instead of open water. Lakes may also be missing in regions close to the coastline where the Copernicus DEM contained zero or no data. Tree species typical for forest occur with reduced size, crown diameter and sparse distribution in the transition zone. Several units which include low shrubs may therefore also include trees.

The current CALU version and presented analyses do not distinguish between natural and artificial barren areas, but a dataset which can be used for separation is available Bartsch et al. (2021a, b). It was derived from Sentinel-1/2 at 10 m nominal resolution. The fraction of artificial areas over the analyses region is, however, comparably small, < 0.02 % versus an overall barren fraction of 14.5 % (Table 2).

5.3 Separation of wetlands

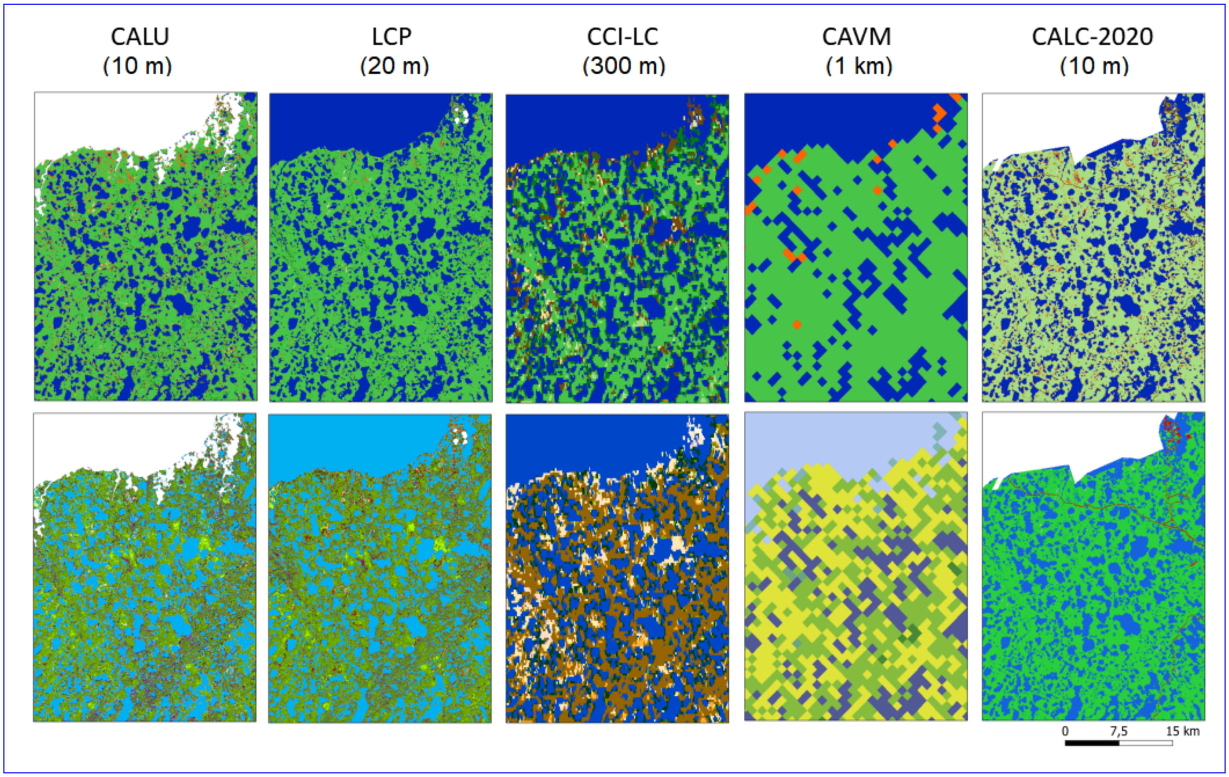

Figure 17. Comparison across all evaluated products for a region dominated by shrub tundra and lakes (CALU - Circumarctic Landcover Units, LCP - landcover prototype, CCI-LC - Climate Change Initiative - Landcover, CAVM - Circumpolar vegetation map, CALC - Circumarctic landcover 2020). Upper row- grouped classes (with name of source and spatial resolution), lower row – original classes (for detailed legend see Tables 1, 2, C1,C2 and C3). For location see Figure 1 (number 6).

Wetlands (in addition to lakes from lakes (Matthews et al., 2020)) are of high relevance for permafrost studies as dry and wet moisture gradients determine carbon fluxes, specifically potential release of methane. The three wetland types represent distinct environments with respect to hydrology and nutrient status. The TN density of #3 (permanent) is lower than for #4 (seasonal) (Table A2). Unit #2 represents permanent inundation. In addition, landcover unit composition and spatial patterns may allow for separation of different wetland types. Especially unit #8 is expected to be very heterogeneous and to include inundated parts (see AVA records in Figure B21). Figure 19 provides examples for different patterns of wetland classesunits. Drained lake basin composition is distinct from wet sites in areas dominated by peat bogs. The high spatial and thematic detail that CALU provides potentially allows for space for time approaches of impact assessment of permafrost related landcover change in addition to classical vegetation index trend analyses, e.g. Nitze et al. (2018); Foster et al. (2022).

The comparison to

5.4 Implications for estimating soil organic carbon and wetland extent across the Arctic

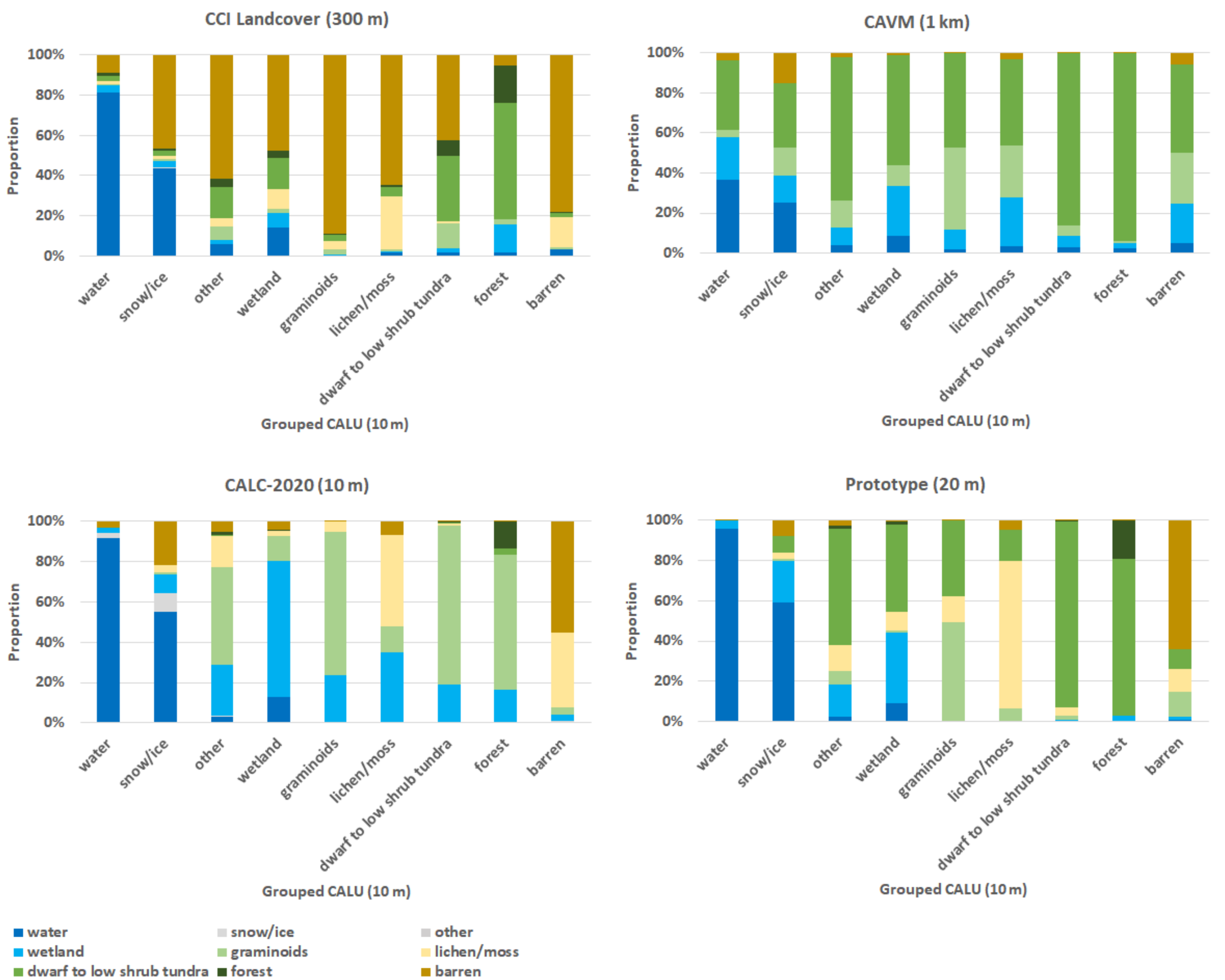

Figure 18. Proportion of grouped Landcover CCI, CAVM, CALC-2020 and prototype classes within grouped CAL Unitsunits (CALU). For grouping schemes see Tables 2 and C3. Matrices are provided in Tables 4, C4, C5 and as Sankey diagram in case of the prototype (Figure D1).

Previous studies used Landcover CCI for estimation of wetland area and soil organic carbon content across the Arctic, but concerns were raised Palmtag et al. (2022). The comparison between CALU and Landcover CCI confirms previous assessments based Landsat derived a previous assessment which used Landsat-derived regional landcover maps (Bartsch et al., 2016a). The thematic content does not match tundra specific landscape types. The barren fraction is in general too large. A large proportion is covered by low vegetation. Palmtag et al. (2022) calculated an

Table 4. Comparison matrix of grouped Climate Change Initiative - CCI Landcover classes and grouped ~~CAL~~ units (Circumarctic Landcover Units - CALU). Values in percent. For grouping schemes see Tables 2 and C1.

		CCI Landcover								
		water	**snow/ice**	**other**	**wetland**	**graminoids**	**lichen/ moss**	**dwarf to low shrub tundra**	**forest**	**barren**
CALU	**water**	65.50	0.45	28.74	7.65	0.18	2.07	0.68	1.35	1.24
	snow/ice	0.50	9.68	0.53	0.10	0.01	0.03	0.01	0.02	0.09
	other	0.65	13.69	0.24	0.65	0.64	0.67	0.51	0.59	1.14
	wetland	15.26	1.14	13.55	20.65	2.12	16.43	4.90	4.77	8.76
	graminoids	0.32	0.00	0.03	0.24	1.44	4.20	0.52	0.56	9.47
	lichen/moss	2.60	47.97	0.10	2.57	1.28	58.38	2.04	1.64	15.97
	dwarf to low shrub tundra	13.53	1.21	40.25	49.63	93.09	13.30	82.50	79.40	60.09
	forest	0.95	0.85	16.51	18.33	1.13	0.02	8.71	11.54	0.46
	barren	0.69	25.01	0.05	0.18	0.11	4.90	0.12	0.14	2.80

Palmtag et al. (2022) used Landcover CCI for upscaling of soil organic carbon. Soil probe data were linked with the landcover units. An average of more than 9 kg C m-2 over the top meter was calculated for the barren classes, which is much higher than in the CALU assessment (2 kg C m-2) due to ~~the inclusion of areas with~~ occurrence of in situ sites representing organic soils in the Landcover CCI barren class. ~~The agreement for~~

The agreement between the wetland classes ~~is similar as was found in (Palmtag et al., 2022), with~~ of Landcover CCI and CALU was very low what confirms the assessment based on in situ observations by Palmtag et al. (2022) (20.65 % (Table 4) and 19 % respectively). This has implication for further use as for example in case of wetland map creation such as in Olefeldt et al. (2021). Palmtag et al. (2022), with reference to Hugelius et al. (2020), suggest a four times larger permafrost wetland area. The underestimation of wetland extent in Landcover CCI can be confirmed with CALU. Just within the extent of the CAVM, our estimate ~~is larger with~~ (1.16 Mio km^2) is larger than the Landcover CCI fraction for the entire high latitude permafrost domain ~~with~~ (1.01 Mio km^2).

The use of terrain information in the retrieval as in the CALC-2020 dataset leads to overestimation of wetland areas in valleys (Figures 14 and 15) and drained lake basins (Figure 19). The heterogeneity in those areas is lost in this case. In total, more area is, however, characterized by wetland in CALU. This might be attributed to the inclusion of shallow water bodies ~~.~~ ~~The classification of areas with shrubs (80% of shrub tundra as defined in CALU)as graminoid tundra leads to differences in dominating class. The most common class of CALU is 'moist tundra, abundant moss, prostrate shrubs' instead.~~ with abundant macrophytes (unit #2).

~~The high number of classes requires cloud free Sentinel-2 at the peak vegetation season. Several years are therefore needed to assemble the circumpolar mosaic. Ingested images span a wide range of acquisition years which may limit application~~

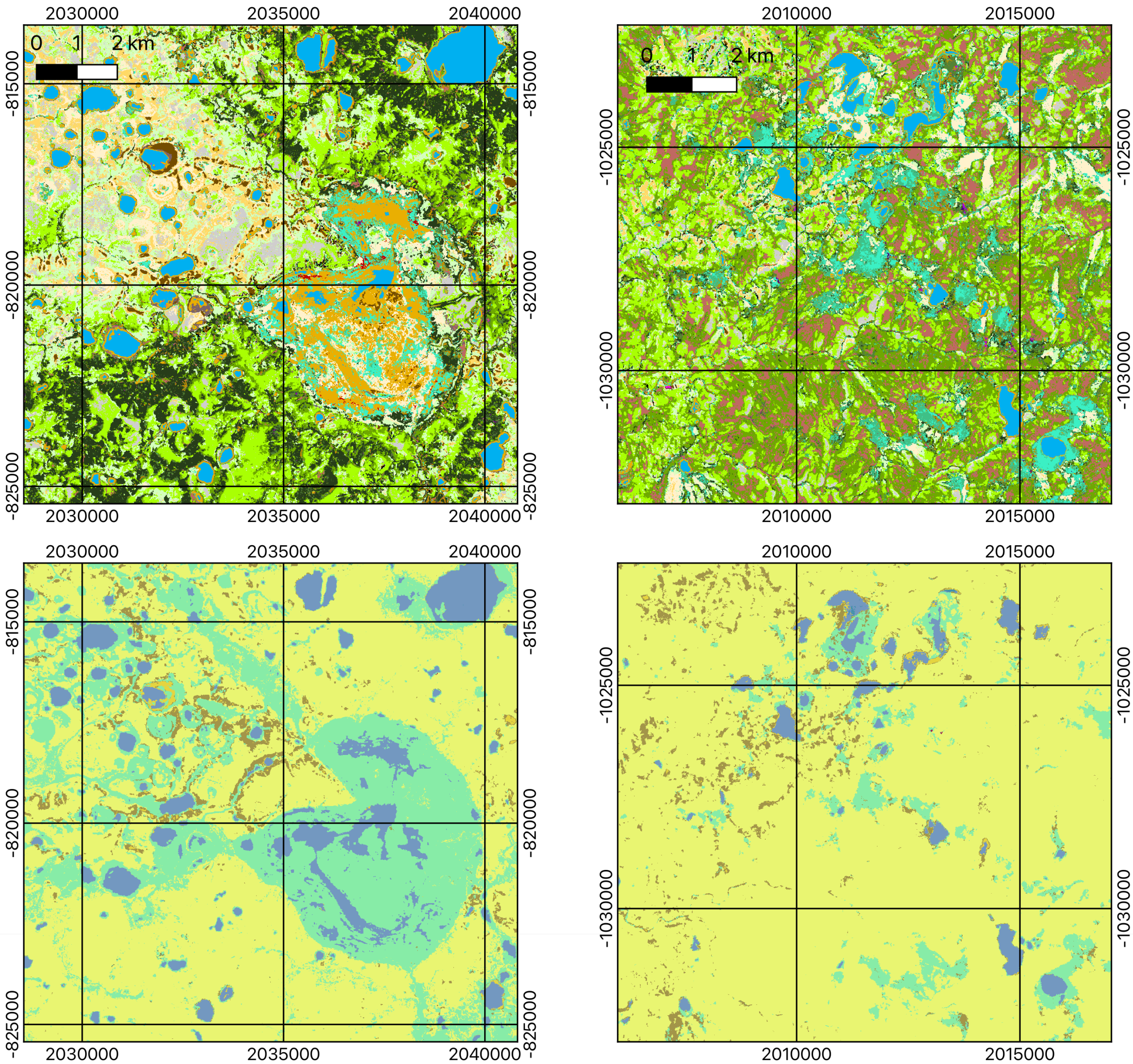

Figure 19. Examples for different wetland types: left - drained lake basins on central Yamal in the tundra zone, right - peat bogs in the hypo-Arctic tundra zone of Western Siberia. top: CALU - for legend see Table 2, bottom: CALC-2020 ((Liu et al., 2023), blue - open water, turquoise - wetland, grey - lichen/moss, light green - graminoid tundra). For detailed legend see Table 2.

~~of landcover change studies. Such analyses should be carried out only locally and the documentation of acquisition dates consulted. In addition, years can differ regarding landsurface hydrology and vegetation state. Wet years with flooding and dry~~

years leading to drought are expected to impact the detectability of specifically the wetland classes. Haze caused by forest fires in general cannot be corrected with the used tools. Affected scenes can not be used. This reduces the number of usable scenes considerably, as fires are abundant and smoke is transported to the tundra area.

5.5 Description of units with in situ records

Although that a very high number of in situ data was were available (almost 40 times more vegetation sites than used for the CALC-2020 assessment (Liu et al., 2023)), more is needed for full characterization of Arctic landscapes. There The used vegetation records represent sites across western Siberia only. The available soil data were collected from regions spread across the Arctic, but there is a lack of soil data (organic layer thickness) for barren areas, and unit #13 (dense shrubs) as it is less common and more difficult to access. The latter also applies to the shallow water wetland class unit (#2) as it is aquatic and thus usually not part of terrestrial vegetation surveys. This class unit might be, however, important for upscaling of methane fluxes. Soil data availability largely represents unit abundance. The most soil data are available for the second most common unit (#11), but much less for the most abundant class unit (#6) what is most likely due to the comparably low organic carbon content and occurrence in high Arctic regions. Soil sampling usually targets soil carbon quantification. Shrub tundra types are in general well sampled (more than 50 % of records). Probes for organic layer thickness come largely from selected environments, often river floodplains (e.g. Lena Delta, Kytalyk) or drained lake basins (e.g. Alaskan North slope). Data for wet unit types (#3-5) come mostly from these type of sites. Paludification is therefore comparably low. OLD was thus rather low for these units. Unit #15 had rather high OLD (Figure 7), but only 25 samples and with a high spread and high mineral volumetric content. In addition to use of more in situ data and region specific retrieval, a stratified random selection of soil probes representing a diversity of settings might be eventually required to allow upscaling of soil properties.

Issues with wrong assignment are common for lakes in Several units represent divers moisture gradients according to the in situ comparison. This applies specifically to #8. This demonstrates that the 10 m are insufficient to fully resolve Arctic landcover heterogeneity, confirming Virtanen and Ek (2014), Siewert et al. (2015) and Treat et al. (2018). There are also uncertainties in geolocation of both the satellite product and the in situ data. The representation of the in situ description for the northern parts. Late floating ice fragments are identified ice10x10 m is also an issue. This mismatch may play a role for the spread of properties within a unit and results in the fuzzy/snow instead of open water. Lakes may also be missing in regions close to the coastline where the Copernicus DEM contained zero or no data. Tree species typical for forest occur with reduced size, crown diameter and sparse distribution in the transition zone. Several unitswhich include low shrubs may therefore also include treesbroad naming of the units.

The current CALU version and presented analyses does not distinguish between natural and artificial barren areas, but a dataset which can be used for separation is available Bartsch et al. (2021a, b). It was derived from Sentinel-1Group assignment was moist in most cases where dry to moist conditions have been observed using both AVA and soil pedon records except for #6. This has been justified based on the comparably high coverage with lichen and relatively low soil water content/2 at 10m nominal resolution. The fraction of artificial areas over the analyses region is, however, comparably small, < 0.02 % versus an overall barren fraction of 14.5% (Table 2) high mineral content values in the pedon records. The previously published

CAWASAR (CircumArctic Wetlands based on Advanced Aperture Radar, Widhalm et al. (2015)) dataset offers also classes for dry, wet and moist. The majority of #6 areas coincides with the class 'dry' (see Supplement Figure 1) what confirms the validity of the group assignment. The comparison to the Alaska landcover map (Supplement Figure 3) also shows that 6 primarily occurs in upland and alpine landscapes.

5.6 Application potential

We are providing description examples based on a limited set of in situ records. Use of CALU subsets, especially outside of the regions with data availability as shown in Figure A1 might require use of additional in situ records, specifically regarding soil conditions including organic layer thickness.

The high spatial and thematic detail of CALU potentially allows for space for time approaches of impact assessment of permafrost related landcover change in addition to classical vegetation index trend analyses, e.g. Nitze et al. (2018); Foster et al. (2022) . Disturbances related to abrupt thaw features are widespread across the Arctic. For example vegetation is removed due to thaw slumping. Lakes drain and allow vegetation regrowth. Both results in specific vegetation succession patterns, not only regarding vegetation types but also wetlands (Wolter et al., 2024). This has implications for carbon cycling. CALU in combination with records of disturbance timing (representing different stages) may support the quantification of abrupt thaw impacts.

6 Conclusions

Tundra regions with wetlands are characterized by high landcover diversity, in addition to the high number of small lakes. Wet, moist and dry landscape types co-occur close to each other in most of the area north of the treeline. Pure wetland coverage over an extent of ~~1x1km~~ 1x1 km are rare. This is expected to be of relevance for any type of analyses related to carbon fluxes, including up-scaling, inversions or landsurface modelling.

Permafrost degradation features are known to lead to changes in landcover type and specifically wetness. For example drained lake basins and also fire scars represent fast changing environments in the years after events. The new circumpolar landcover unit map provides three types of wetland ~~classes~~ units in addition to 14 terrestrial tundra units covering barren area as well as different types of shrub physiognomy and soil moisture gradients at 10x10 m. This level of detail is unprecedented. Both, vegetation and soil type variations can be documented with extensive in situ datasets. Some landcover units with less extensive coverage, specifically disturbed sites (fires) are under-represented in available records.

The high thematic content requires good quality of input data. Although data availability from Sentinel-1 and -2 is good since 2016, the seven years of records ~~have not been~~ were not sufficient for complete coverage~~(1%)~~. Cloud coverage in case of Sentinel-2 and inconsistent acquisition strategies for Sentinel-1 lead to quality issues. Several years of Sentinel-2 ~~have been~~ were combined for robustness where sufficient acquisitions ~~have been~~ were available. This needs to be considered when combined with other records specifically with respect to ~~impact of~~ assessment of cryosphere change impacts on landsurface hydrology.

Data availability. The CALU dataset will be made openly available.

Author contributions. AB developed the concept for the study, analysed the results and wrote the first draft of the manuscript. KE and GH contributed to the in situ surveys, their compilation and analyses and to the writing of the manuscript. AE, BW, XM, CB processed the satellite data and contributed to in situ and other reference data statistical analyses. HB supported the postprocessing and analyses of results. BH and ML supported the interpretation and documentation of the results as well as writing of the manuscript.

Competing interests. The authors declare no competing interests.

Acknowledgements. This work was supported by the European Space Agency CCI+ Permafrost and AMPAC-Net projects, the European Research Council project No. 951288 (Q-Arctic), and has received funding under the European Union's Horizon 2020 Research and Innovation Programme under Grant Agreement No. 869471 (CHARTER).

We acknowledge all AVA data collectors for the western Siberia region, specifically Olga Khitun and Elena Troeva for photographs. We further acknowledge Mareike Wieczorek for provision of photographs from the Kolyma region.

References

Ackerman, D., Griffin, D., Hobbie, S. E., and Finlay, J. C.: Arctic shrub growth trajectories differ across soil moisture levels, Global Change Biology, 23, 4294–4302, https://doi.org/10.1111/gcb.13677, 2017.

Albuhaisi, Y. A. Y., van der Velde, Y., Jeu, R. D., Zhang, Z., and Houweling, S.: High-Resolution Estimation of Methane Emissions from Boreal and Pan-Arctic Wetlands Using Advanced Satellite Data, Remote Sensing, 15, 3433, https://doi.org/10.3390/rs15133433, 2023.

Ali, I., Cao, S., Naeimi, V., Paulik, C., and Wagner, W.: Methods to Remove the Border Noise From Sentinel-1 Synthetic Aperture Radar Data: Implications and Importance For Time-Series Analysis, IEEE Journal of Selected Topics in Applied Earth Observations and Remote Sensing, 11, 777–786, https://doi.org/10.1109/JSTARS.2017.2787650, 2018.

Bartsch, A., Höfler, A., Kroisleitner, C., and Trofaier, A. M.: Land Cover Mapping in Northern High Latitude Permafrost Regions with Satellite Data: Achievements and Remaining Challenges, Remote Sensing, 8, 979, https://doi.org/10.3390/rs8120979, 2016a.

Bartsch, A., Widhalm, B., Kuhry, P., Hugelius, G., Palmtag, J., and Siewert, M. B.: Can C-band synthetic aperture radar be used to estimate soil organic carbon storage in tundra?, Biogeosciences, 13, 5453–5470, https://doi.org/10.5194/bg-13-5453-2016, 2016b.

Bartsch, A., Leibman, M., Strozzi, T., Khomutov, A., Widhalm, B., Babkina, E., Mullanurov, D., Ermokhina, K., Kroisleitner, C., and Bergstedt, H.: Seasonal Progression of Ground Displacement Identified with Satellite Radar Interferometry and the Impact of Unusually Warm Conditions on Permafrost at the Yamal Peninsula in 2016, Remote Sensing, 11, 1865, https://doi.org/10.3390/rs11161865, 2019a.

Bartsch, A., Widhalm, B., Pointner, G., Ermokhina, K., Leibman, M., and Heim, B.: Landcover derived from Sentinel-1 and Sentinel-2 satellite data (2015-2018) for subarctic and arctic environments, https://doi.org/10.1594/pangaea.897916, 2019b.

Bartsch, A., Pointner, G., Ingeman-Nielsen, T., and Lu, W.: Towards Circumpolar Mapping of Arctic Settlements and Infrastructure Based on Sentinel-1 and Sentinel-2, Remote Sensing, 12, 2368, https://doi.org/10.3390/rs12152368, 2020.

Bartsch, A., Pointner, G., and Nitze, I.: Sentinel-1/2 derived Arctic Coastal Human Impact dataset (SACHI), ZENODO, https://doi.org/10.5281/ZENODO.4925911, 2021a.

Bartsch, A., Pointner, G., Nitze, I., Efimova, A., Jakober, D., Ley, S., Högström, E., Grosse, G., and Schweitzer, P.: Expanding infrastructure and growing anthropogenic impacts along Arctic coasts, Environmental Research Letters, 16, 115 013, https://doi.org/10.1088/1748-9326/ac3176, 2021b.

Bartsch, A., Strozzi, T., and Nitze, I.: Permafrost Monitoring from Space, Surveys in Geophysics, https://doi.org/10.1007/s10712-023-09770-3, 2023.

Bergstedt, H., Zwieback, S., Bartsch, A., and Leibman, M.: Dependence of C-Band Backscatter on Ground Temperature, Air Temperature and Snow Depth in Arctic Permafrost Regions, Remote Sensing, 10, 142, https://doi.org/10.3390/rs10010142, 2018.

Bergstedt, H., Bartsch, A., Neureiter, A., Hofler, A., Widhalm, B., Pepin, N., and Hjort, J.: Deriving a Frozen Area Fraction From Metop ASCAT Backscatter Based on Sentinel-1, IEEE Transactions on Geoscience and Remote Sensing, 58, 6008–6019, https://doi.org/10.1109/tgrs.2020.2967364, 2020.

Crist, E. P.: A TM Tasseled Cap equivalent transformation for reflectance factor data, Remote Sensing of Environment, 17, 301 – 306, https://doi.org/10.1016/0034-4257(85)90102-6, 1985.

Defourny, P., Lamarche, C., Brockmann, C., Boettcher, M., Bontemps, S., Maet, T. D., Duveiller, G. L., Harper, K., Hartley, A., Kirches, G., Moreau, I., Peylin, P., Ottlé, C., Radoux, J., Bogaert, E. V., Ramoino, F., Albergel, C., and Arino, O.: Observed annual global land-use change from 1992 to 2020 three times more dynamic than reported by inventory-based statistics, in preparation.

Dvornikov, Y., Leibman, M., Heim, B., Bartsch, A., Haas, A., Khomutov, A., Gubarkov, A., Mikhaylova, M., Mullanurov, D., Widhalm, B., Skorospekhova, T., and Irina, F.: Geodatabase and WebGIS project for long-term permafrost monitoring at the Vaskiny Dachi research station, Yamal, Russia, Polarforschung, 85, 107–115, https://doi.org/10.2312/polfor.2016.007, 2016.

ESA: Sentinel-1. ESA's Radar Observatory Mission for GMES Operational Services., Tech. rep., 2012.

ESA: Sentinel-2 User Handbook, Tech. rep., 2015.

Foster, A. C., Wang, J. A., Frost, G. V., Davidson, S. J., Hoy, E., Turner, K. W., Sonnentag, O., Epstein, H., Berner, L. T., Armstrong, A. H., Kang, M., Rogers, B. M., Campbell, E., Miner, K. R., Orndahl, K. M., Bourgeau-Chavez, L. L., Lutz, D. A., French, N., Chen, D., Du, J., Shestakova, T. A., Shuman, J. K., Tape, K., Virkkala, A.-M., Potter, C., and Goetz, S.: Disturbances in North American boreal forest and Arctic tundra: impacts, interactions, and responses, Environmental Research Letters, 17, 113 001, https://doi.org/10.1088/1748-9326/ac98d7, 2022.

Hersbach, H., Bell, B., Berrisford, P., Biavati, G., Horányi, A., Muñoz Sabater, J., Nicolas, J., Peubey, C., Radu, R., Rozum, I., Schepers, D., Simmons, A., Soci, C., Dee, D., and Thépaut, J.-N.: ERA5 hourly data on single levels from 1940 to present. Copernicus Climate Change Service (C3S) Climate Data Store (CDS), https://doi.org/DOI: 10.24381/cds.adbb2d47, 2023.

Hogstrom, E. and Bartsch, A.: Impact of Backscatter Variations Over Water Bodies on Coarse-Scale Radar Retrieved Soil Moisture and the Potential of Correcting With Meteorological Data, IEEE Transactions on Geoscience and Remote Sensing, 55, 3–13, https://doi.org/10.1109/tgrs.2016.2530845, 2017.

Högström, E., Heim, B., Bartsch, A., Bergstedt, H., and Pointner, G.: Evaluation of a MetOp ASCAT-Derived Surface Soil Moisture Product in Tundra Environments, Journal of Geophysical Research: Earth Surface, 123, 3190–3205, https://doi.org/10.1029/2018jf004658, 2018.

Hugelius, G., Bockheim, J. G., Camill, P., Elberling, B., Grosse, G., Harden, J. W., Johnson, K., Jorgenson, T., Koven, C. D., Kuhry, P., Michaelson, G., Mishra, U., Palmtag, J., Ping, C.-L., O'Donnell, J., Schirrmeister, L., Schuur, E. A. G., Sheng, Y., Smith, L. C., Strauss, J., and Yu, Z.: A new data set for estimating organic carbon storage to 3 m depth in soils of the northern circumpolar permafrost region, Earth System Science Data, 5, 393–402, https://doi.org/10.5194/essd-5-393-2013, 2013.

Hugelius, G., Strauss, J., Zubrzycki, S., Harden, J. W., Schuur, E. A. G., Ping, C.-L., Schirrmeister, L., Grosse, G., Michaelson, G. J., Koven, C. D., O'Donnell, J. A., Elberling, B., Mishra, U., Camill, P., Yu, Z., Palmtag, J., and Kuhry, P.: Estimated stocks of circumpolar permafrost carbon with quantified uncertainty ranges and identified data gaps, Biogeosciences, 11, 6573–6593, https://doi.org/10.5194/bg-11-6573-2014, 2014.

Hugelius, G., Loisel, J., Chadburn, S., Jackson, R. B., Jones, M., MacDonald, G., Marushchak, M., Olefeldt, D., Packalen, M., Siewert, M. B., Treat, C., Turetsky, M., Voigt, C., and Yu, Z.: Large stocks of peatland carbon and nitrogen are vulnerable to permafrost thaw, Proceedings of the National Academy of Sciences, 117, 20 438–20 446, https://doi.org/10.1073/pnas.1916387117, 2020.

Kåresdotter, E., Destouni, G., Ghajarnia, N., Hugelius, G., and Kalantari, Z.: Mapping the Vulnerability of Arctic Wetlands to Global Warming, Earth's Future, 9, https://doi.org/10.1029/2020ef001858, 2021.

Kasischke, E. S., Williams, D., and Barry, D.: Analysis of the patterns of large fires in the boreal forest region of Alaska, International Journal of Wildland Fire, 11, 131, https://doi.org/10.1071/wf02023, 2002.

Kraev, G., Belonosov, A., Veremeeva, A., Grabovskii, V., Sheshukov, S., Shelokhov, I., and Smirnov, A.: Fluid Migration through Permafrost and the Pool of Greenhouse Gases in Frozen Soils of an Oil and Gas Field, Remote Sensing, 14, 3662, https://doi.org/10.3390/rs14153662, 2022.

Lanaras, C., Bioucas-Dias, J., Galliani, S., Baltsavias, E., and Schindler, K.: Super-resolution of Sentinel-2 images: Learning a globally applicable deep neural network, ISPRS Journal of Photogrammetry and Remote Sensing, 146, 305–319, https://doi.org/10.1016/j.isprsjprs.2018.09.018, 2018.

Liljedahl, A. K., Boike, J., Daanen, R. P., Fedorov, A. N., Frost, G. V., Grosse, G., Hinzman, L. D., Iijma, Y., Jorgenson, J. C., Matveyeva, N., Necsoiu, M., Raynolds, M. K., Romanovsky, V. E., Schulla, J., Tape, K. D., Walker, D. A., Wilson, C. J., Yabuki, H., and Zona, D.: Pan-Arctic ice-wedge degradation in warming permafrost and its influence on tundra hydrology, Nature Geoscience, 9, 312–318, https://doi.org/10.1038/ngeo2674, 2016.

Liu, C., Xu, X., Feng, X., Cheng, X., Liu, C., and Huang, H.: CALC-2020: a new baseline land cover map at 10 m resolution for the circumpolar Arctic, Earth System Science Data, 15, 133–153, https://doi.org/10.5194/essd-15-133-2023, 2023.

Matthews, E., Johnson, M. S., Genovese, V., Du, J., and Bastviken, D.: Methane emission from high latitude lakes: methane-centric lake classification and satellite-driven annual cycle of emissions, Sci Rep, 10, https://doi.org/10.1038/s41598-020-68246-1, 2020.

Melvaer, Y.: Terrengmodell Svalbard (S0 Terrengmodell) [Data set], Norwegian Polar Institute, https://doi.org/10.21334/npolar.2014.dce53a47, 2014.

Muster, S., Riley, W. J., Roth, K., Langer, M., Aleina, F. C., Koven, C. D., Lange, S., Bartsch, A., Grosse, G., Wilson, C. J., Jones, B. M., and Boike, J.: Size Distributions of Arctic Waterbodies Reveal Consistent Relations in Their Statistical Moments in Space and Time, Frontiers in Earth Science, 7, https://doi.org/10.3389/feart.2019.00005, 2019.

Nitze, I. and Grosse, G.: Detection of landscape dynamics in the Arctic Lena Delta with temporally dense Landsat time-series stacks, Remote Sensing of Environment, 181, 27–41, https://doi.org/10.1016/j.rse.2016.03.038, 2016.

Nitze, I., Grosse, G., Jones, B. M., Romanovsky, V. E., and Boike, J.: Remote sensing quantifies widespread abundance of permafrost region disturbances across the Arctic and Subarctic, Nature Communications, 9, https://doi.org/10.1038/s41467-018-07663-3, 2018.

Obu, J., Westermann, S., Bartsch, A., Berdnikov, N., Christiansen, H. H., Dashtseren, A., Delaloye, R., Elberling, B., Etzelmüller, B., Kholodov, A., Khomutov, A., Kääb, A., Leibman, M. O., Lewkowicz, A. G., Panda, S. K., Romanovsky, V., Way, R. G., Westergaard-Nielsen, A., Wu, T., Yamkhin, J., and Zou, D.: Northern Hemisphere permafrost map based on TTOP modelling for 2000-2016 at 1?km2 scale, Earth-Science Reviews, 193, 299–316, https://doi.org/10.1016/j.earscirev.2019.04.023, 2019.

Obu, J., Westermann, S., Barboux, C., Bartsch, A., Delaloye, R., Grosse, G., Heim, B., Hugelius, G., Irrgang, A., Kääb, A. M., Kroisleitner, C., Matthes, H., Nitze, I., Pellet, C., Seifert, F. M., Strozzi, T., Wegmüller, U., Wieczorek, M., and Wiesmann, A.: ESA Permafrost Climate Change Initiative (Permafrost_cci): Permafrost ground temperature for the Northern Hemisphere, v3.0, CEDA, https://doi.org/10.5285/b25d4a6174de4ac78000d034f500a268, 2021.

Olefeldt, D., Hovemyr, M., Kuhn, M. A., Bastviken, D., Bohn, T. J., Connolly, J., Crill, P., Euskirchen, E. S., Finkelstein, S. A., Genet, H., Grosse, G., Harris, L. I., Heffernan, L., Helbig, M., Hugelius, G., Hutchins, R., Juutinen, S., Lara, M. J., Malhotra, A., Manies, K., McGuire, A. D., Natali, S. M., O'Donnell, J. A., Parmentier, F.-J. W., RÃ¤sÃ¤nen, A., SchÃ¤del, C., Sonnentag, O., Strack, M., Tank, S., Treat, C., Varner, R. K., Virtanen, T., Warren, R. K., and Watts, J. D.: The Boreal-Arctic Wetland and Lake Dataset (BAWLD), Earth System Science Data, pp. 5127–5149, https://doi.org/10.5194/essd-13-5127-20210, 2021.

Ou, C., LaRocque, A., Leblon, B., Zhang, Y., Webster, K., and McLaughlin, J.: Modelling and mapping permafrost at high spatial resolution using Landsat and Radarsat-2 images in Northern Ontario, Canada: Part 2 – regional mapping, International Journal of Remote Sensing, 37, 2751–2779, https://doi.org/10.1080/01431161.2016.1151574, 2016.

Palmtag, J., Obu, J., Kuhry, P., Richter, A., Siewert, M. B., Weiss, N., Westermann, S., and Hugelius, G.: A high spatial resolution soil carbon and nitrogen dataset for the northern permafrost region based on circumpolar land cover upscaling, Earth System Science Data, 14, 4095–4110, https://doi.org/10.5194/essd-14-4095-2022, 2022.

Raynolds, M. K., Walker, D. A., Balser, A., Bay, C., Campbell, M., Cherosov, M. M., DaniÃ«ls, F. J., Eidesen, P. B., Ermokhina, K. A., Frost, G. V., Jedrzejek, B., Jorgenson, M. T., Kennedy, B. E., Kholod, S. S., Lavrinenko, I. A., Lavrinenko, O. V., Magnússon, B., Matveyeva, N. V., Metúsalemsson, S., Nilsen, L., Olthof, I., Pospelov, I. N., Pospelova, E. B., Pouliot, D., Razzhivin, V., Schaepman-Strub, G., Šibík, J., Telyatnikov, M. Y., and Troeva, E.: A raster version of the Circumpolar Arctic Vegetation Map (CAVM), Raynolds2019, 232, 111 297, https://doi.org/10.1016/j.rse.2019.111297, 2019.

Reschke, J., Bartsch, A., Schlaffer, S., and Schepaschenko, D.: Capability of C-Band SAR for Operational Wetland Monitoring at High Latitudes, Remote Sensing, 4, 2923–2943, https://doi.org/10.3390/rs4102923, 2012.

Saunois, M., Bousquet, P., Poulter, B., Peregon, A., Ciais, P., Canadell, J. G., Dlugokencky, E. J., Etiope, G., Bastviken, D., Houweling, S., Janssens-Maenhout, G., Tubiello, F. N., Castaldi, S., Jackson, R. B., Alexe, M., Arora, V. K., Beerling, D. J., Bergamaschi, P., Blake, D. R., Brailsford, G., Brovkin, V., Bruhwiler, L., Crevoisier, C., Crill, P., Covey, K., Curry, C., Frankenberg, C., Gedney, N., Höglund-Isaksson, L., Ishizawa, M., Ito, A., Joos, F., Kim, H.-S., Kleinen, T., Krummel, P., Lamarque, J.-F., Langenfelds, R., Locatelli, R., Machida, T., Maksyutov, S., McDonald, K. C., Marshall, J., Melton, J. R., Morino, I., Naik, V., O'Doherty, S., Parmentier, F.-J. W., Patra, P. K., Peng, C., Peng, S., Peters, G. P., Pison, I., Prigent, C., Prinn, R., Ramonet, M., Riley, W. J., Saito, M., Santini, M., Schroeder, R., Simpson, I. J., Spahni, R., Steele, P., Takizawa, A., Thornton, B. F., Tian, H., Tohjima, Y., Viovy, N., Voulgarakis, A., van Weele, M., van der Werf, G. R., Weiss, R., Wiedinmyer, C., Wilton, D. J., Wiltshire, A., Worthy, D., Wunch, D., Xu, X., Yoshida, Y., Zhang, B., Zhang, Z., and Zhu, Q.: The global methane budget 2000–2012, Earth System Science Data, 8, 697–751, https://doi.org/10.5194/essd-8-697-2016, 2016.

Scheer, J., Caduff, R., How, P., Marcer, M., Strozzi, T., Bartsch, A., and Ingeman-Nielsen, T.: Thaw-Season InSAR Surface Displacements and Frost Susceptibility Mapping to Support Community-Scale Planning in Ilulissat, West Greenland, Remote Sensing, 15, 3310, https://doi.org/10.3390/rs15133310, 2023.

Schubert, A., Miranda, N., Geudtner, D., and Small, D.: Sentinel-1A/B Combined Product Geolocation Accuracy, Remote Sensing, 9, 2017.

Siewert, M. B., Hanisch, J., Weiss, N., Kuhry, P., Maximov, T. C., and Hugelius, G.: Comparing carbon storage of Siberian tundra and taiga permafrost ecosystems at very high spatial resolution, Journal of Geophysical Research: Biogeosciences, 120, 1973–1944, https://doi.org/10.1002/2015JG002999, 2015.

Silvertown, J., Araya, Y., and Gowing, D.: Hydrological niches in terrestrial plant communities: a review, Journal of Ecology, 103, 93–108, https://doi.org/10.1111/1365-2745.12332, 2014.

Small, D.: Flattening Gamma: Radiometric Terrain Correction for SAR Imagery, IEEE Transactions on Geoscience and Remote Sensing, 49, 3081–3093, https://doi.org/10.1109/tgrs.2011.2120616, 2011.

Spiegel, M. P., Volkovitskiy, A., Terekhina, A., Forbes, B. C., Park, T., and Macias-Fauria, M.: Top-Down Regulation by a Reindeer Herding System Limits Climate-Driven Arctic Vegetation Change at a Regional Scale, Earth's Future, 11, https://doi.org/10.1029/2022ef003407, 2023.

Treat, C. C., Marushchak, M. E., Voigt, C., Zhang, Y., Tan, Z., Zhuang, Q., Virtanen, T. A., Räsänen, A., Biasi, C., Hugelius, G., Kaverin, D., Miller, P. A., Stendel, M., Romanovsky, V., Rivkin, F., Martikainen, P. J., and Shurpali, N. J.: Tundra landscape heterogeneity, not interannual variability, controls the decadal regional carbon balance in the Western Russian Arctic, Global Change Biology, 24, 5188–5204, https://doi.org/10.1111/gcb.14421, 2018.

Viereck, L., Dyrness, C., and Batten, A.R. aand Wenzlick, K.: The Alaskavegetation classification, no. PNW-GTR-286 in Gen. Tech. Rep, U.S.Department of Agriculture, Forest Service, Pacific Northwest Research Station, Portland, OR, 1992.

Virtanen, T. and Ek, M.: The fragmented nature of tundra landscape, International Journal of Applied Earth Observation and Geoinformation, 27, 4–12, https://doi.org/10.1016/j.jag.2013.05.010, 2014.

Walker, D. A., Raynolds, M. K., Danii¿½ls, F. J., Einarsson, E., Elvebakk, A., Gould, W. A., Katenin, A. E., Kholod, S. S., Markon, C. J., Melnikov, E. S., Moskalenko, N. G., Talbot, S. S., Yurtsev, B. A., and other members of the CAVM Team, T.: The Circumpolar Arctic vegetation map, Journal of Vegetation Science, 16, 267–282, 2005.

Walker, D. A., Daniëls, F. J., Matveyeva, N. V., Šibík, J., Walker, M. D., Breen, A. L., Druckenmiller, L. A., Raynolds, M. K., Bültmann, H., Hennekens, S., Buchhorn, M., Epstein, H. E., Ermokhina, K., Fosaa, A. M., Hei∂marsson, S., Heim, B., Jónsdóttir, I. S., Koroleva, N., Lévesque, E., MacKenzie, W. H., Henry, G. H., Nilsen, L., Peet, R., Razzhivin, V., Talbot, S. S., Telyatnikov, M., Thannheiser, D., Webber, P. J., and Wirth, L. M.: Circumpolar Arctic Vegetation Classification, Phytocoenologia, 48, 181–201, https://doi.org/10.1127/phyto/2017/0192, 2018.

Westermann, S., Peter, M., Langer, M., Schwamborn, G., Schirrmeister, L., EtzelmÃ¼ller, B., and Boike, J.: Transient modeling of the ground thermal conditions using satellite data in the Lena River delta, Siberia, The Cryosphere, 11, 1441–1463, https://doi.org/10.5194/tc-11-1441-2017, 2017.

Widhalm, B., Bartsch, A., and Heim, B.: A novel approach for the characterization of tundra wetland regions with C-band SAR satellite data, International Journal of Remote Sensing, 36, 5537–5556, 2015.

Widhalm, B., Bartsch, A., and Goler, R.: Simplified Normalization of C-Band Synthetic Aperture Radar Data for Terrestrial Applications in High Latitude Environments, Remote Sensing, 10, https://doi.org/10.3390/rs10040551, 2018.

Wolter, J., Jones, B. M., Fuchs, M., Breen, A. L., Bussmann, I., Koch, B. P., Lenz, J., Myers-Smith, I. H., Sachs, T., Strauss, J., Nitze, I., and Grosse, G.: Post-drainage vegetation, microtopography and organic matter in Arctic drained lake basins, Environmental Research Letters, https://doi.org/10.1088/1748-9326/ad2eeb, 2024.

Wrona, E., Rowlandson, T. L., Nambiar, M., Berg, A. A., Colliander, A., and Marsh, P.: Validation of the Soil Moisture Active Passive (SMAP) satellite soil moisture retrieval in an Arctic tundra environment, Geophysical Research Letters, 44, 4152–4158, https://doi.org/10.1002/2017gl072946, 2017.

Zemlianskii, V., Ermokhina, K., Schaepman-Strub, G., Matveyeva, N., Troeva, E., Lavrinenko, I., Telyatnikov, M., Pospelov, I., Koroleva, N., Leonova, N., Khitun, O., Walker, D., Breen, A., Kadetov, N., Lavrinenko, O., Ivleva, T., Kholod, S., Petrzhik, N., Gunin, Y., Kurysheva, M., Lapina, A., Korolev, D., Kudr, E., and Plekhanova, E.: Russian Arctic Vegetation Archive—A new database of plant community composition and environmental conditions, Global Ecology and Biogeography, https://doi.org/10.1111/geb.13724, 2023.

Zhang, Z., Fluet-Chouinard, E., Jensen, K., McDonald, K., Hugelius, G., Gumbricht, T., Carroll, M., Prigent, C., Bartsch, A., and Poulter, B.: Development of the global dataset of Wetland Area and Dynamics for Methane Modeling (WAD2M), Earth System Science Data, 13, 2001–2023, https://doi.org/10.5194/essd-13-2001-2021, 2021.

Appendix A: ~~Class~~ Selected statistics from in situ measurements

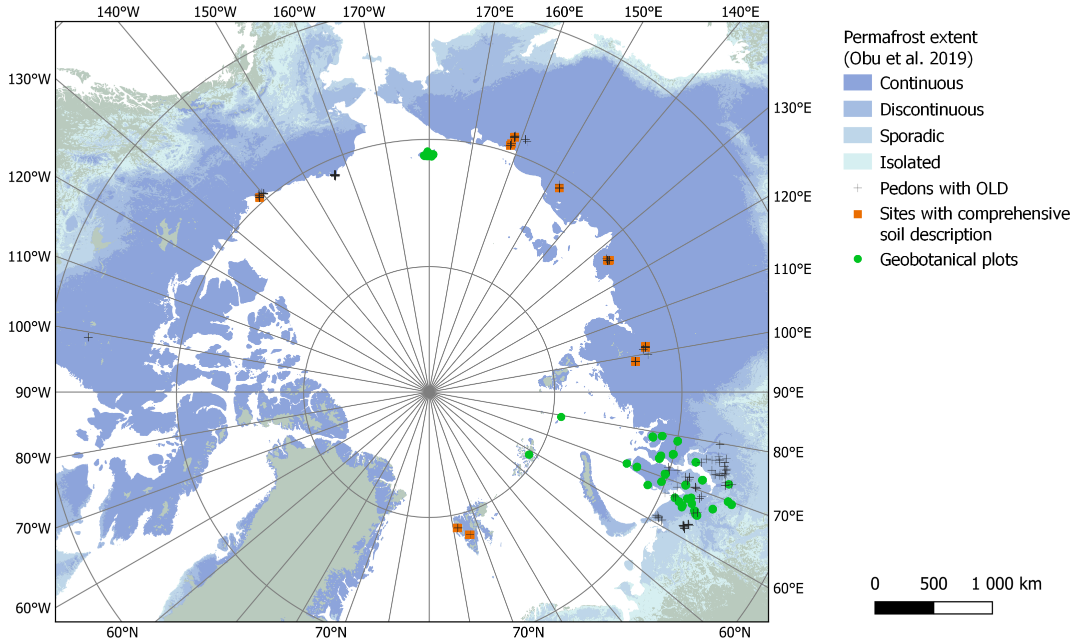

Figure A1. Location of in situ records (vegetation (Zemlianskii et al., 2023), soils (Hugelius et al., 2013, 2014, 2020; Palmtag et al., 2022)) and permafrost extent (source: Obu et al. (2019)). OLD - organic layer depth.

Table A1. Soil surface organic horizon depth statistics extracted from several different sources, including (Hugelius et al., 2013, 2014, 2020) and (Palmtag et al., 2022).

Unit	Samples	Mean	Median	Std
2	23	105	62	103
15	25	93	72	99
12	42	74	15	112
14	51	74	20	98
16	21	64	8	109
6	44	62	33	78
8	43	59	30	65
11	157	41	12	74
17	5	40	18	36
3	54	40	20	54
4	64	39	20	39
7	30	37	19	55
9	123	34	18	42
10	74	29	15	37
5	19	28	20	20
13	10	23	11	33
21	3	13	0	19

Table A2. Average soil characteristics based on Palmtag et al. (2022)

Type	Dry bulk density (g/cm3)	Wet bulk density (g/cm3)	Organic volumetric content	Water volumetric content	Mineral volumetric content	SOC density (kg C m-2)	TN density (kg N m-2)	Samples
3	0.61	1.11	4.53	50.38	20.61	29.41	1.47	22
4	0.92	1.48	3.97	46.87	27.34	30.97	2.07	6
5	1.27	1.62	3.36	33.03	46.42	22.19	1.61	5
6	1.18	1.53	3.03	34.64	44.02	21.19	1.04	31
7	0.86	1.24	4.04	40.51	30.42	26.64	1.16	4
8	0.86	1.38	3.72	44.70	27.35	26.77	1.49	20
9	0.85	1.35	4.60	50.25	29.48	30.79	1.43	56
10	0.74	1.27	5.90	52.82	24.60	38.20	1.63	27
11	0.75	1.28	5.54	50.55	25.06	36.90	1.63	52
12	0.63	1.06	3.56	43.48	22.82	23.05	1.28	8
13	0.74	1.13	3.69	38.62	26.08	23.83	1.58	1
14	0.86	1.34	4.69	47.33	30.43	30.31	1.56	16
15	1.27	1.62	2.26	35.84	47.31	15.14	1.03	7
16	1.30	1.73	3.50	39.72	44.99	22.77	1.91	6
19	1.47	1.90	2.13	38.01	58.59	14.69	0.65	3
20	0.76	1.17	4.12	41.00	27.35	26.89	1.55	2
21	1.83	2.03	0.30	16.77	68.82	2.98	0.39	11

Table A3. Average characteristics for vegetation types of used sites of the Russian Arctic Vegetation Archive (AVA) (Zemlianskii et al., 2023)
.

AVA type	**Samples**	**Mean**	**Median**	**Std**
Tree layer	5.1	5.1	3.6	5.8
Tall shrubs	3.4	3.4	0.2	9.2
Low shrubs	11.1	11.1	4.2	15.9
Erect dwarf shrubs	11.4	11.4	4.9	14.9
Prostrate dwarf shrubs	7.6	7.6	0.8	14.2
Graminoids	19.7	19.7	11.0	22.5
Tussok graminioids	2.2	2.2	0.0	6.5
Forbs	12.1	12.1	6.1	15.3
Seedless vascular plants	2.4	2.4	0.1	6.3
Mosses and liverworts	48.0	48.0	44.8	32.8
Lichen	11.8	11.8	3.7	17.8
Crust	1.7	1.7	0.0	5.5
Algae	0.3	0.3	0.0	1.9
Bare soil	5.4	5.4	1.3	10.2
Bare rock	1.9	1.9	0.0	6.1
Litter	16.4	16.4	0.0	21.7

Appendix B: ~~Class~~ Example unit descriptions

B1 ~~Class~~ CALU #1

Description: Open water

B2 ~~Class~~ CALU #2

Description: Shallow water/abundant macrophytes

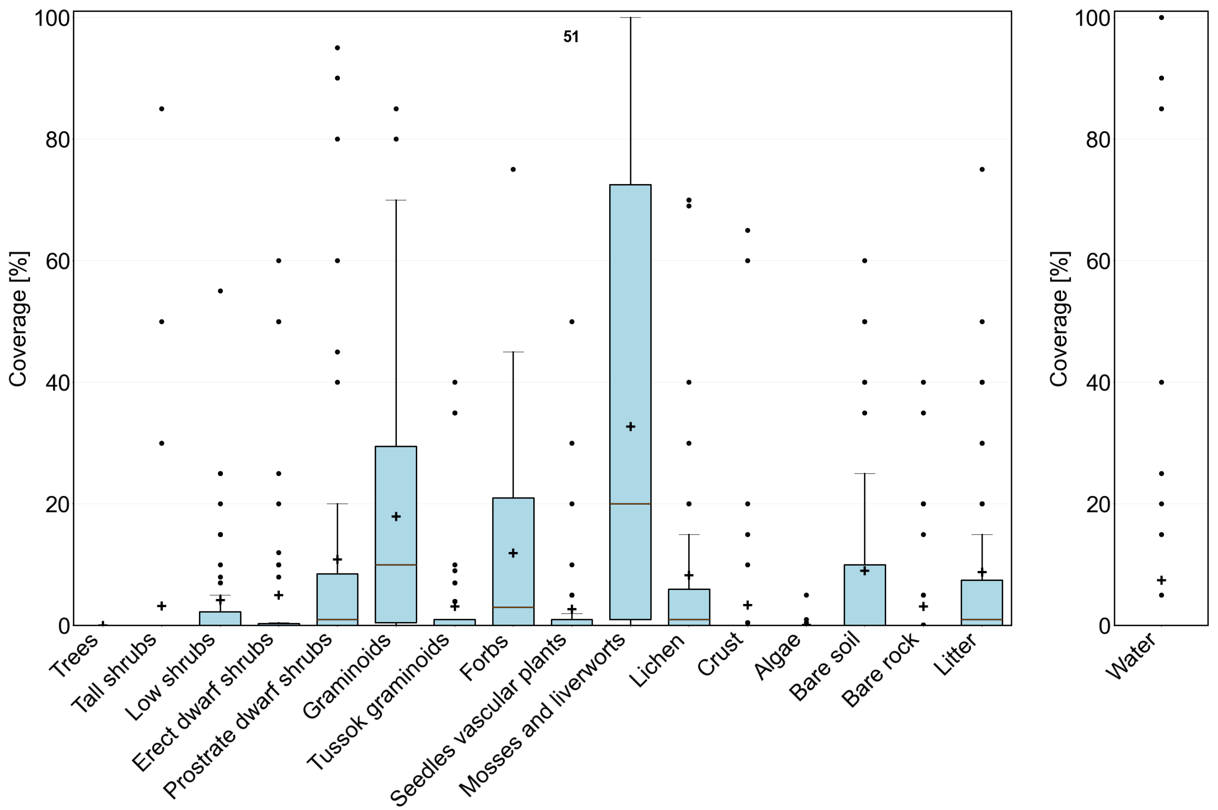

Figure B1. ~~Class~~ CALU #2 vegetation properties based on AVA (Zemlianskii et al., 2023).

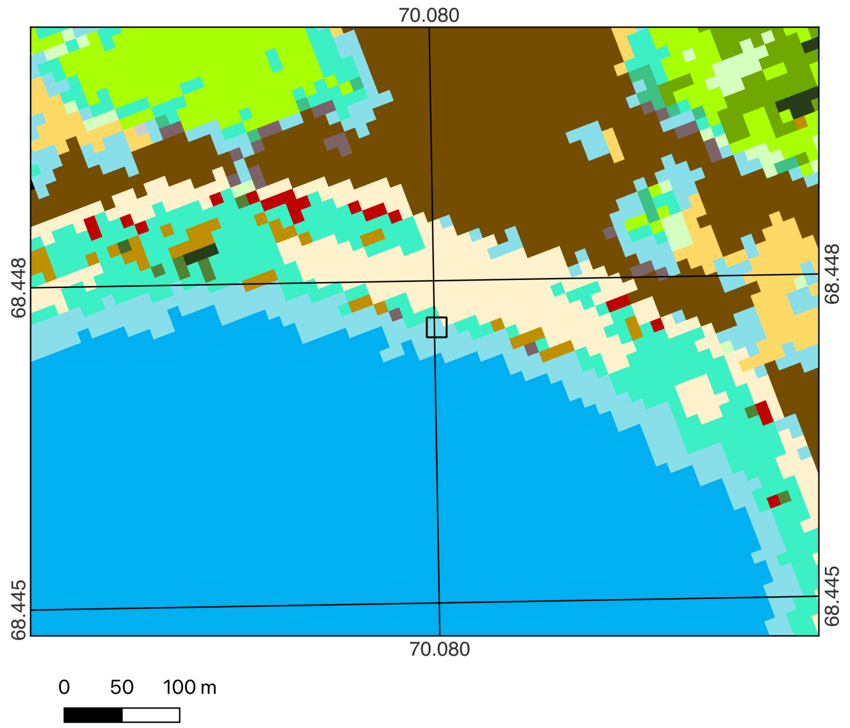

Figure B2. Example for a typical vegetation plot (Zemlianskii et al., 2023) located along a lake margin (square), falling into unit #2 (light blue; for full legend see Table 2). In situ values: 15 % land covered by mostly graminoids, occurrence of 1 % forbs with height 50 cm, 85 % water, wetness category 'moist'.

Figure B3. Example photograph ~~class~~ CALU #2, lake margin with patches of macrophytes, water depth approximately 22 cm (Annett Bartsch, 21.07.2023, Inuvik region)

Figure B4. Example photograph ~~class~~ CALU #2, lake with patches of macrophytes in the centre (Annett Bartsch, 2023, Inuvik region)

B3 ~~Class~~ CALU #3

Description: ~~permanent~~ Permanent wetland, aquatic, low to medium organic layer thickness, medium mineral volumetric content.

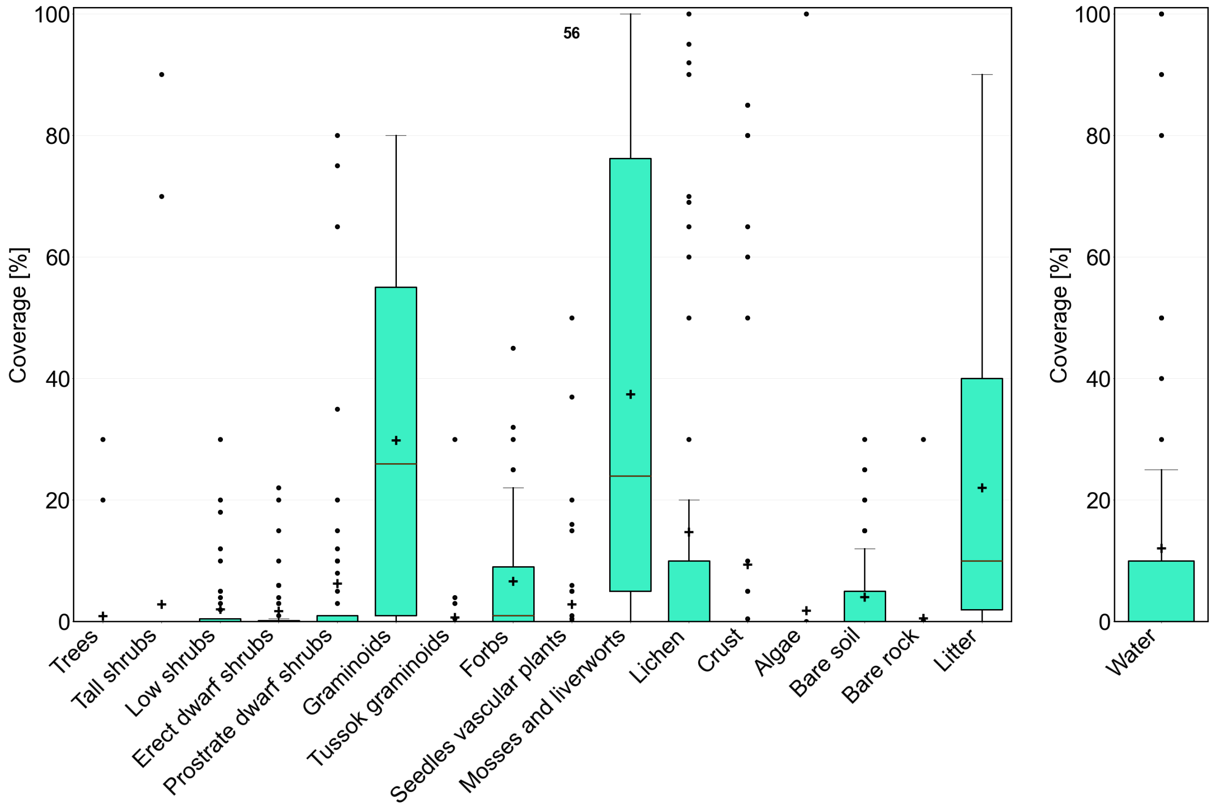

Figure B5. ~~Class~~ CALU #3 vegetation properties based on AVA (Zemlianskii et al., 2023).

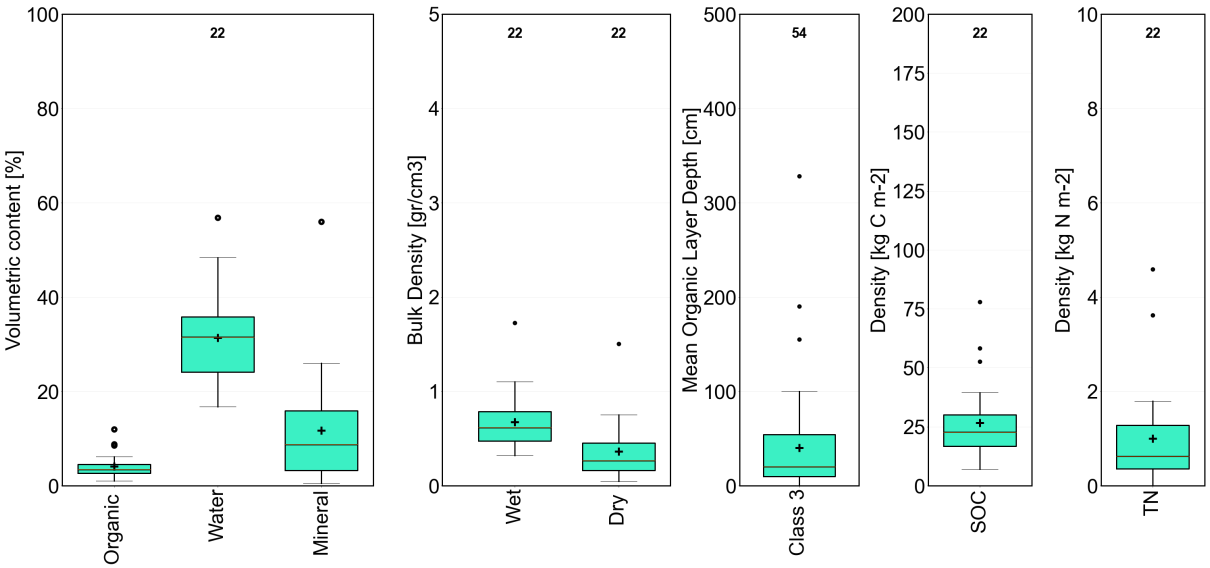

Figure B6. ~~Class~~ CALU #3 soil properties based on Palmtag et al. (2022).

Figure B7. Example photograph ~~class~~ CALU #3 (Birgit Heim, Lena Delta, Samoylov polygonal tundra)

Figure B8. Example photograph ~~class~~ CALU #3 (Annett Bartsch, 2023, Inuvik region)

B4 ~~Class~~ CALU #4

Description: ~~wet~~ Wet to aquatic (seasonal wetland), abundant moss, low to medium organic layer thickness, low mineral volumetric content.

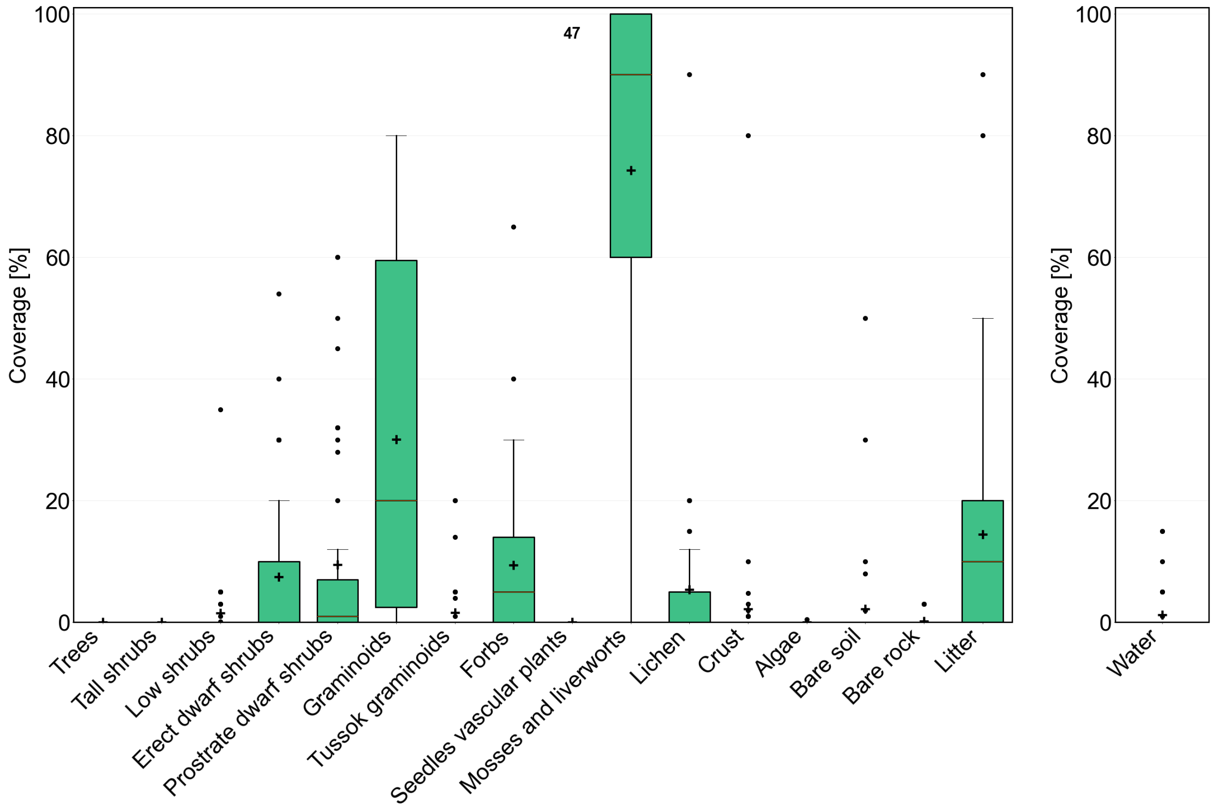

Figure B9. ~~Class~~ CALU #4 vegetation properties based on AVA (Zemlianskii et al., 2023).

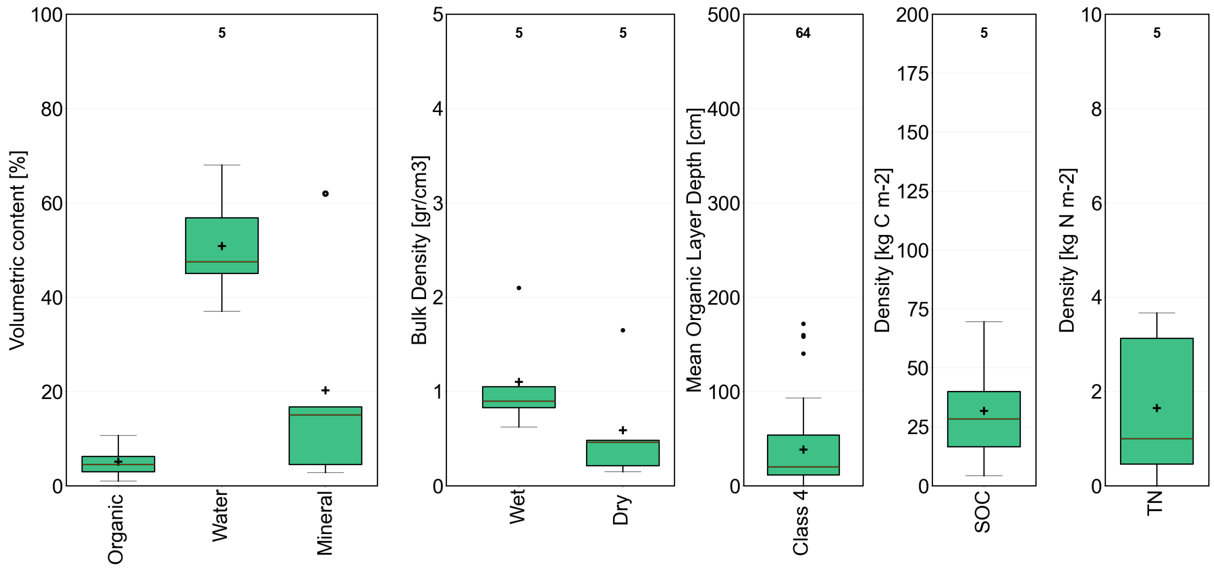

Figure B10. ~~Class~~ CALU #4 soil properties based on Palmtag et al. (2022).

B5 ~~Class~~ CALU #5

Description: ~~moist~~ Moist to wet tundra, abundant moss, prostrate shrubs; low to medium organic layer thickness, medium mineral volumetric content.

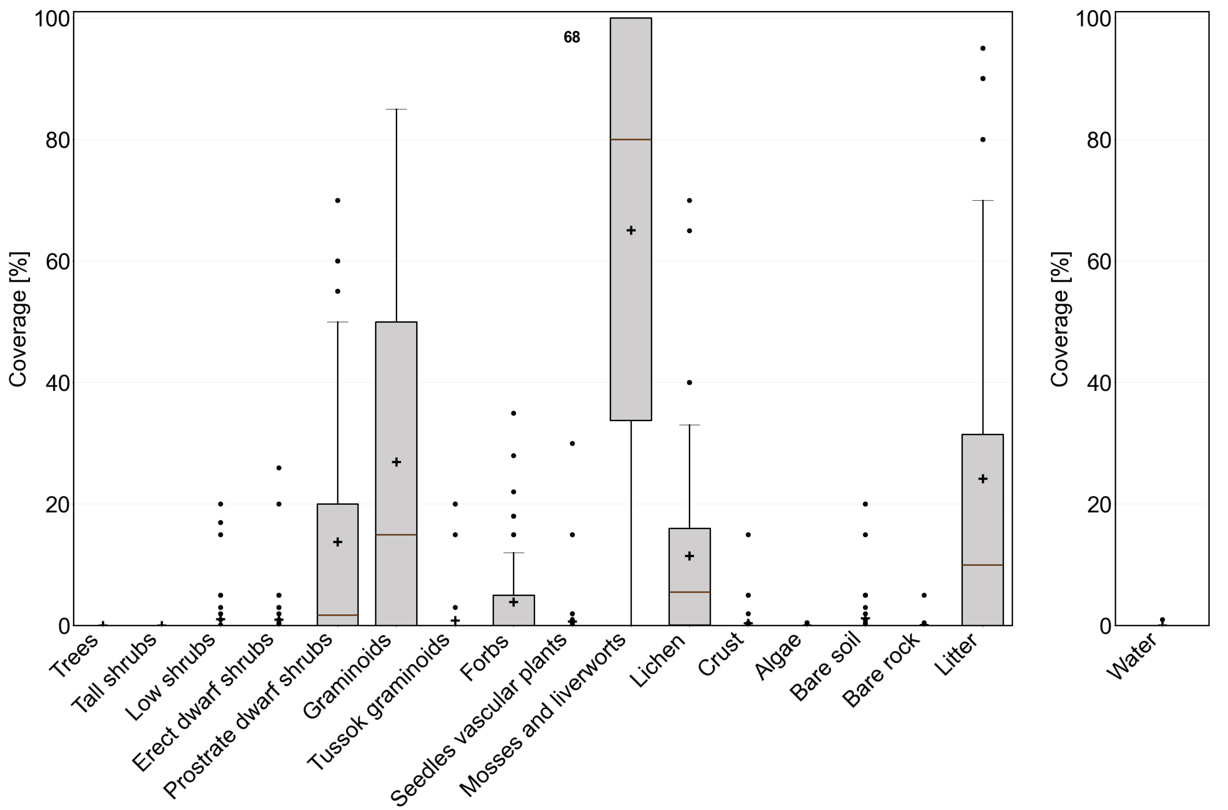

Figure B11. ~~Class~~ CALU #5 vegetation properties based on AVA (Zemlianskii et al., 2023).

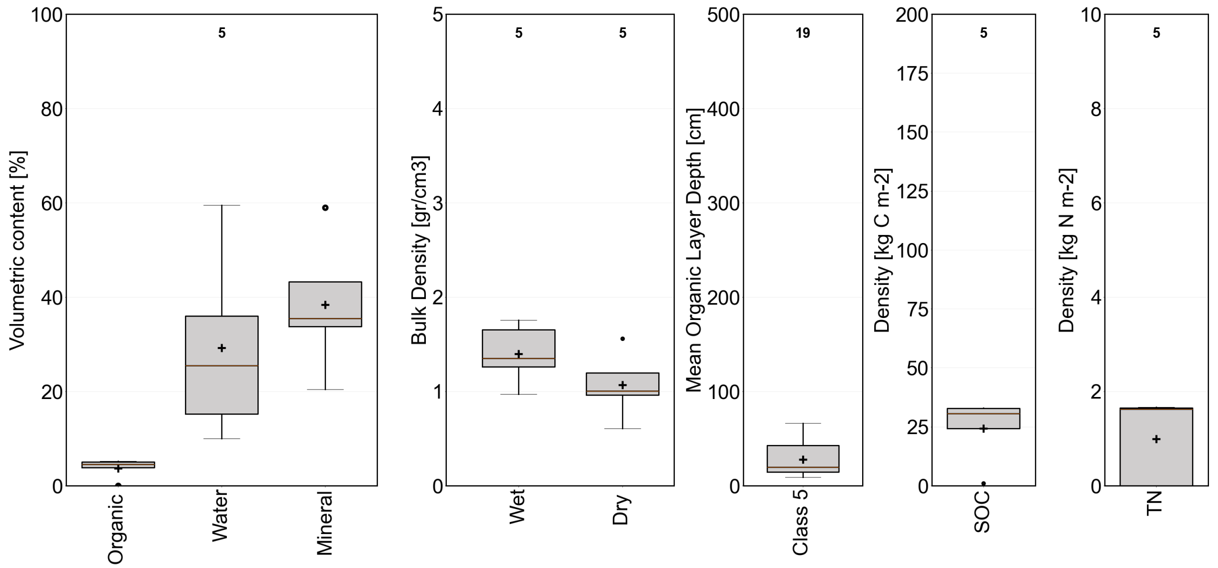

Figure B12. ~~Class~~ CALU #5 soil properties based on Palmtag et al. (2022).

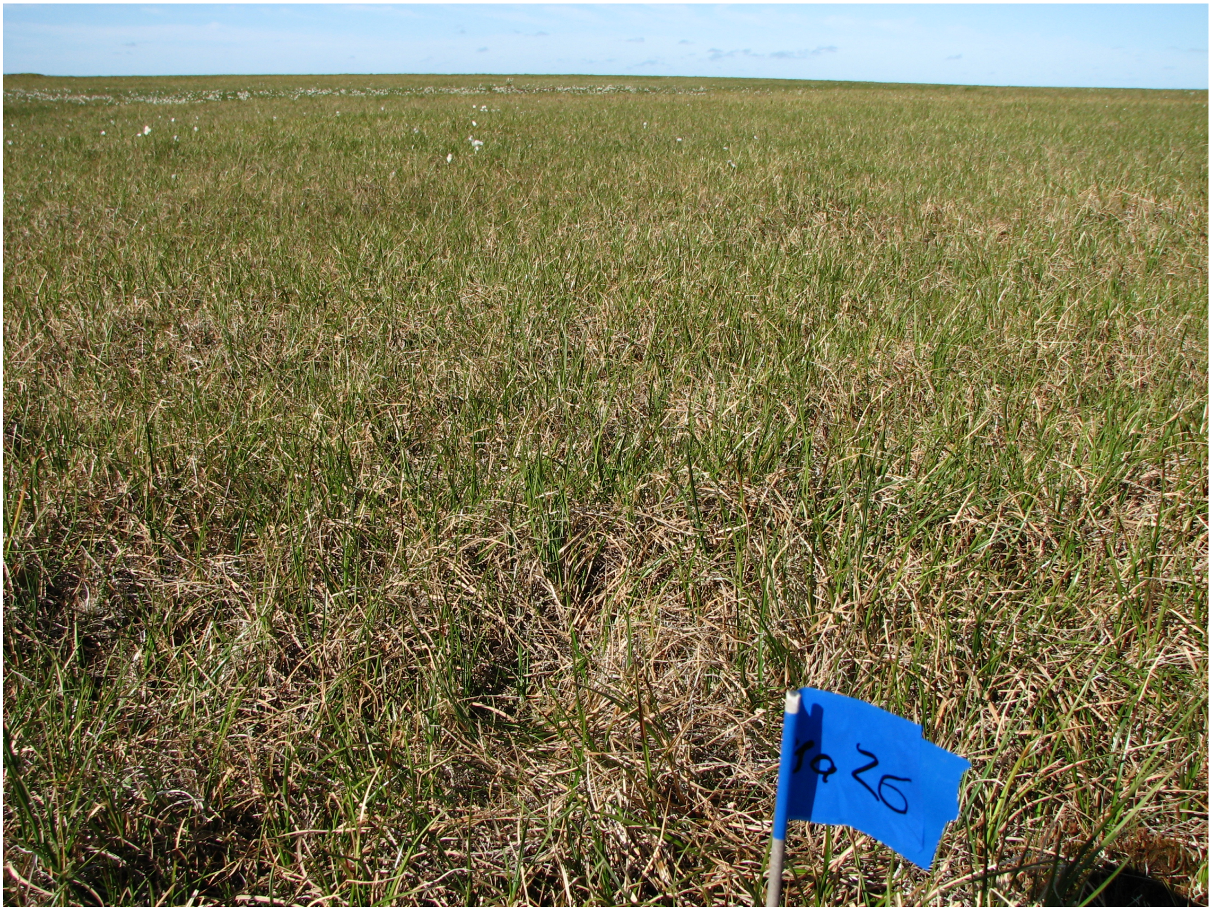

Figure B13. Example photograph ~~class~~ CALU #5 (Elena Troeva, 2017, Northern Yamal)

B6 ~~Class~~ CALU #6

Description: ~~dry~~ Dry to moist tundra, partially barren, prostrate shrubs; medium organic layer thickness, high mineral volumetric content.

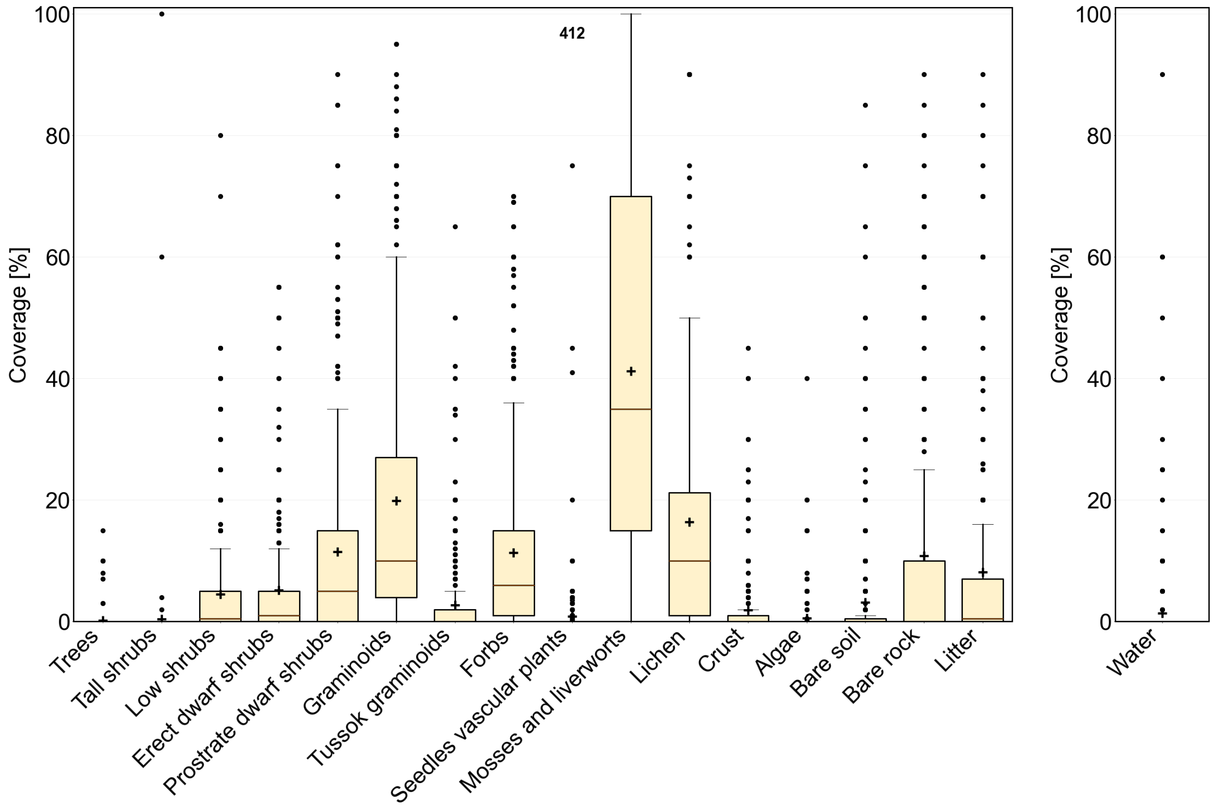

Figure B14. ~~Class~~ CALU #6 vegetation properties based on AVA (Zemlianskii et al., 2023).

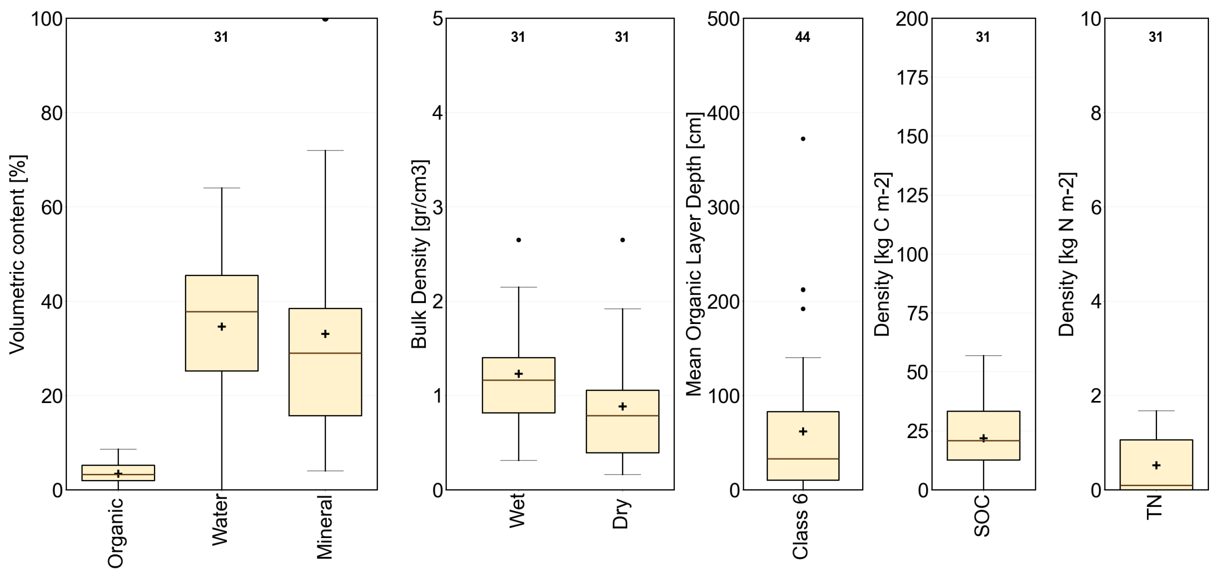

Figure B15. ~~Class~~ CALU #6 soil properties based on Palmtag et al. (2022).

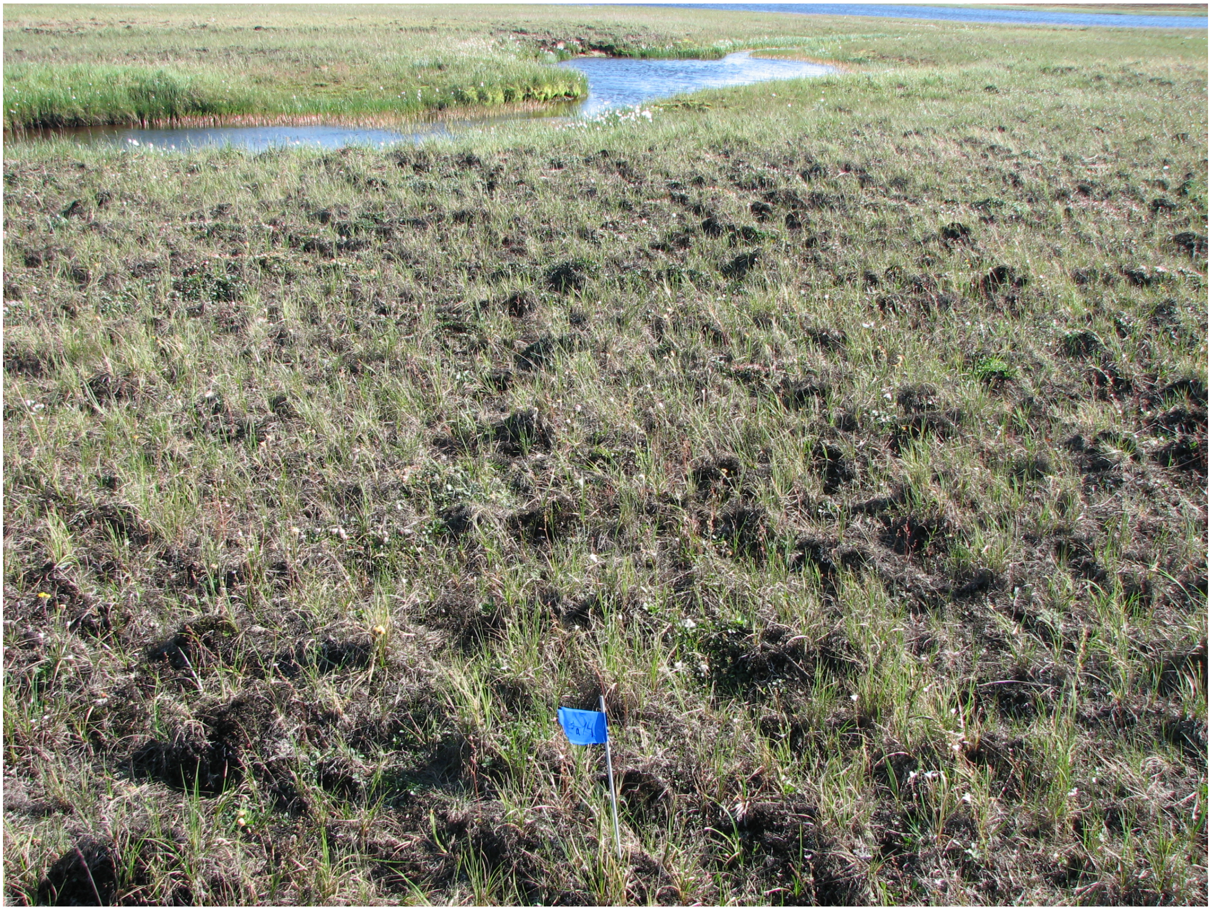

Figure B16. Example photograph ~~class~~ CALU #6, foreground (Elena Troeva, 2017, Northern Yamal)

B7 Class CALU #7

Description: dry Dry tundra, abundant lichen, prostrate shrubs; low to medium organic layer thickness, high mineral volumetric content.

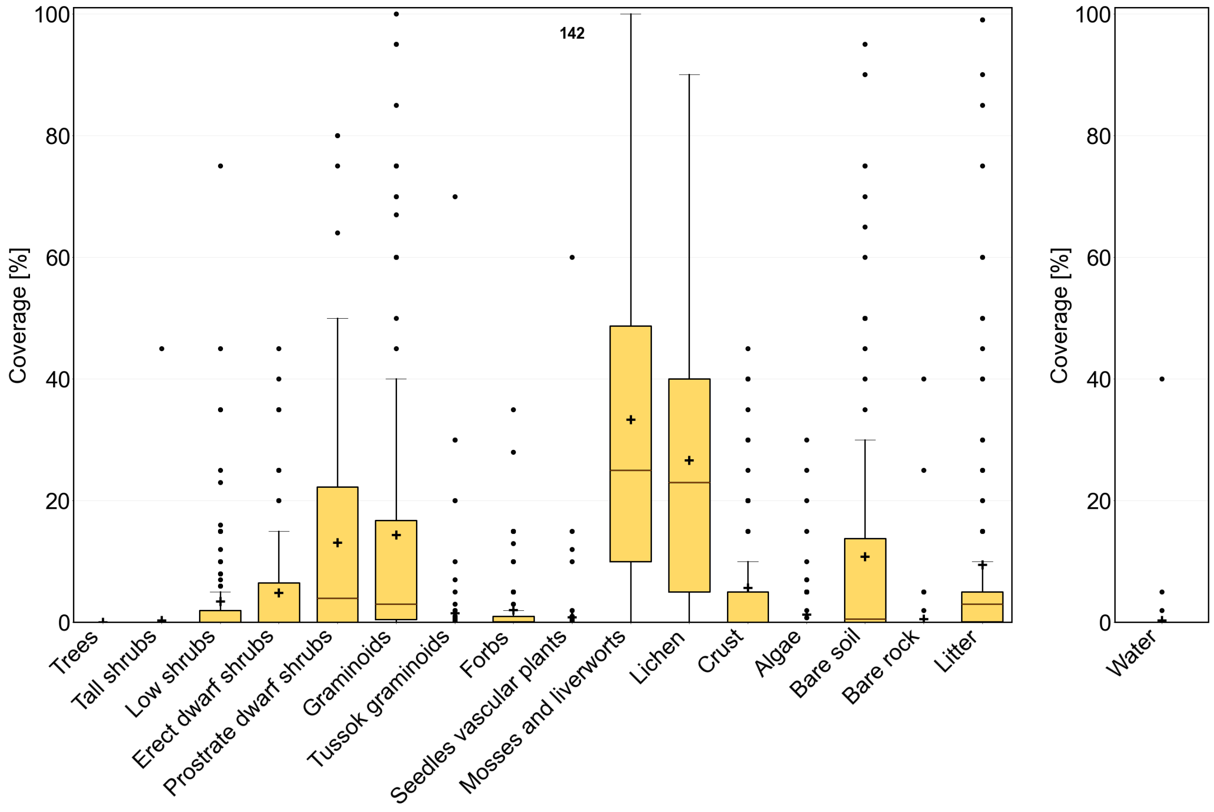

Figure B17. Class CALU #7 vegetation properties based on AVA (Zemlianskii et al., 2023).

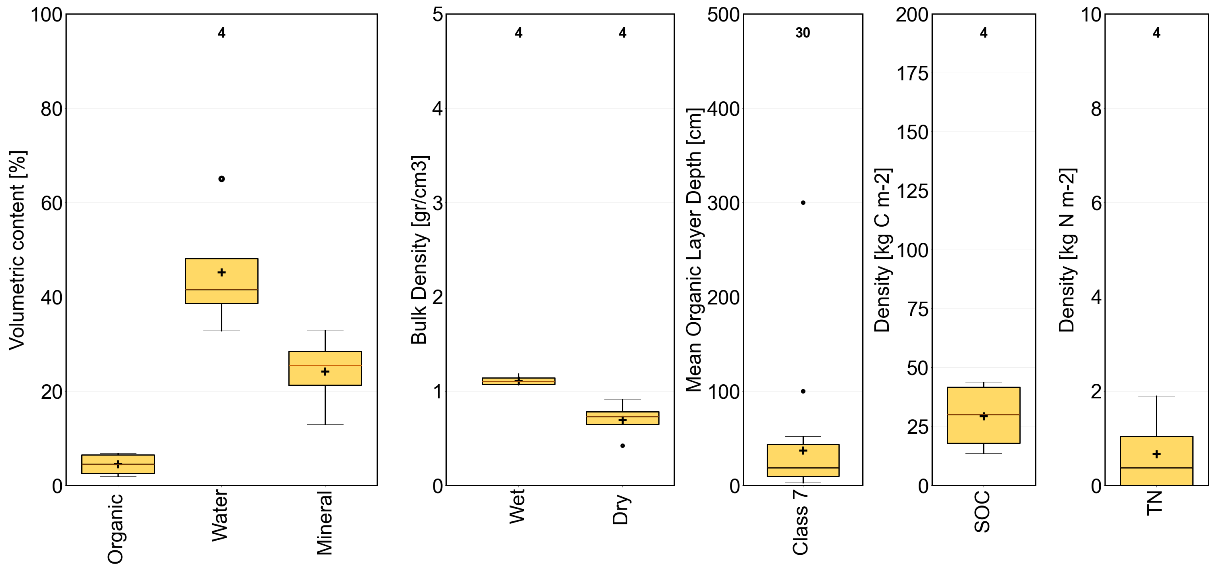

Figure B18. ~~Class~~ CALU #7 soil properties based on Palmtag et al. (2022).

Figure B19. Example photograph ~~class~~ CALU #7 (Annett Bartsch 2018, Polar Ural)

Figure B20. Example photograph ~~class~~ CALU #7 (Olga Khitun, 2017, Central Gydan)

B8 ~~Class~~ CALU #8

Description: ~~dry~~ Dry to aquatic tundra, dwarf shrubs (sparse tree cover along treeline, woodlands and open stands); medium organic layer thickness, medium mineral volumetric content.

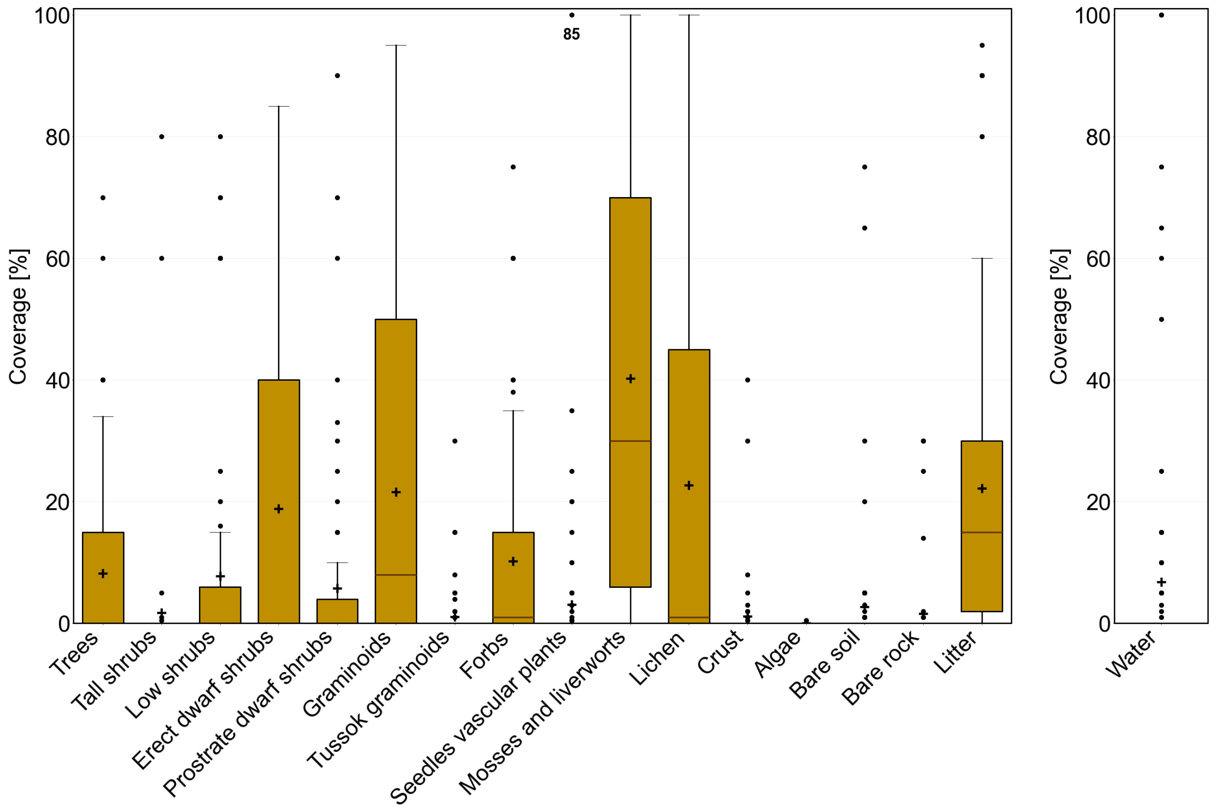

Figure B21. ~~Class~~ CALU #8 vegetation properties based on AVA (Zemlianskii et al., 2023).

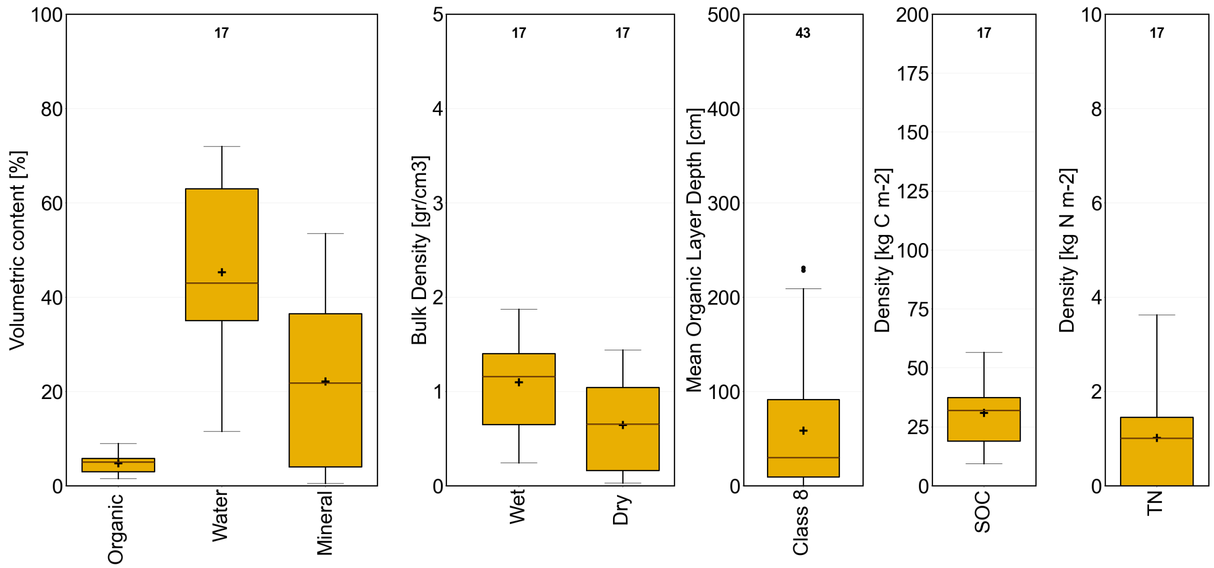

Figure B22. ~~Class~~ CALU #8 soil properties based on Palmtag et al. (2022).

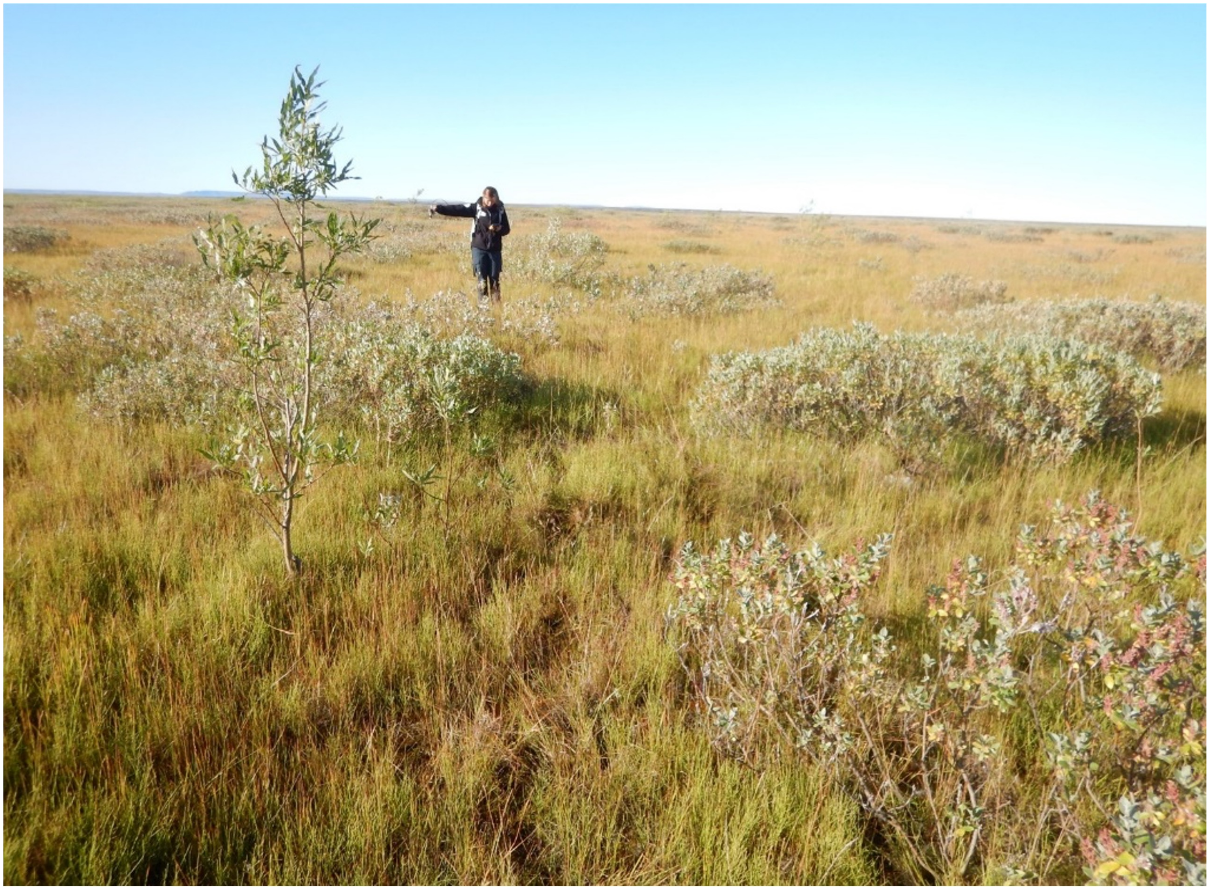

Figure B23. Example photograph ~~class~~ CALU #8 (Birgit Heim, Lena delta)

Figure B24. Example photograph ~~class~~ CALU #8 (Annett Bartsch, 2023, Inuvik region)

B9 ~~Class~~ CALU #9

Description: ~~dry~~ Dry to moist tundra, prostrate to low shrubs, tussocks; low to medium organic layer thickness, medium mineral volumetric content.

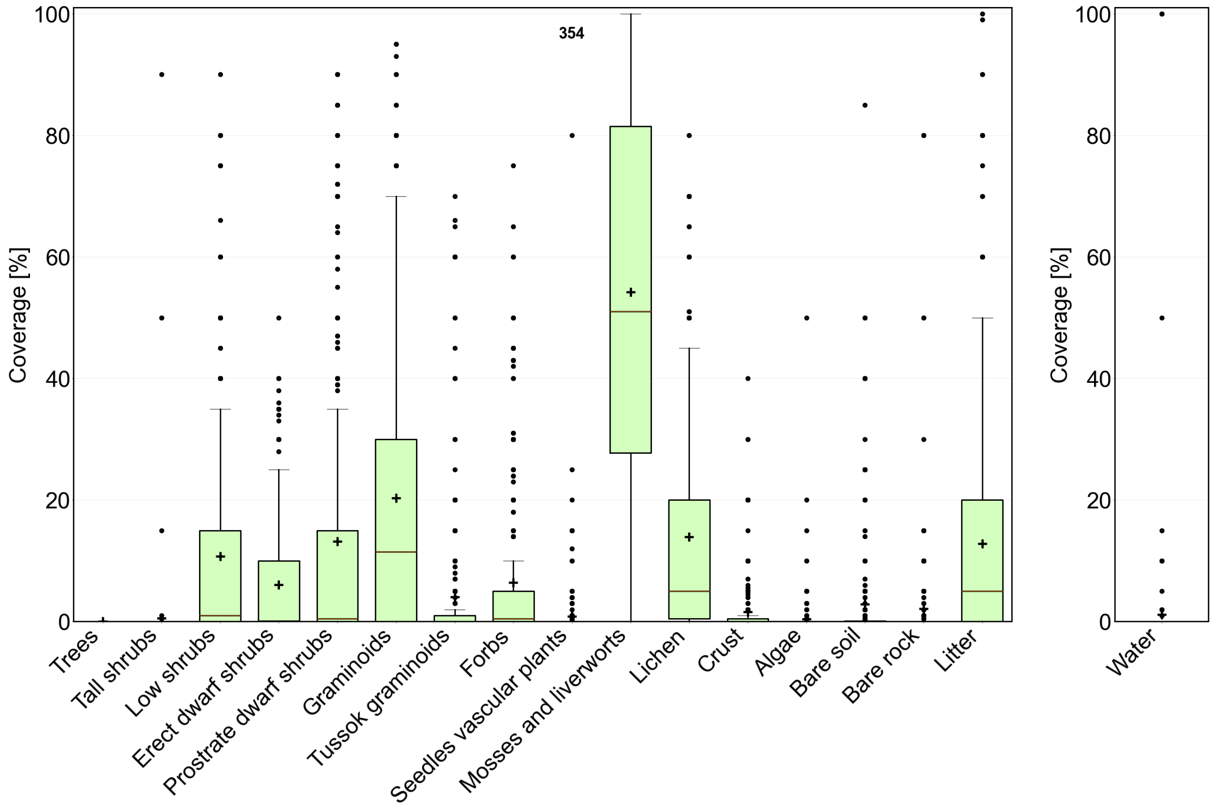

Figure B25. ~~Class~~ CALU #9 vegetation properties based on AVA (Zemlianskii et al., 2023).

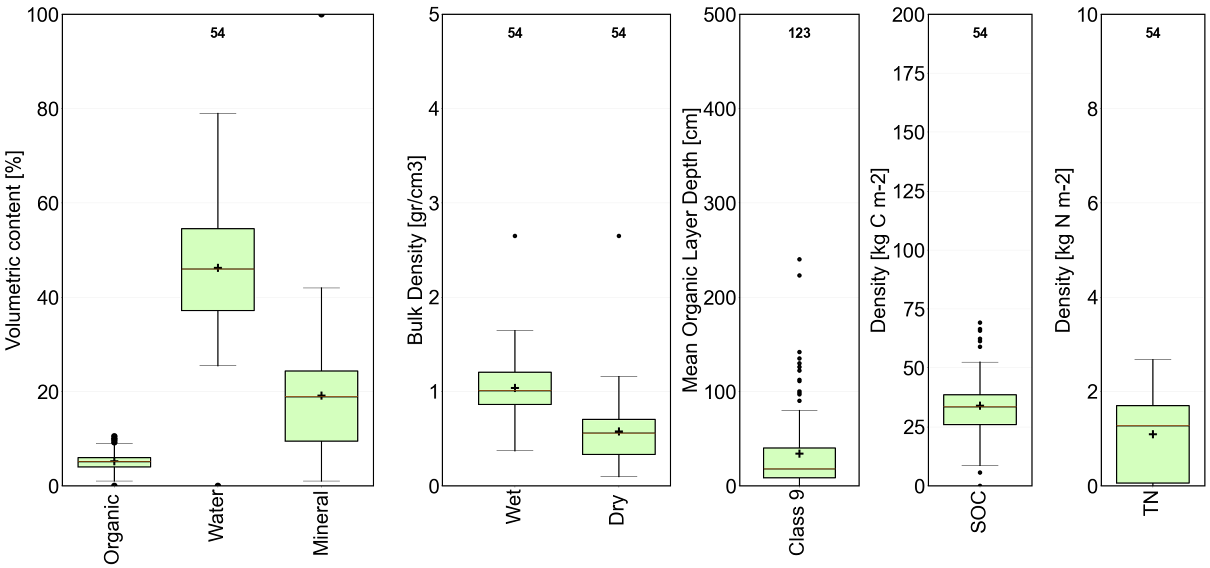

Figure B26. ~~Class~~ CALU #9 soil properties based on Palmtag et al. (2022).

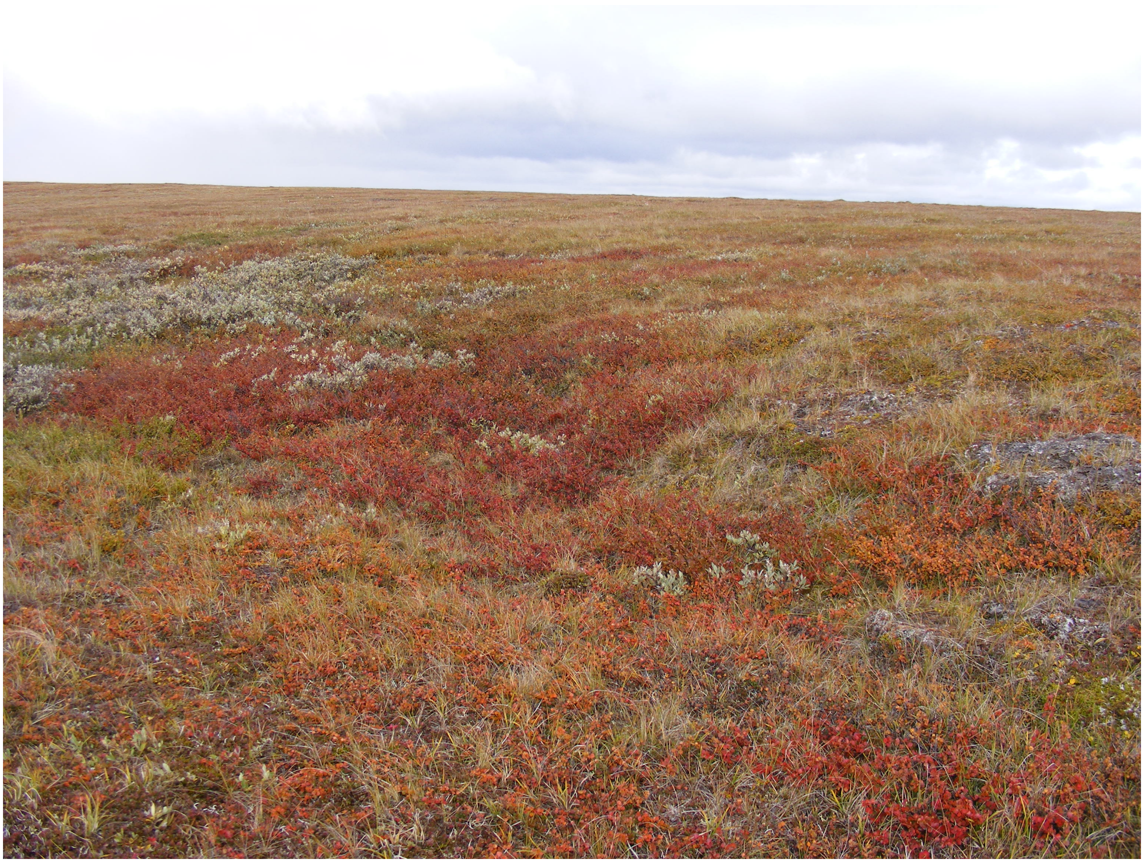

Figure B27. Example photograph ~~class~~ CALU #9 (Marina Leibman, 29.08.2014, central Yamal)

Figure B28. Example photograph ~~class~~ CALU #9 (Annett Bartsch, 2023, Inuvik region)

Figure B29. Example photograph ~~class~~ CALU #9 (Birgit Heim, 2018, Lena Delta 3rd terrace)

B10 ~~Class~~ CALU #10

Description: ~~moist~~ Moist tundra, abundant moss, prostrate to low shrubs, tussocks; low organic layer thickness, medium mineral volumetric content.

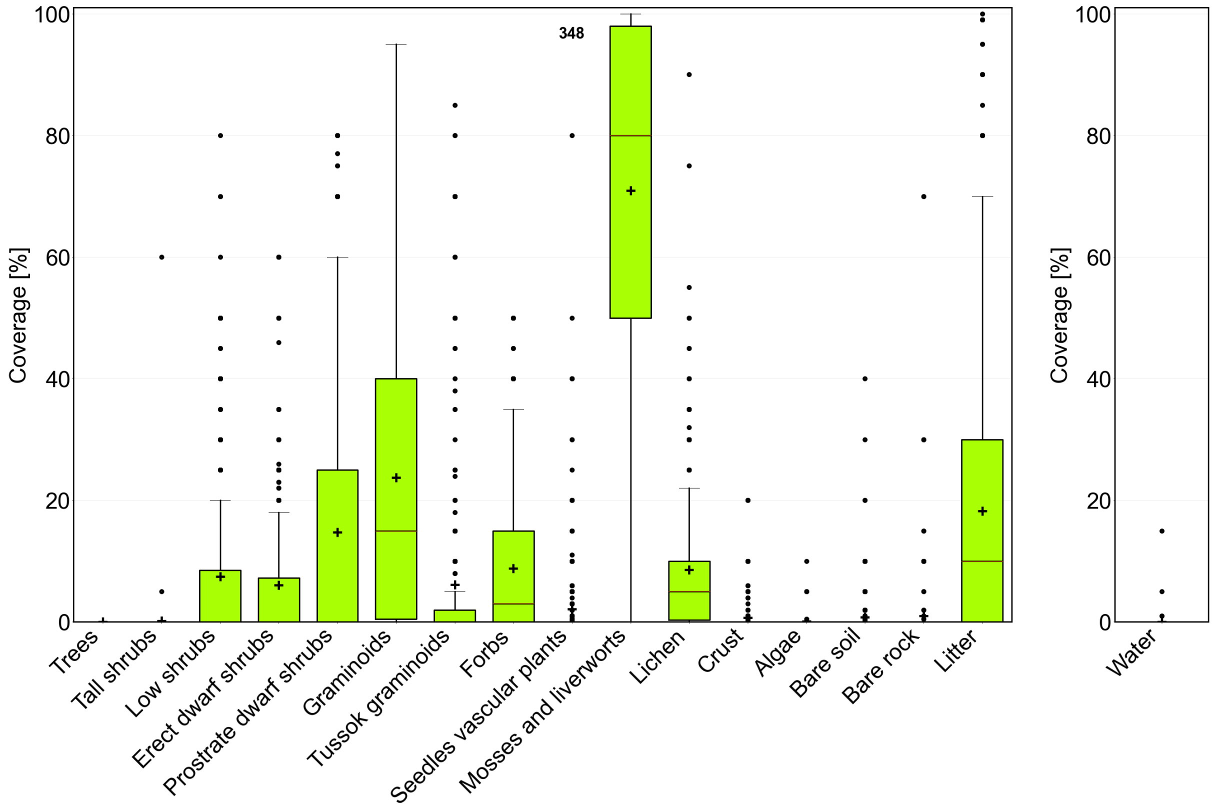

Figure B30. ~~Class~~ CALU #10 vegetation properties based on AVA (Zemlianskii et al., 2023).

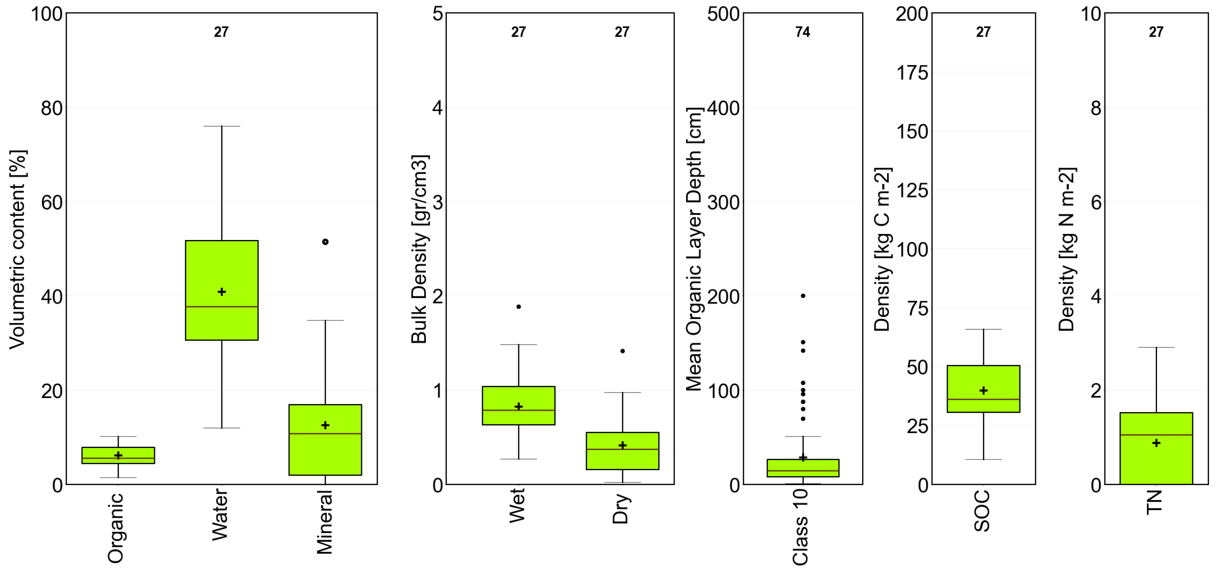

Figure B31. ~~Class~~ CALU #10 soil properties based on Palmtag et al. (2022).

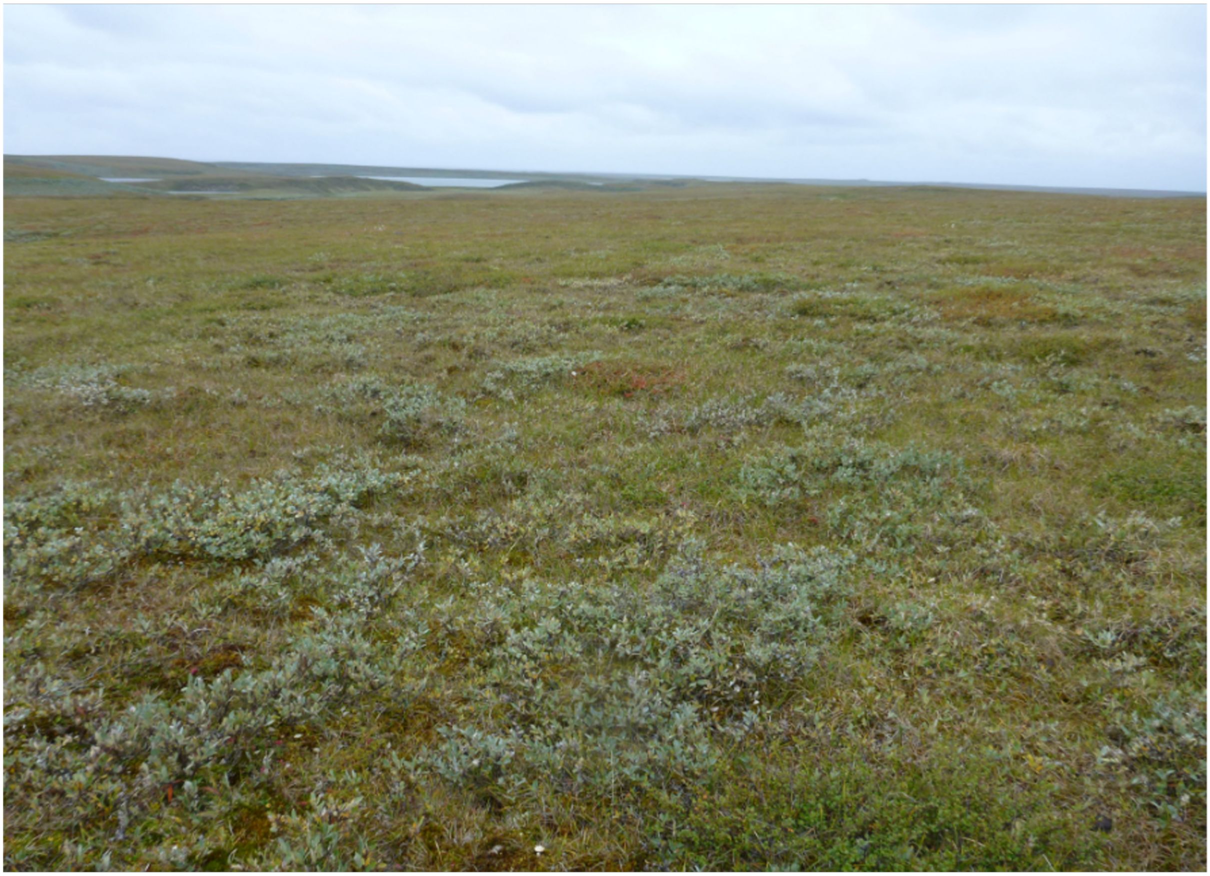

Figure B32. Example photograph ~~class~~ CALU #10 (Marina Leibmann, central Yamal)

B11 ~~Class~~ CALU #11

Description: ~~moist~~ Moist tundra, abundant moss, dwarf and low shrubs, tussocks; low organic layer thickness, medium mineral volumetric content.

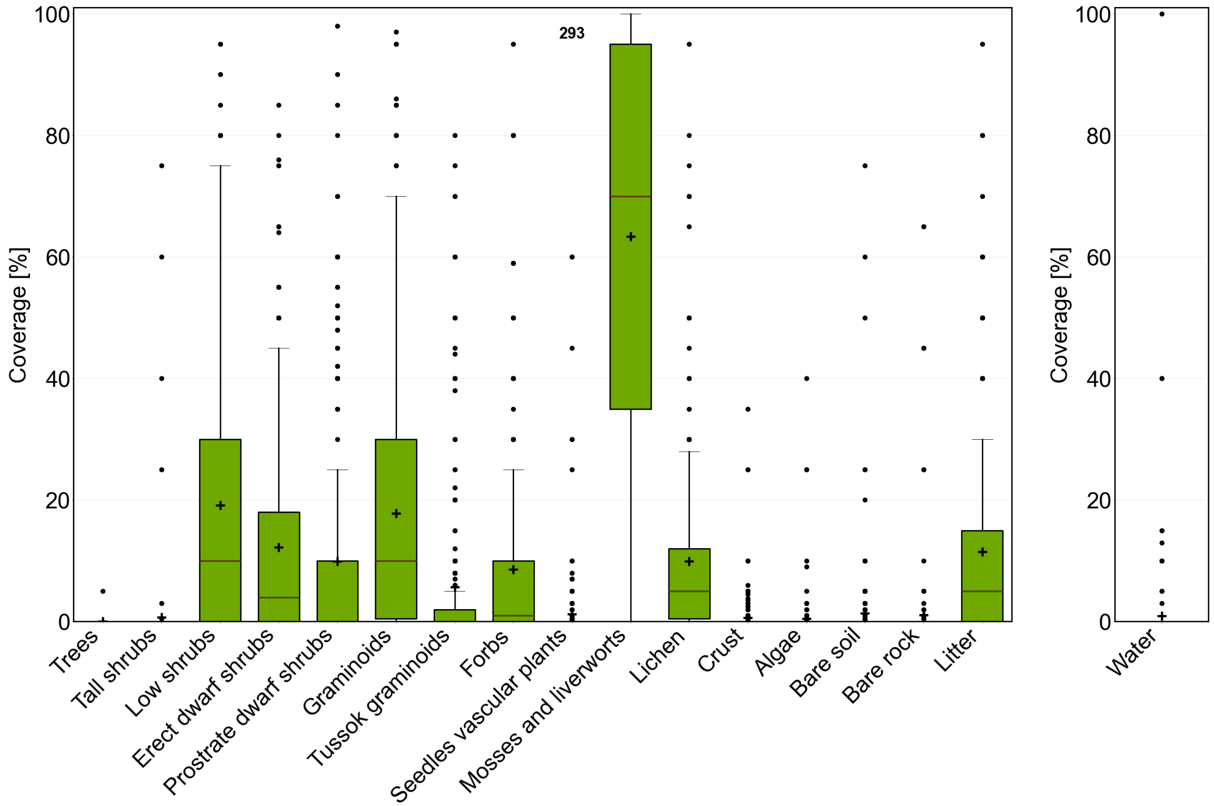

Figure B33. ~~Class~~ CALU #11 vegetation properties based on AVA (Zemlianskii et al., 2023).

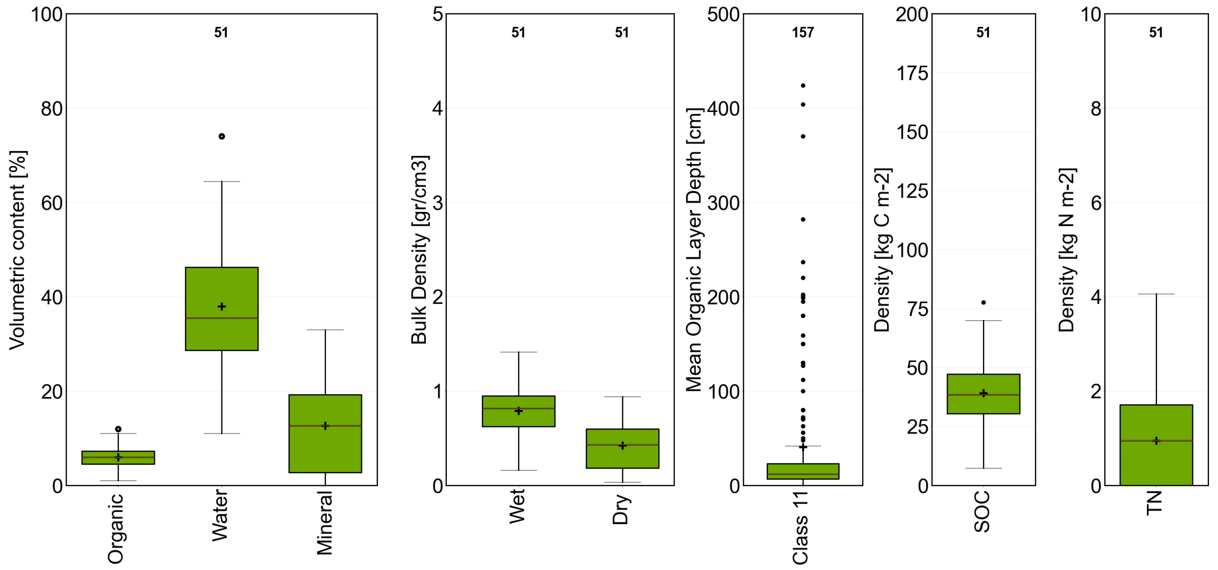

Figure B34. ~~Class~~ CALU #11 soil properties based on Palmtag et al. (2022).

Figure B35. Example photograph ~~class~~ CALU #11 (Annett Bartsch 2018, Polar Ural)

Figure B36. Example photograph ~~class~~ CALU #11 (Annett Bartsch 2023, Inuvik region)

B12 ~~Class~~ CALU #12

Description: ~~moist~~ Moist tundra, dense dwarf and low shrubs (sparse tree cover along treeline, woodlands with open stands); medium organic layer thickness, low mineral volumetric content.

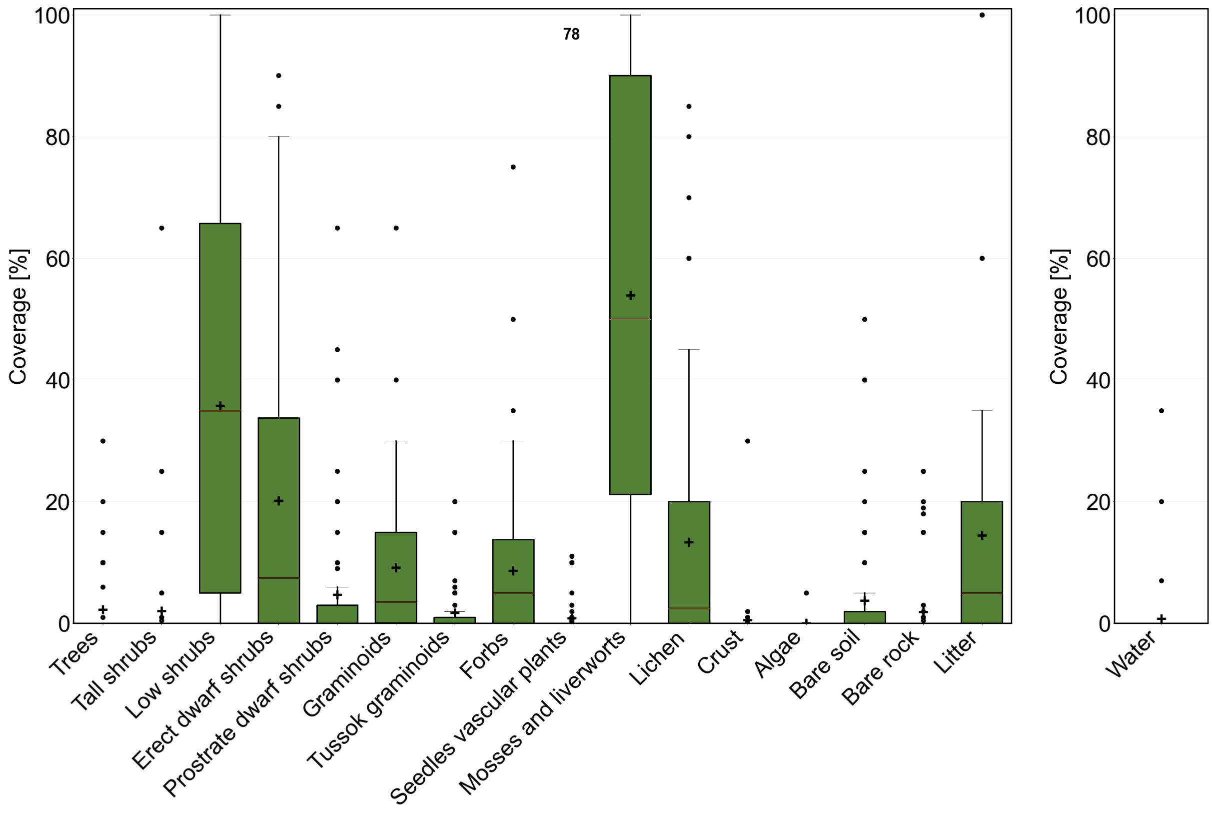

Figure B37. ~~Class~~ CALU #12 vegetation properties based on AVA (Zemlianskii et al., 2023).

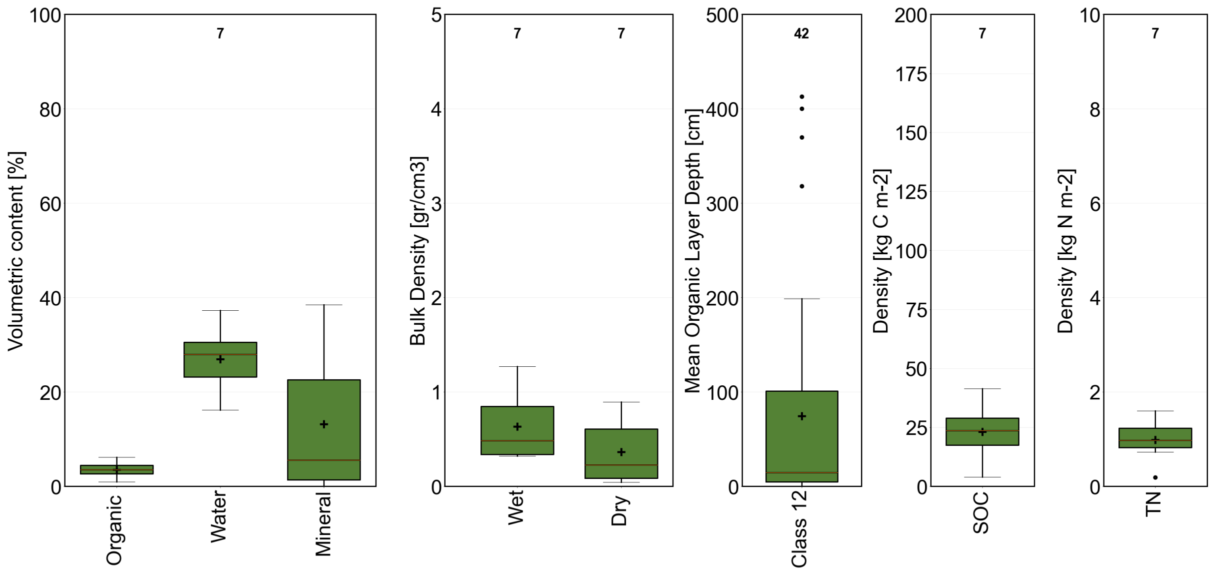

Figure B38. ~~Class~~ CALU #12 soil properties based on Palmtag et al. (2022).

Figure B39. Example photograph ~~class~~ CALU #12, foreground (Ksenia Ermokhina , 01.08. 2011, Polar Urals; mostly *Betula nana*, scattered *Salix* ssp.).

Figure B40. Example photograph ~~class~~ CALU #12 (Mareike Wieczorek, 11.08.2012, Kolyma region; mostly *Betula nana* in proximity to patches of ~~class~~ CALU ##3.

B13 Class CALU #13

Description: moist Moist to wet tundra, dense dwarf and low shrubs (sparse tree cover along treeline, woodlands with open stands).

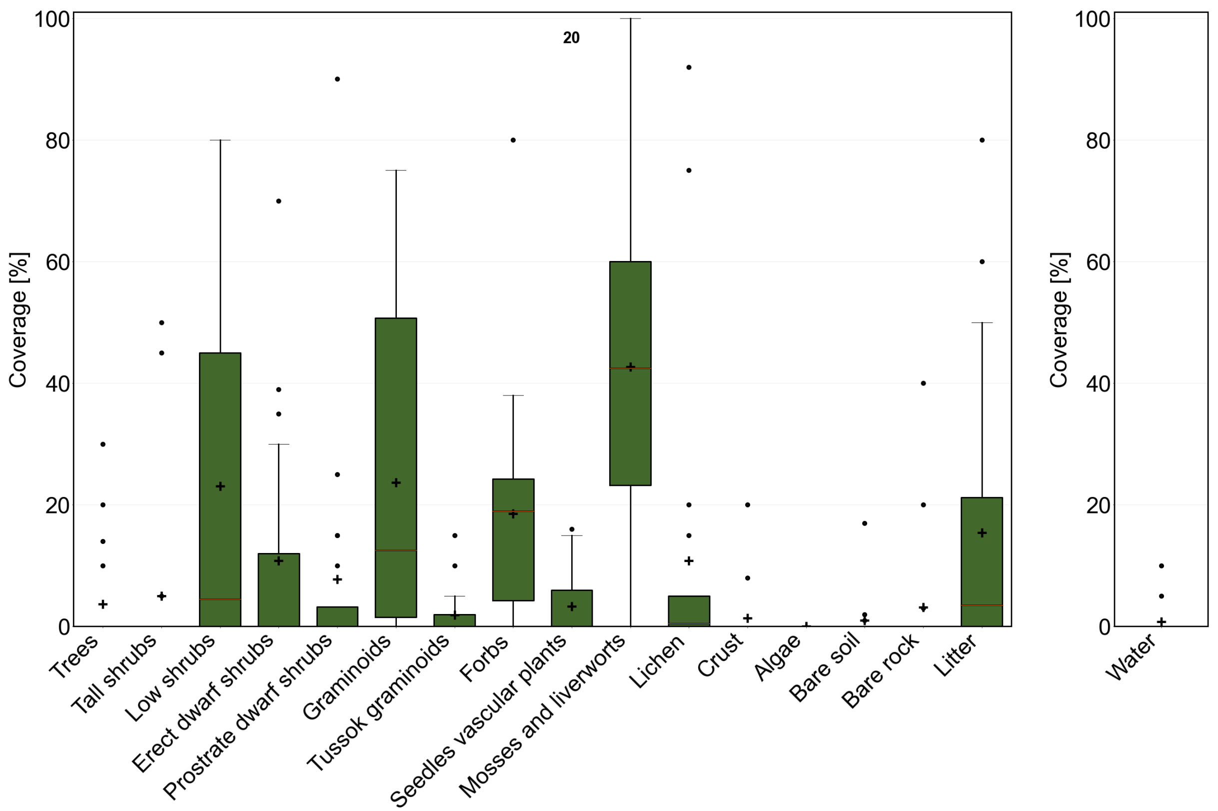

Figure B41. Class CALU #13 vegetation properties based on AVA (Zemlianskii et al., 2023).

Figure B42. Example photograph ~~class~~ CALU #13 (Clemens von Baeckmann, 25.07.2023, Inuvik region).

B14 ~~Class~~ CALU #14

Description: ~~moist~~ Moist tundra, low shrubs; medium organic layer thickness, medium mineral volumetric content.

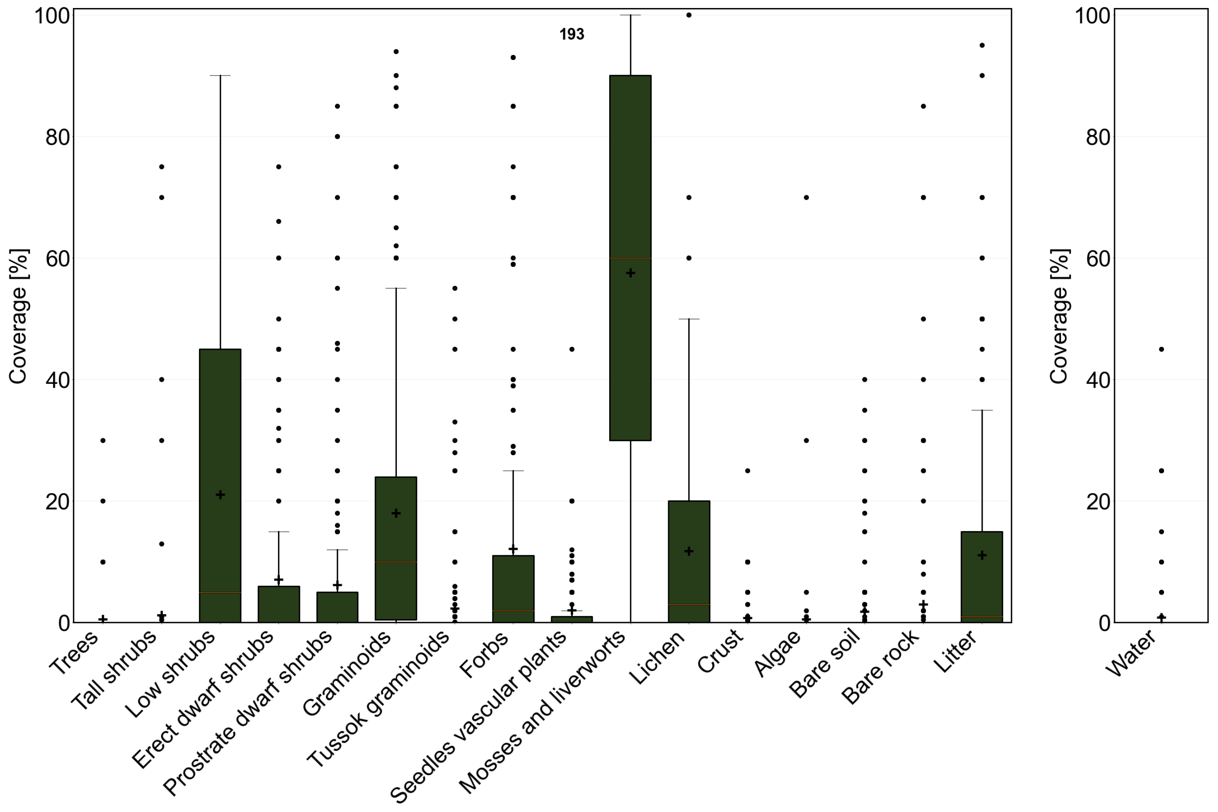

Figure B43. ~~Class~~ CALU #14 vegetation properties based on AVA (Zemlianskii et al., 2023).

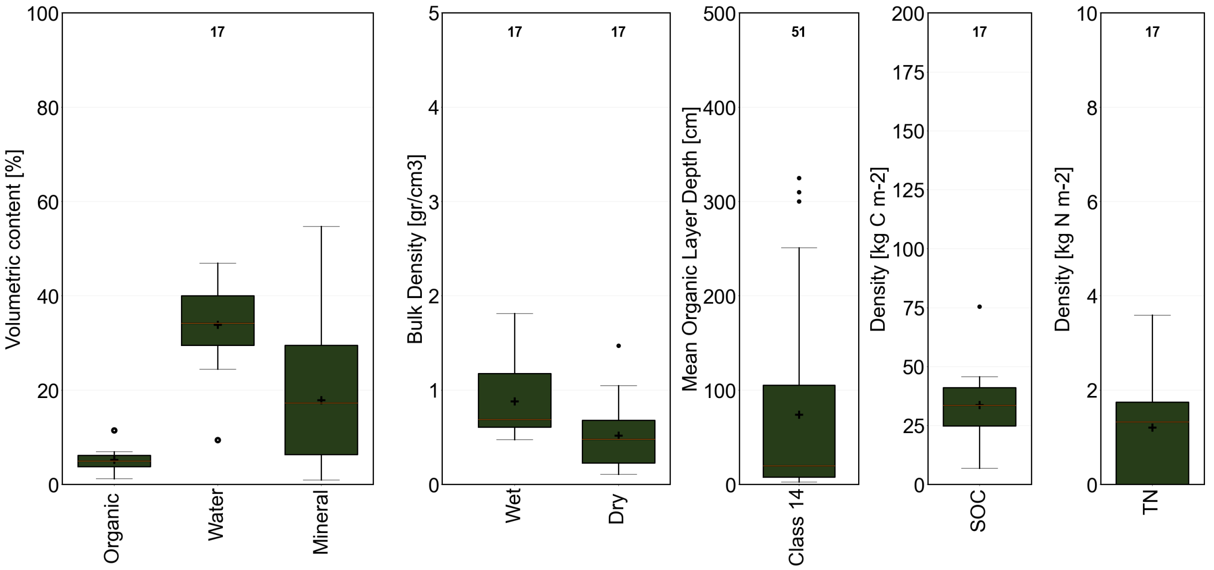

Figure B44. ~~Class~~ CALU #14 soil properties based on Palmtag et al. (2022).

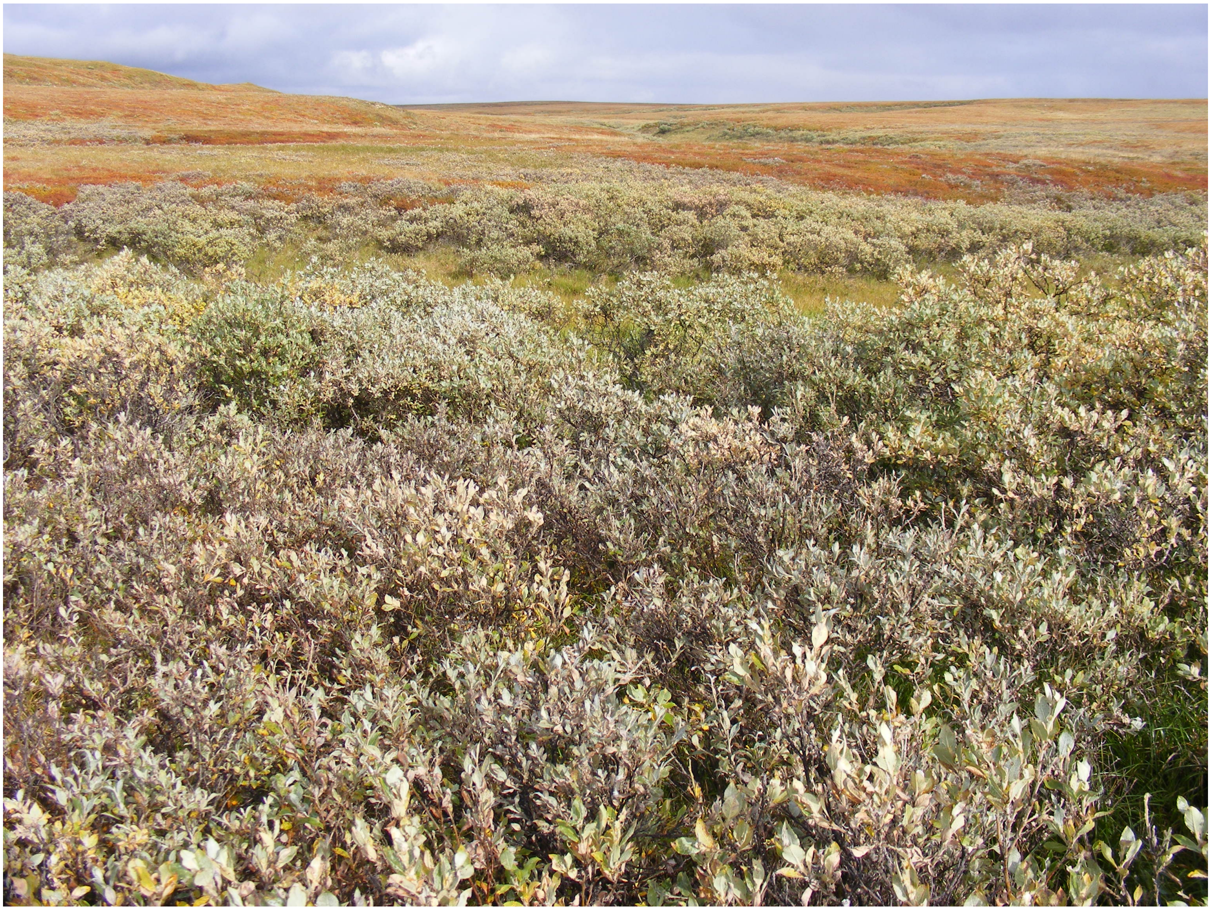

Figure B45. Example photograph ~~class~~ CALU #14 (Marina Leibmann, 29.08.2014, central Yamal; mostly *Salix* ssp.)

Figure B46. Example photograph ~~class~~ CALU #14 (Annett Bartsch 24.07.2023, Inuvik region, backround *Salix* ssp., left and right *Alnus* ssp.)

B15 ~~Class~~ CALU #15

Description: ~~moist~~ Moist to wet tundra, abundant lichen, in some cases partially barren (disturbed).

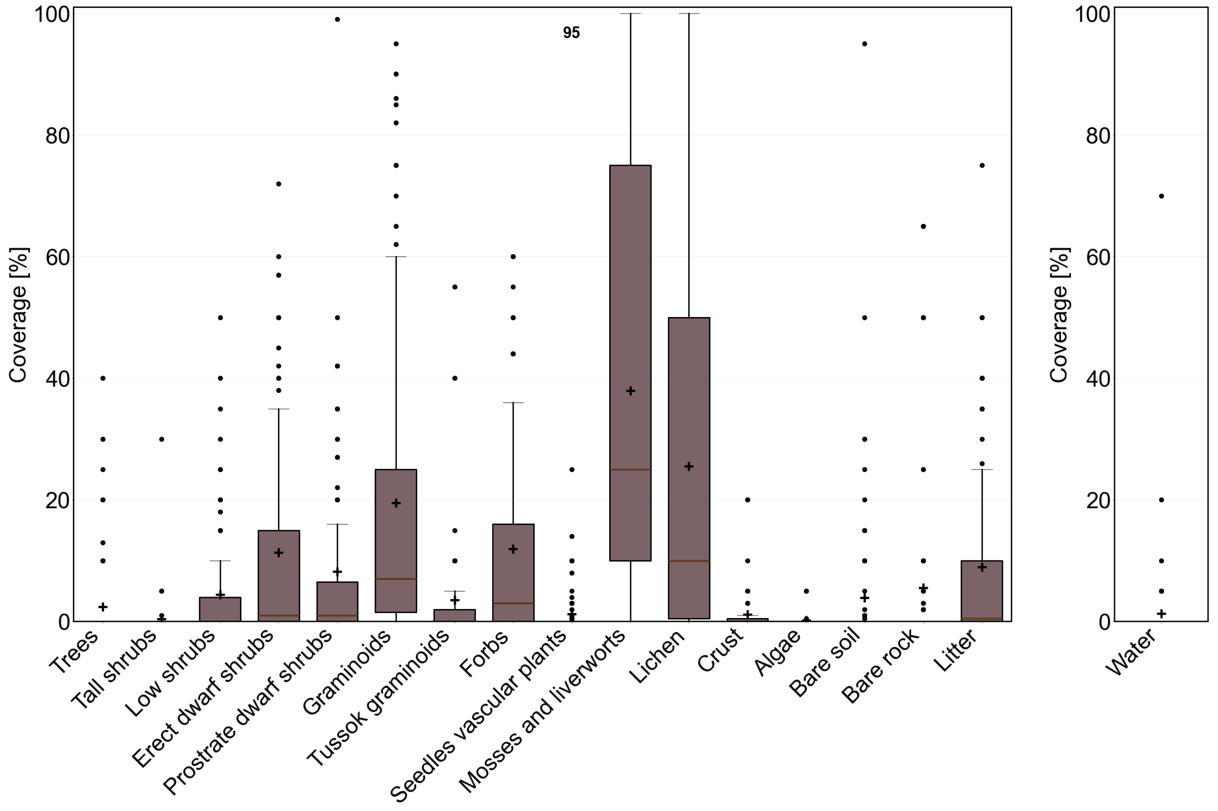

Figure B47. ~~Class~~ CALU #15 vegetation properties based on AVA (Zemlianskii et al., 2023).

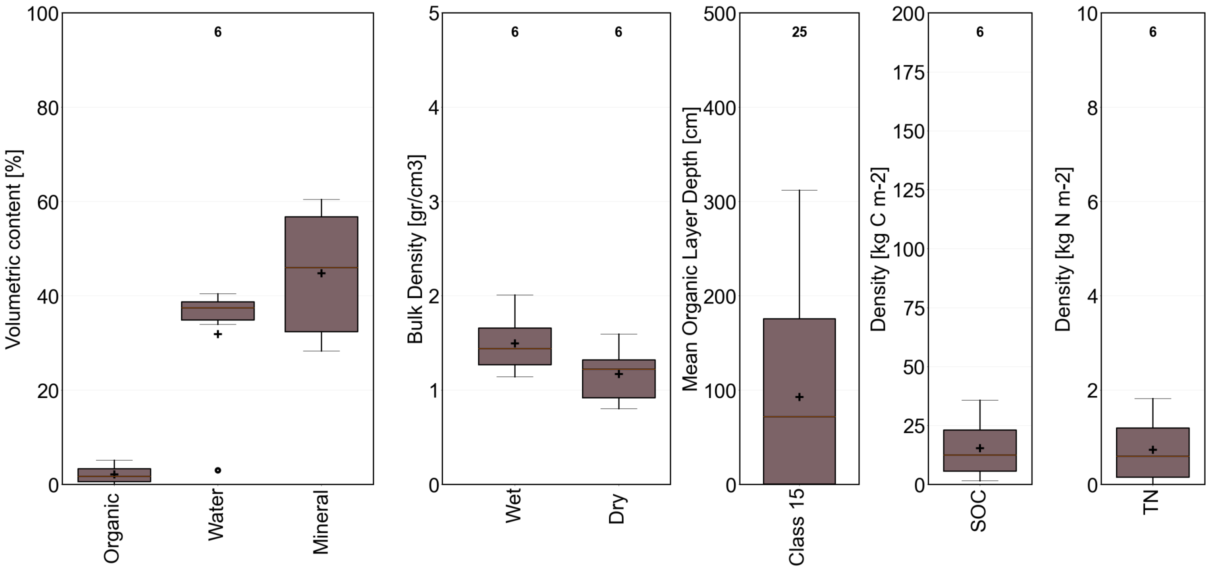

Figure B48. ~~Class~~ CALU #15 soil properties based on Palmtag et al. (2022).

Figure B49. Example photograph ~~class~~ CALU #15 (Veronika Döpfer, 17.07.2023, Inuvik region)

B16 ~~Class~~ CALU #16

Description: ~~moist~~ Moist tundra, abundant forbs, dwarf to tall shrubs; medium organic layer thickness.

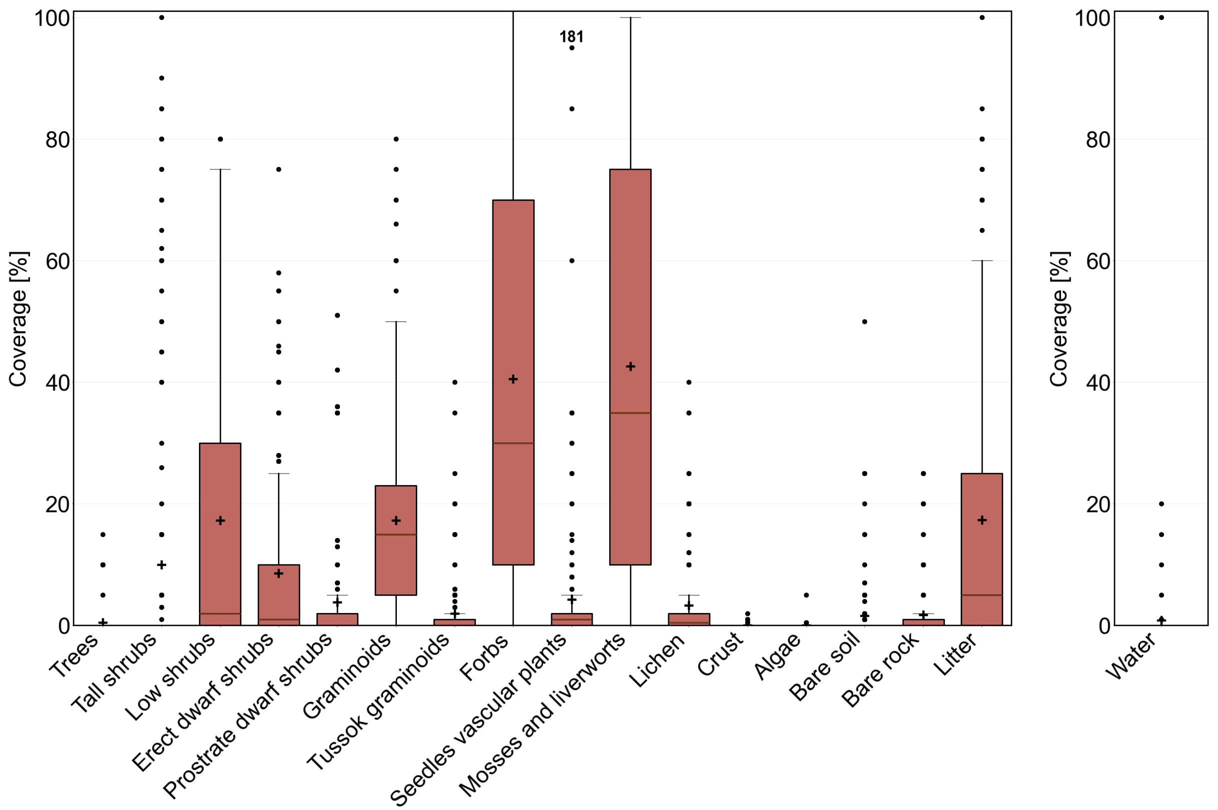

Figure B50. ~~Class~~ CALU #16 vegetation properties based on AVA (Zemlianskii et al., 2023).

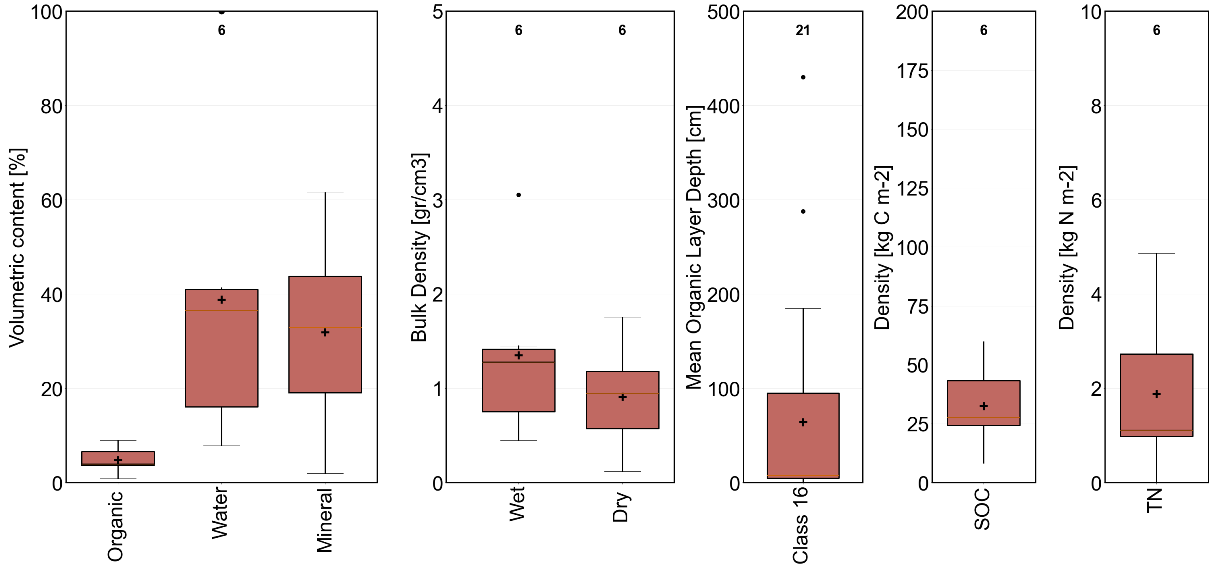

Figure B51. ~~Class~~ CALU #16 soil properties based on Palmtag et al. (2022).

Figure B52. Example photograph ~~class~~ CALU #16 (Annett Bartsch 2018, Polar Ural)

B17 ~~Class~~ **CALU #17**

Description: ~~recently~~ Recently burned or flooded, partially barren.

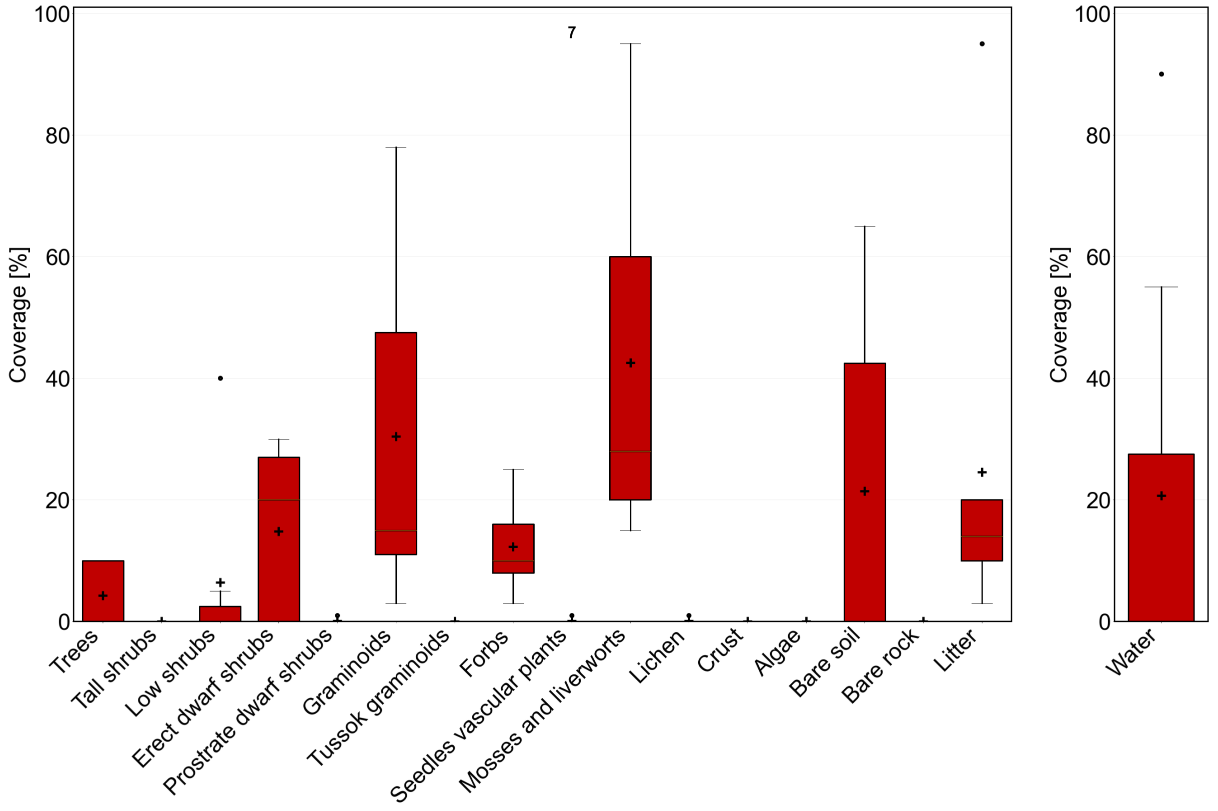

Figure B53. ~~Class~~ CALU #17 vegetation properties based on AVA (Zemlianskii et al., 2023).

Figure B54. Example photograph ~~class~~ CALU #17 (Annett Bartsch 27.07.2023, Inuvik)

B18 ~~Class~~ CALU #18

Description: Forest (deciduous) with dwarf to tall shrubs.

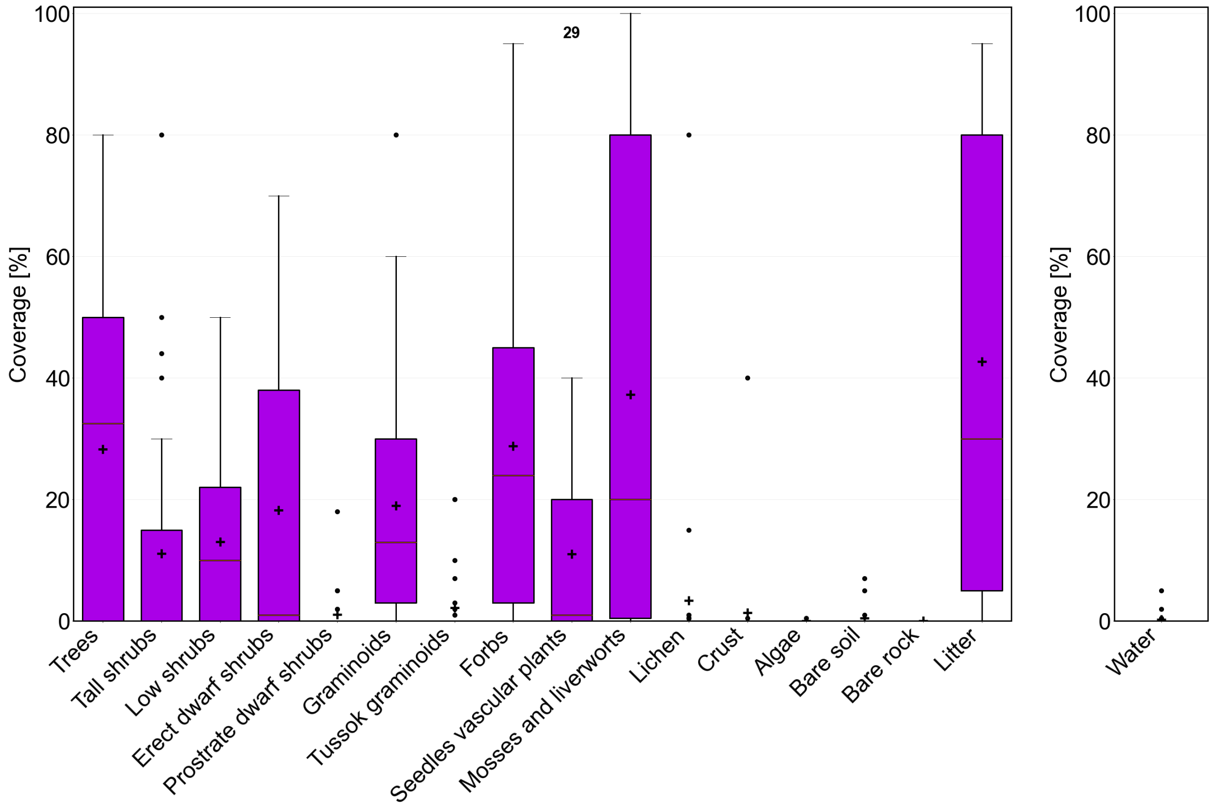

Figure B55. ~~Class~~ CALU #18 vegetation properties based on AVA (Zemlianskii et al., 2023).

B19 ~~Class~~ CALU #19

Description: Forest (mixed) with dwarf to tall shrubs.

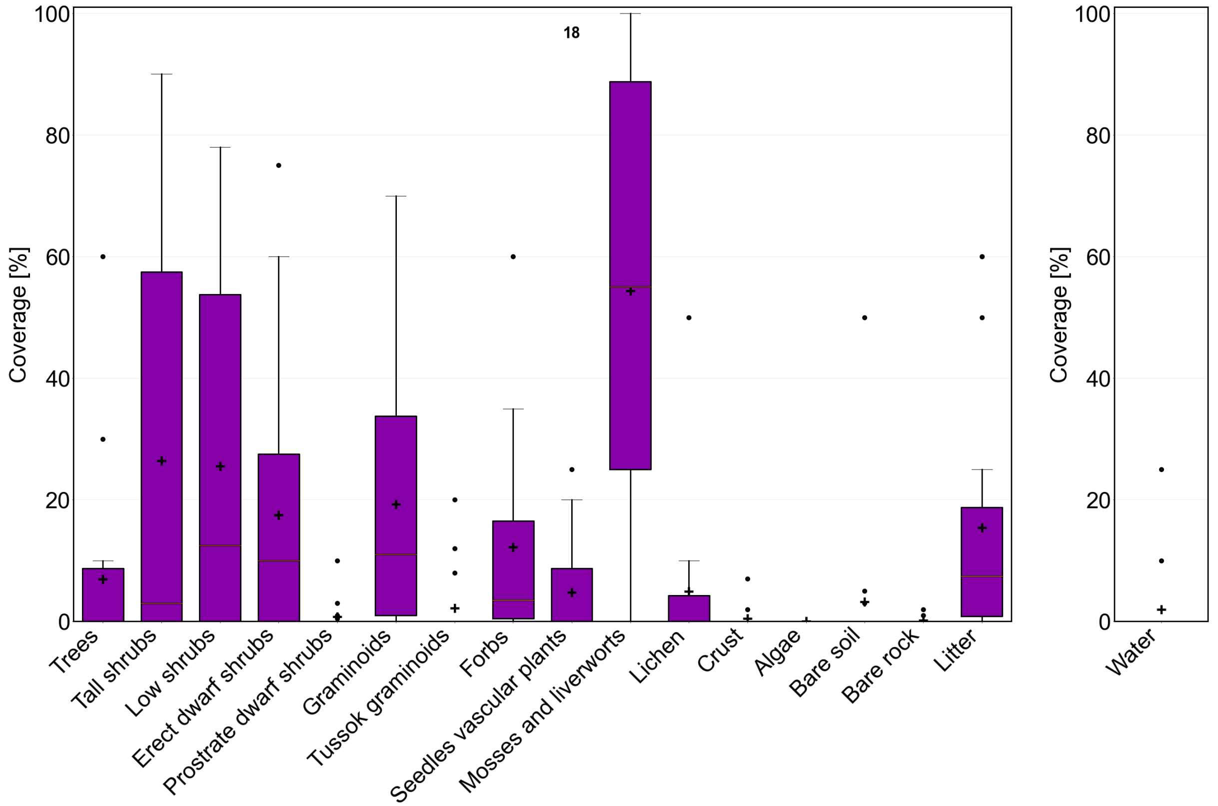

Figure B56. ~~Class~~ CALU #19 vegetation properties based on AVA (Zemlianskii et al., 2023).

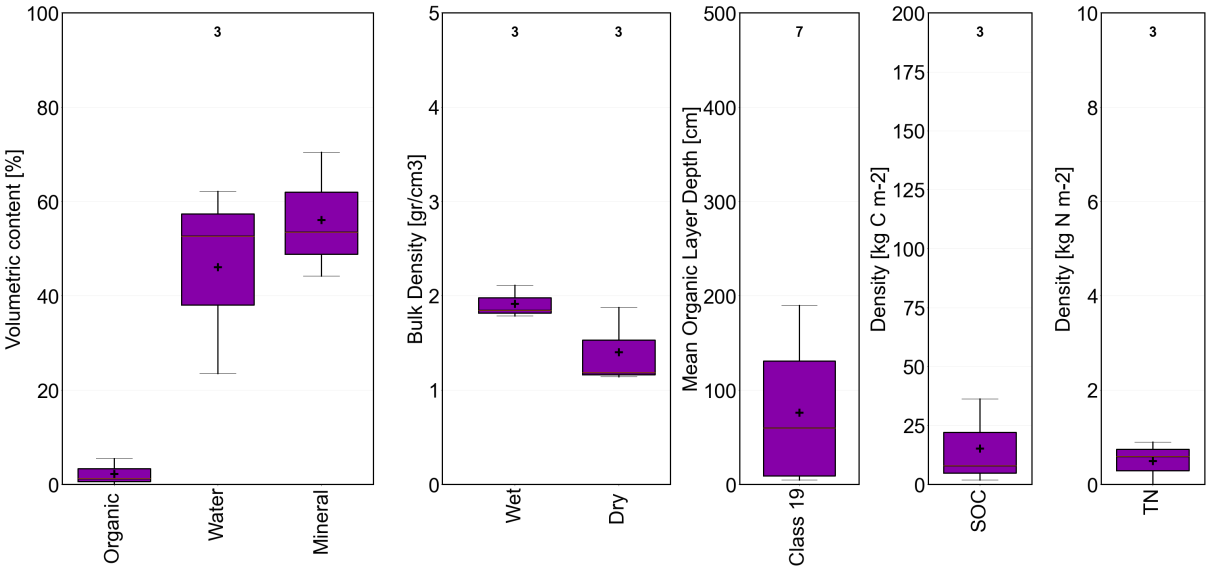

Figure B57. ~~Class~~ CALU #19 soil properties based on Palmtag et al. (2022).

B20 ~~Class~~ CALU #20

Description: Forest (needle leave) with dwarf and low shrubs.

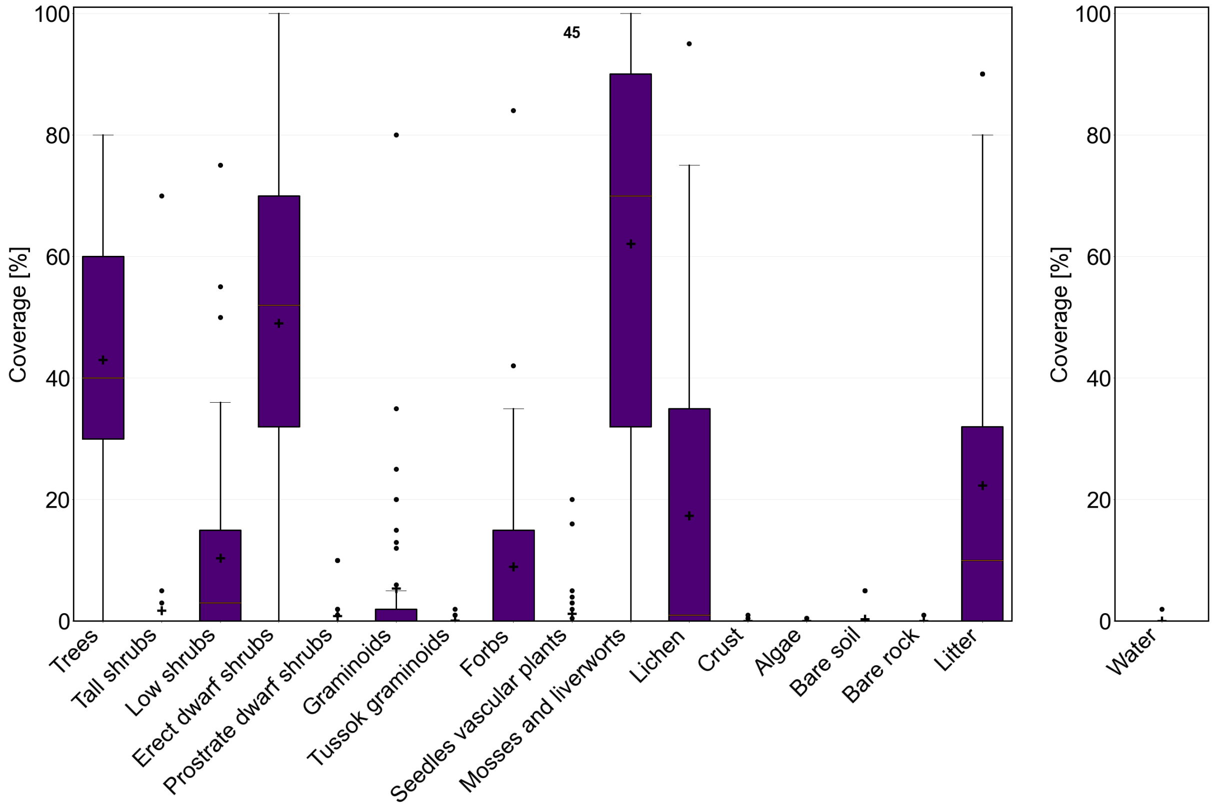

Figure B58. ~~Class~~ CALU #20 vegetation properties based on AVA (Zemlianskii et al., 2023).

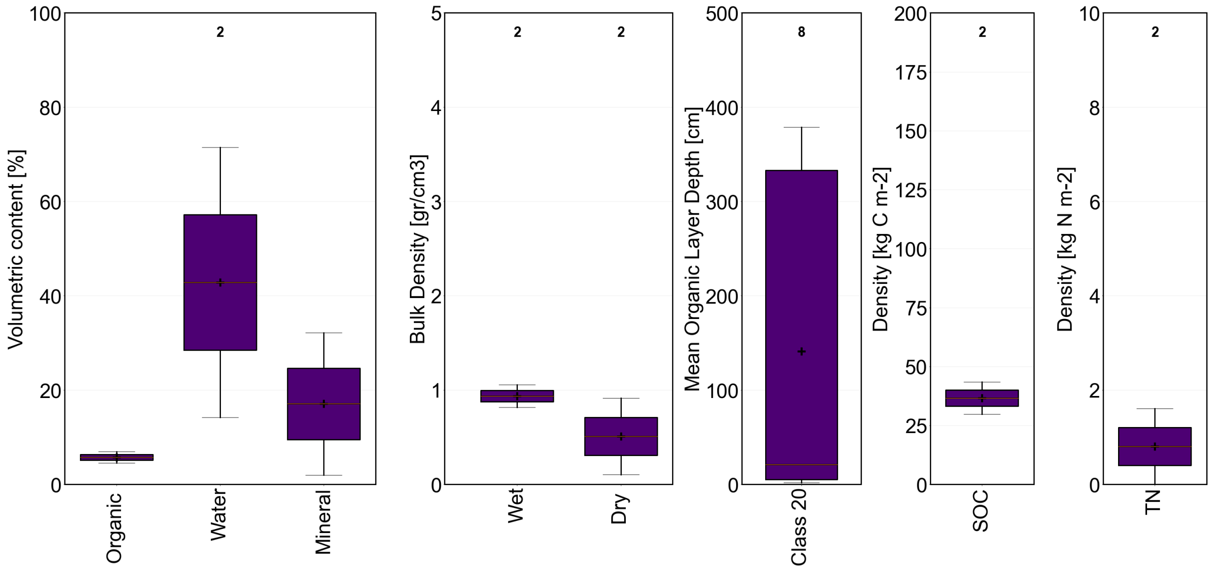

Figure B59. ~~Class~~ CALU #20 soil properties based on Palmtag et al. (2022).

B21 ~~Class~~ CALU #21

820 **Description:** Partially barren, dry.

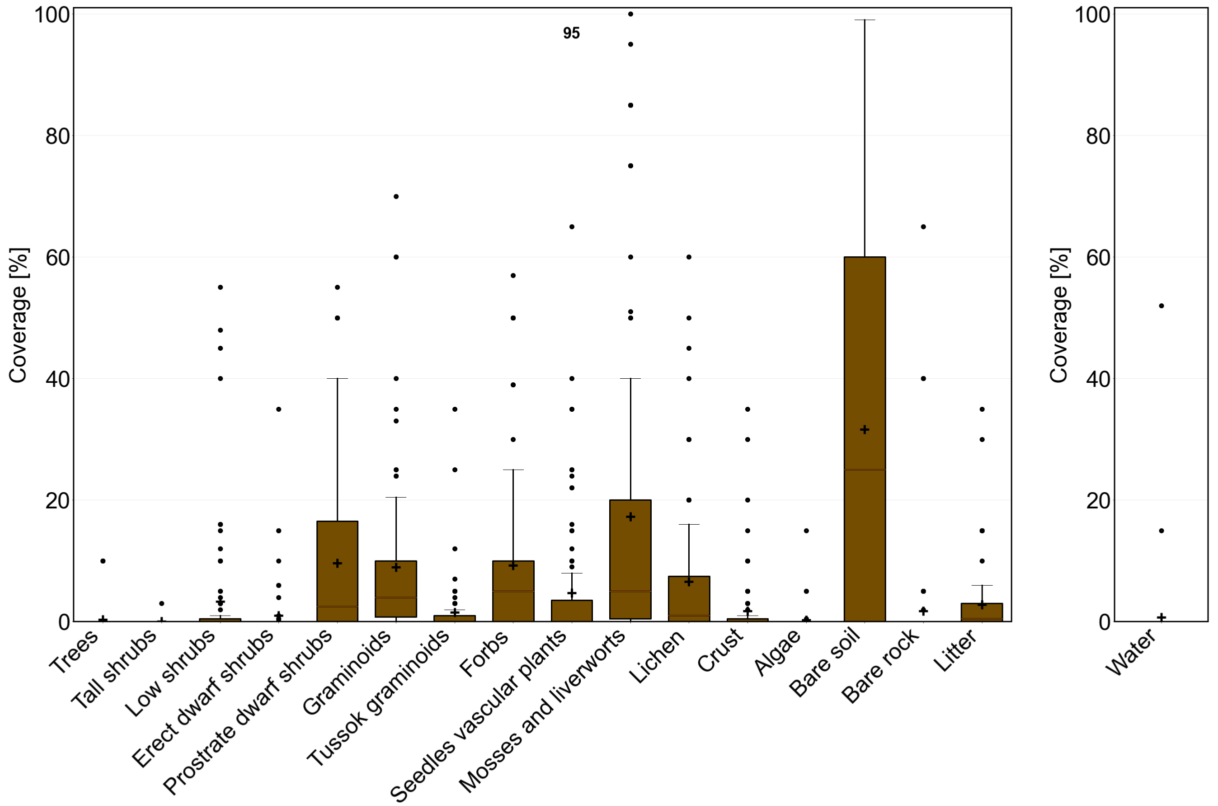

Figure B60. ~~Class~~ CALU #21 vegetation properties based on AVA (Zemlianskii et al., 2023).

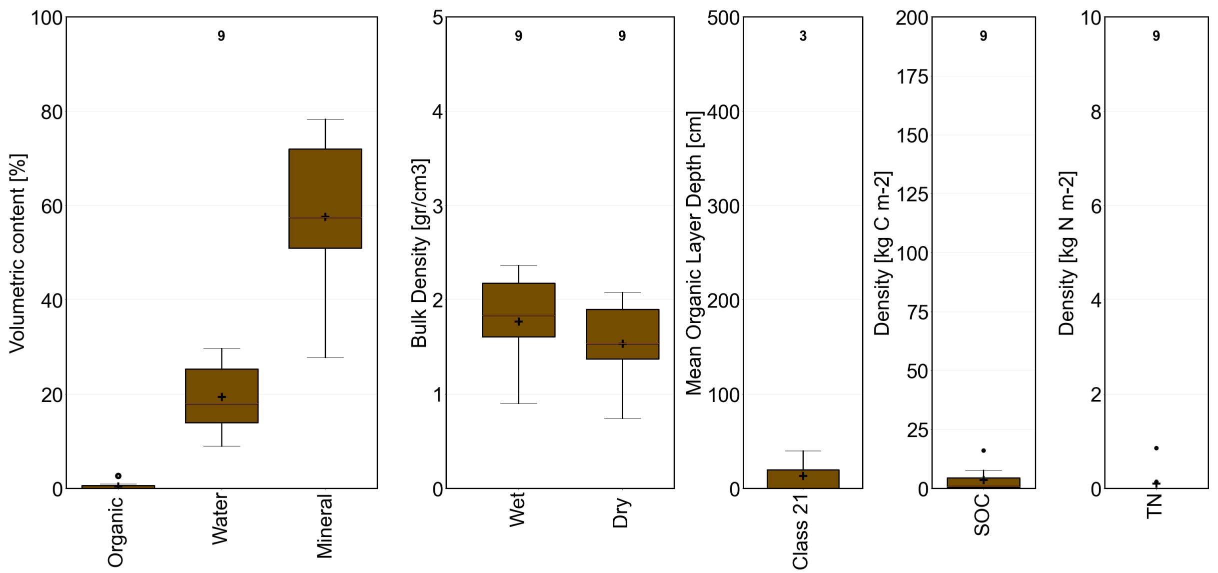

Figure B61. ~~Class~~ CALU #21 soil properties based on Palmtag et al. (2022).

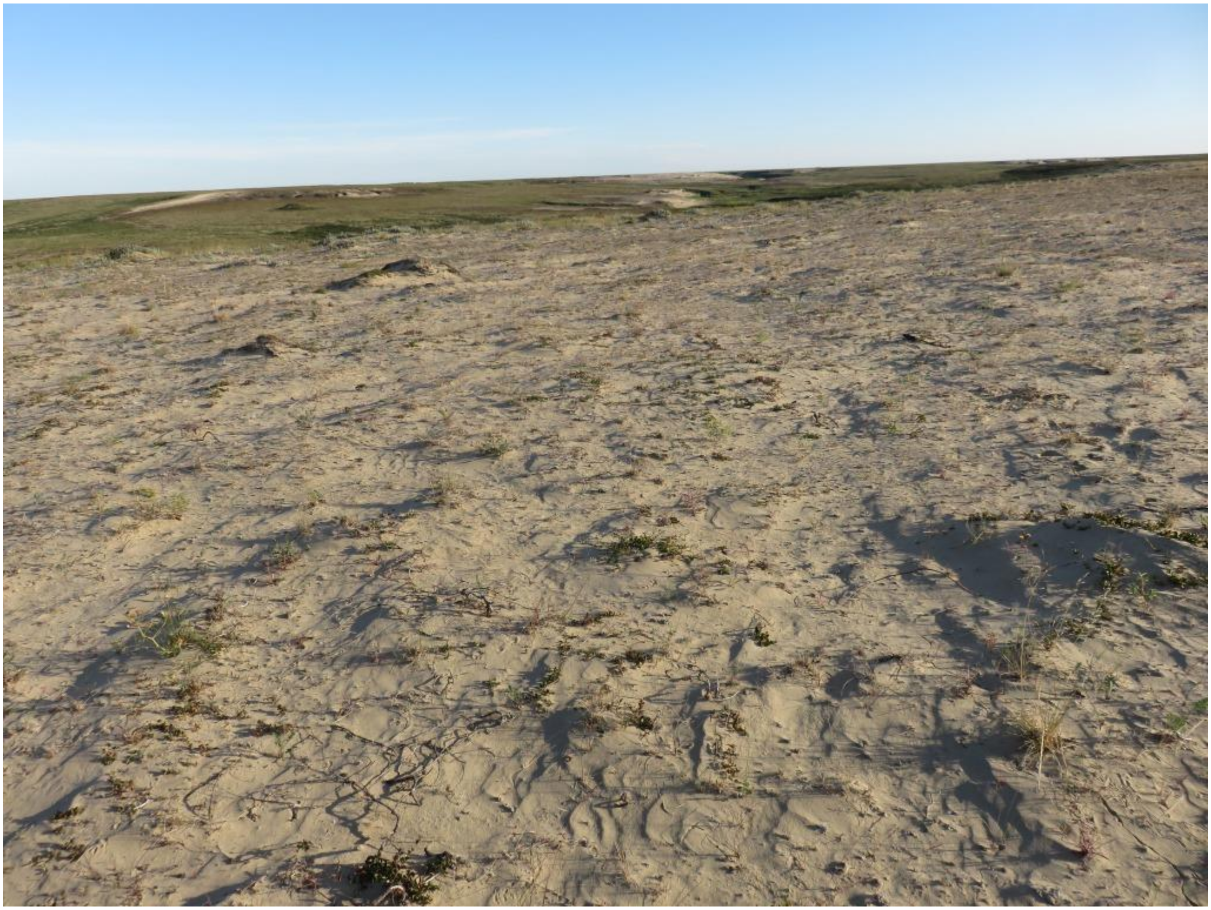

Figure B62. Example photograph ~~class~~ CALU #21 (Olga Khitun, 2017, Tazovskiy Peninsula)

Figure B63. Example photograph ~~class~~ CALU #21 (Elena Troeva, 2017, Northern Yamal)

Appendix C: Comparison schemes and matrices for external landcover ~~dataset~~datasets

Table C1. Classes of ESA CCI Landcover (Defourny et al., in preparation) (http://maps.elie.ucl.ac.be/CCI/viewer/index.php, last access: 1 September 2023) and grouping for comparison (see Table 2).

Group A	**Description**
other	0 No Data
other	10 Cropland, rainfed
other	11 Herbaceous cover
other	12 Tree or shrub cover
other	20 Cropland, irrigated or post-flooding
other	30 Mosaic cropland (>50 %) / natural vegetation (tree, shrub, herbaceous cover) (<50 %)
other	40 Mosaic natural vegetation (tree, shrub, herbaceous cover) (>50 %) / cropland (<50 %)
forest	50 Tree cover, broadleaved, evergreen, closed to open (>15 %)
forest	60 Tree cover, broadleaved, deciduous, closed to open (>15 %)
forest	61 Tree cover, broadleaved, deciduous, closed (>40 %)
forest	62 Tree cover, broadleaved, deciduous, open (15-40 %)
forest	70 Tree cover, needleleaved, evergreen, closed to open (>15 %)
forest	71 Tree cover, needleleaved, evergreen, closed (>40 %)
forest	72 Tree cover, needleleaved, evergreen, open (15-40 %)
forest	80 Tree cover, needleleaved, deciduous, closed to open (>15 %)
forest	81 Tree cover, needleleaved, deciduous, closed (>40 %)
forest	82 Tree cover, needleleaved, deciduous, open (15-40 %)
forest	90 Tree cover, mixed leaf type (broadleaved and needleleaved)
forest	100 Mosaic tree and shrub (>50 %) / herbaceous cover (<50 %)
dwarf to low shrub tundra	110 Mosaic herbaceous cover (>50 %) / tree and shrub (<50 %)
dwarf to low shrub tundra	120 Shrubland
dwarf to low shrub tundra	121 Evergreen shrubland
dwarf to low shrub tundra	122 Deciduous shrubland
grassland graminoids	130 Grassland
lichen/moss	140 Lichens and mosses
barren	150 Sparse vegetation (tree, shrub, herbaceous cover) (<15 %)
barren	151 Sparse tree (<15 %)
barren	152 Sparse shrub (<15 %)
barren	153 Sparse herbaceous cover (<15 %)
wetland	160 Tree cover, flooded, fresh or brakish water
wetland	170 Tree cover, flooded, saline water
wetland	180 Shrub or herbaceous cover, flooded, fresh/saline/brakish water
barren	190 Urban areas
barren	200 Bare areas
barren	201 Consolidated bare areas
barren	202 Unconsolidated bare areas
water	210 Water bodies
snow/ice	220 Permanent snow and ice

Table C2. Classes of the CAVM (Raynolds et al., 2019) and grouping for comparison (see Table 2).

Group A	CAVM Code	Unit
barren	B1	Cryptogam, herb barren
~~grassland~~ graminoids	B2a	Cryptogam, barren complex
~~shrubland~~ dwarf to low shrub tundra	B2b	Cryptogam, barren, dwarf-shrub complex
~~other~~ barren	B3	Non-carbonate mountain complex
~~other~~ barren	B4	Carbonate mountain complex
~~grassland~~ graminoids	G1	Graminoid, forb, cryptogam tundra
~~grassland~~ graminoids	G2	Graminoid, prostrate dwarf-shrub, forb, moss tundra
dwarf to low shrub tundra	G3	Non-tussock sedge, dwarf-shrub, moss tundra
dwarf to low shrub tundra	G4	Tussock-sedge, dwarf-shrub, moss tundra
~~grassland~~ graminoids	P1	Prostrate dwarf-shrub, herb, lichen tundra
dwarf to low shrub tundra	P2	Prostrate/hemi-prostrate dwarf-shrub, lichen tundra
dwarf to low shrub tundra	S1	Erect dwarf-shrub, moss tundra
dwarf to low shrub tundra	S2	Low-shrub, moss tundra
wetland	W1	Sedge/grass, moss wetland complex
wetland	W2	Sedge, moss, dwarf-shrub wetland complex
wetland	W3	Sedge, moss, low-shrub wetland complex
water	FW	Fresh water
water	SW	Saline water

Table C3. Classes of the CALC-2020 (Liu et al., 2023) and grouping for comparison (see Table 2).

Group A	Class	Description
other	cropland	Arable land that is sowed or planted at least once within a 12-month period
forest	forest	Land covered by trees, with canopy coverage greater than 30 %
~~grassland~~ graminoids	graminoid tundra	Land covered by herbaceous vegetation with plant height typically ranging 5–15 cm
dwarf to low shrub tundra	shrub tundra	Land covered by shrubs of any stature with plant height typically ranging 20–50 cm
wetland	wetland	Land featured by aquatic plants and periodically saturated with or covered by water
water	open water	Inland open water bodies
lichen/moss	lichen/moss	Bedrock covered by cryptogam communities
barren	barren man-made	Impermeable land surface paved by man-made structures
barren	barren	less than 10 % vegetation
ice/snow	ice/snow	Land covered with snow and ice all year round

Table C4. Comparison matrix of grouped Circumpolar Arctic Vegetation Map - CAVM classes and grouped units (Circumarctic Landcover Units - CALU). Values in percent. For grouping schemes see Tables 2 and C2.

	CAVM					
CALU		**water**	**wetland**	**graminoids**	**dwarf to low shrub tundra**	**barren**
	water	41.10	12.12	2.42	2.89	25.91
	snow/ice	0.39	0.11	0.12	0.04	1.46
	other	0.58	0.68	1.15	0.81	2.00
	wetland	12.82	18.93	8.79	6.17	8.32
	graminoids	1.64	4.35	19.99	3.08	1.04
	lichen/moss	6.43	25.39	29.55	6.48	38.39
	dwarf to low shrub tundra	33.92	34.62	33.43	74.67	12.06
	forest	1.67	0.88	0.36	4.89	0.48
	barren	1.46	2.92	4.19	0.96	10.36

Table C5. Comparison matrix of grouped Circumarctic Landcover - CALC-2020 Landcover classes and grouped units (Circumarctic Landcover Units - CALU). Values in percent. For grouping schemes see Tables 2 and C3.

	CALC-2020								
CALU		**water**	**snow/ice**	**wetland**	**graminoids**	**lichen/ moss**	**dwarf to low shrub tundra**	**forest**	**barren**
	water	83.02	88.27	0.62	0.00	0.07	0.00	0.02	8.41
	snow/ice	0.70	4.41	0.03	0.00	0.05	0.00	0.00	0.82
	other	0.39	1.14	0.89	0.69	1.80	1.36	1.67	1.91
	wetland	15.53	1.81	23.38	1.70	3.37	2.30	3.42	14.82
	graminoids	0.00	0.00	4.73	5.75	3.65	0.00	0.00	0.07
	lichen/moss	0.01	0.84	16.27	2.38	72.96	0.44	0.03	32.87
	dwarf to low shrub tundra	0.17	0.00	51.26	85.06	9.44	63.57	33.78	2.12
	forest	0.05	0.00	2.60	4.33	0.06	32.32	61.06	0.18
	barren	0.13	3.52	0.21	0.09	8.61	0.01	0.01	38.82

Appendix D: **Changes between prototype and CALU**

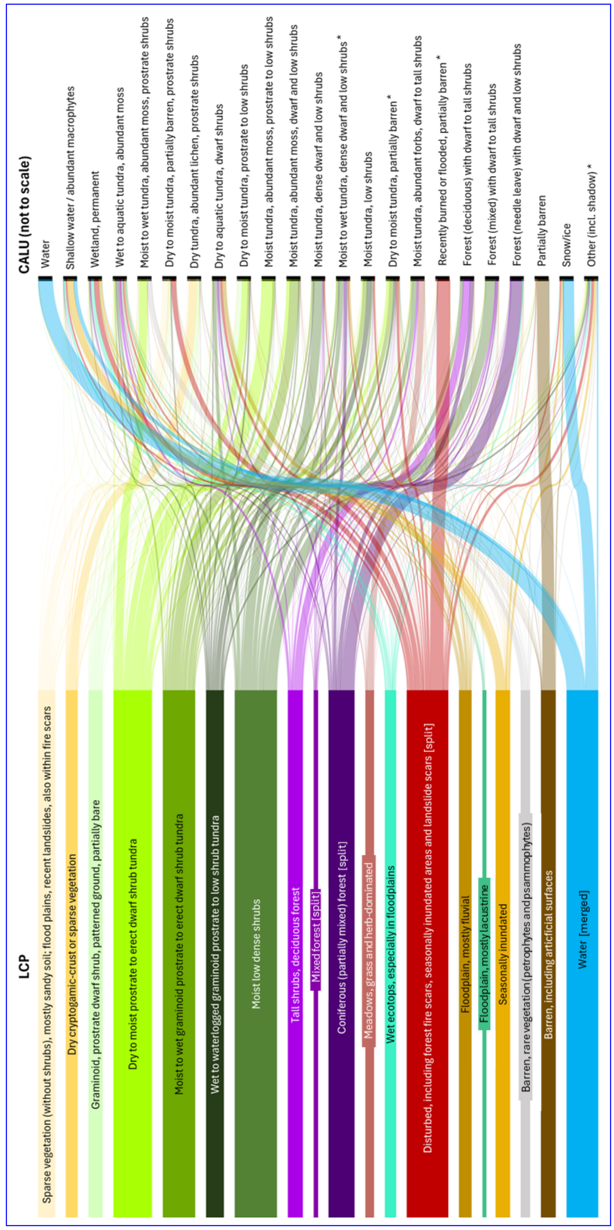

Figure D1. Visualisation of changed mapping units from the landcover prototype (LCP, 20m) to CALU (10m). The three water classes of the LCP are merged. New units are are marked with *.